

A Role for SIRT-1 in Dendritic and Spine Morphology of  
Medium Spiny Neurons in the Nucleus Accumbens

by

Tanessa Call

A Dissertation Presented in Partial Fulfillment  
of the Requirements for the Degree  
Doctor of Philosophy

Approved June 2022 by the  
Graduate Supervisory Committee:

Deveroux Ferguson, Co-Chair

Janet Neiswander, Co-Chair

Ron Hammer

Shenfeng Qiu

ARIZONA STATE UNIVERSITY

August 2022

## ABSTRACT

Major depressive disorders affect 350 million people globally and are the leading cause of disability worldwide. Chronic or prolonged stress can trigger development of depression. Key symptoms of depression are anhedonia, helplessness, and decreased socialization. These behavioral outcomes suggest a dysfunction within the brain's reward system, the mesolimbic system. The nucleus accumbens (NAc) is regarded as the brain's reward hub, integrating signals from multiple brain regions to influence motivated behavioral output. The NAc consists of medium spiny neurons (MSNs) which represent 95% of the cellular landscape. These neurons can be separated into two distinct groups, dopamine receptor-1 (DR1 or D1) and dopamine receptor-2 (DR2 or D2). Differentiating between these two cell types is ideal as activation results in opposing outcomes. One protein of interest sirtuin-1 (SIRT1) has been found to alter dendritic morphology in brain regions involved in stress. Discovery that SIRT1, a histone deacetylase (HDAC), has cell-type-specific action in the NAc in a mouse model of depression and resulting behavioral changes suggest possible underlying morphological changes. Neuronal morphology includes measurement of the dendritic arbor and dendritic spines, small protrusions from the dendritic shaft. These studies seek to elucidate morphological changes following knockout or overexpression of SIRT1 in either D1-or D2-MSNs in both male and female mice. Results show that SIRT1 overexpression in male D1-MSNs results in a significant increase in stubby spines and a decrease in mushroom spines. Conversely, in female mice with SIRT1 OVEXP in D1-MSNs, there was found a significant increase in mushroom spines accompanied by a significant decrease in stubby spines. The D2-targeted mice also showed significant changes across spine types. In both

treatment types, D2- males had a significant increase in stubby spines, filopodia, and thin spines. Females with SIRT1 knocked out had a significant decrease in filopodia and thin spines. SIRT1 overexpression in D2- females showed a significant decrease in stubby spines. These results suggest SIRT1 has a regulatory role in the density of spine type and possibly the maturation of spines. This discovery of an increase in stubby spines in male D1-MSNs overexpressing mice establishes a role for SIRT1 in stubby spine formation.

## ACKNOWLEDGMENTS & DEDICATION

First and foremost, I would like to thank my mentor, Deveroux Ferguson. It was a journey, but we made it! I can't even begin to express how grateful I am for you taking me on as a graduate student. I appreciate the way you urged me to really grasp the concepts I was trying to learn, not just a surface knowledge. Your push for me to read and continue to learn has had a very positive affect on me. Also, the time you spent training me on how to- and how not to- conduct various techniques is a time I'll remember fondly. Like that one time we poured water onto LiCl, and the bottle got so hot we thought it might explode. I wish you, your family, and laboratory the best for all future endeavors. I would also like to thank the rest of my committee members. Janet Neiswander, thank you for your though provoking questions. They caused me to slow down and really digest what I was talking about and how to present it. Thank you also for the great support you provided for me when I wasn't sure if or how to keep moving forward. You were always so kind to me. Ron Hammer, when I began volunteering in your lab in 2012 I had absolutely no idea what I was doing. Thank you for taking a chance with me. I am pleased you were on my committee and got to watch me grow into a more knowledgeable and confident scientist. Shenfeng Qiu, thank you for your lively discussions about electrophysiology and all the time you shared helping me learn the procedure. I will always remember your sense of humor and still can't look at avocados without thinking of bloated and dying neurons.

I would like to thank everyone who has played a mentor to me. Firstly, Amanda Maple, without you I truly believe I would not be here. Your patience with me while I was your assistant is commendable. The time you spent showing me how to do

injections, handle animals, run animals was indispensable for me to getting into graduate school. You spoiled me as a mentor, and I have held others to the standard you set. I can only hope I will one day have your way of explaining difficult concepts. Taleen Der-Ghazarian, if I had 1/10<sup>th</sup> of your energy and drive, I could probably take over the world. You juggled so many different things while in school, yet you always made time to help and answer questions. I miss your positive energy and I know you are doing amazing things.

I would also like to thank members of my lab. Dr. Hee-Dae Kim, you are the hardest working, most amazing person I probably know. Your unending patience is enviable. Never did you turn down a request for help from anybody. You were always happy to answer questions, explain a difficult technique, or help me find which box that dang virus is kept in. You deserve the absolute best. I wish nothing but amazing things for you and your sweet family. I hope we will keep in touch over the years. Samantha Carotenuto is tied with Hee-Dae for the nicest person I've ever met. The way you handle every situation with grace is impressive. I am so excited we will be living near each other in CA. I do hope we keep in touch. I would like to thank Alex (AJ) Summers, your help processing dendrites allowed me to work on other experiments and was so greatly appreciated. I know you will do great things, just hang in there. I would also like to thank our undergraduate volunteers, Ross Johnson, and Julia Jackman for spending their precious remaining time helping around the lab. We can't do what we do without your help. I know you will both become wonderful MDs.

Next, I would like to thank my family and friends. Josh, I love you. You've been with me from the very beginning. Thank you for all your support, emotionally,

financially, and scholarly. Your input and discussions have provided different ways of thinking about common concepts and framed them in a new way. I am so excited to move to California to be together again. I'd like to thank my sisters, Brittny, Ashlyn, and Kelsie, and my mother, Cathie Call. The unending and unconditional support you all provided me helped me so much on this journey. I would also like to thank Annika Vannan and Mark Namba, my partners in crime during grad school. Without you two, I really would have struggled through the program. I will always remember the fun-and not so fun- game nights, homemade meals, and the cheesecake- that was a fun one. Finally, thank you for all the conversations of encouragement and support, the help they provided is immeasurable. I cannot wait to continue our friendship long-distance. I am probably forgetting a slew of people, but I extend my thanks and gratitude to everyone I crossed paths with along this journey.

Finally, I have dedicated this work to my cousin Stephen Justensen. I was in my second year of graduate school when he lost his battle with depression. We weren't very close, but he was young and had a beautiful young family. Suffering from depression myself, it was very difficult to learn of. During times I felt stuck and just wanted to give up, I would try to remember my cousin and the deal I made myself to finish my degree because there are those out there who no longer have that opportunity.

Lastly, I would like to thank the animals, without who these studies would not be possible. I would like to thank the Harry Lowell Swift advancing science group for their scholarship. I would also like to extend the deepest gratitude to Daryl and Christine Burton who supported me for two years through the (ARCS). Without your support, I would have had difficulty making ends meet every month. Thank you so very much.

## TABLE OF CONTENTS

	Page
LIST OF TABLES .....	ix
LIST OF FIGURES .....	x
LIST OF SUPPLEMENTARY FIGURES .....	xi
CHAPTER	
1 INTRODUCTION AND OVERVIEW.....	1
Mesocorticolimbic System.....	4
Nucleus Accumbens.....	6
Nucleus Accumbens Core Versus Shell .....	7
Medium Spiny Neurons .....	9
Nucleus Accumbens and Dopamine .....	11
Nucleus Accumbens and Stress .....	12
Dendritic Spines .....	14
Stress and Dendritic Morphology .....	20
Beyond Monoamines .....	22
Sirtuin-1 .....	23
Stress and Females .....	27
2 MATERIALS AND METHODS .....	28
Experimental Designs .....	29
Development of Triple-Transgenic Mouse Models .....	29
DiOlistic Labeling .....	29
Tissue collection .....	30

CHAPTER	Page
Bullets .....	30
Tissue Labeling .....	31
Imaging .....	32
Neuron and Dendritic Reconstruction .....	32
Data Analysis.....	32
3 EXPERIMENTS 1 & 2 .....	33
Introduction .....	33
Experiment 1 .....	33
Results .....	34
Experiment 2 .....	35
Results .....	35
Discussion.....	36
4 EXPERIMENTS 3 & 4 .....	38
Introduction .....	38
Experiment 3 .....	41
Results.....	41
Experiment 4 .....	42
Results .....	42
Discussion.....	44
5 EXPERIMENTS 5 & 6 .....	45
Experiment 5 .....	45
Results .....	45



CHAPTER	Page
Experiment 6 .....	46
Results .....	47
Discussion.....	48
6 EXPERIMENTS 7 & 8 .....	49
Experiment 7 .....	49
Results .....	49
Experiment 8 .....	50
Results .....	50
7 FINAL DISCUSSION .....	51
REFERENCES .....	63
APPENDIX	
A TABLES .....	83
B FIGURES .....	84

## TABLES

Table	Page
1. Comparison of All Groups' Sholl Analysis and Total Dendritic Spine Densities...	83

## LIST OF FIGURES

Figure	Page
1. Dendritic Morphology of Male SIRT1-KO in D1-MSNs.....	85
2. Whole Cell Dendritic Spine Density of Male SIRT1-KO in D1-MSNs .....	86
3. Dendritic Morphology of Male SIRT1-OVEXP in D1-MSNs.....	87
64. Whole Cell Dendritic Spine Density of Male SIRT1-OVEXP in D1-MSNs.....	88
5. Dendritic Morphology of Female SIRT1-KO in D1-MSNs .....	89
6. Whole Cell Dendritic Spine Density of Female SIRT1-OVEXP in D1-MSNs. ....	90
7. Dendritic Morphology of Female SIRT1-OVEXP in D1-MSNs .....	91
8. Whole Cell Dendritic Spine Density of Female SIRT1-OVEXP in D1-MSNs.....	92
9. Dendritic Morphology of Male SIRT1-KO in D2-MSNs.....	93
10. Whole Cell Dendritic Spine Density of Male SIRT1-KO in D2-MSNs .....	94
11. Dendritic Morphology of Male SIRT1-OVEXP in D2-MSNs.....	95
12. Whole Cell Dendritic Spine Density of Male SIRT1-OVEXP in D2-MSNs.....	96
13. Dendritic Morphology of Female SIRT1-KO in D2-MSNs.....	97
14. Whole Cell Dendritic Spine Density of Female SIRT1-KO in D2- MSNs.....	98
15. Dendritic Morphology of Female SIRT1-OVEXP in D2-MSNs .....	99
16. Whole Cell Dendritic Spine Density of Female SIRT1-OVEXP in D2-MSNs.....	100
17. Changes in Dendritic Spine Type by Distance, SIRT1-KO-D1 Male.....	101
18. Changes in Dendritic Spine Type by Distance, SIRT1-OVEXP-D1 Male .....	102
19. Changes in Dendritic Spine Type by Distance, SIRT1-KO-D1 Female .....	103
20. Changes in Dendritic Spine Type by Distance, SIRT1-OVEXP-D1 Female... ..	104
21. Changes in Dendritic Spine Type by Distance, SIRT1-KO-D2 Male.....	105

Figure	Page
22. Changes in Dendritic Spine Type by Distance, SIRT1-OVEXP-D2 Male.....	106
23. Changes in Dendritic Spine Type by Distance, SIRT1-KO-D2 Female .....	107
24. Changes in Dendritic Spine Type by Distance, SIRT1-OVEXP-D2 Female .....	108

## CHAPTER 1

### INTRODUCTION

Major depressive disorder (MDD) affects 350 million people globally and is the leading cause of disability worldwide ([www.who.int](http://www.who.int), 2016); approximately 800,000 deaths occur every year due to this illness ([http://www.who.int/mental\\_health/prevention/genderwomen/en/](http://www.who.int/mental_health/prevention/genderwomen/en/)). In the US, more than 90% of suicides are committed by individuals suffering from a mental illness with suicide from depression accounting for 30-70% of the suicide rate (<http://www.mentalhealthamerica.net/suicide>). The highest rates of depression and suicides occur in men and women between the ages of 15-29 ([http://www.who.int/mental\\_health/prevention/genderwomen/en/](http://www.who.int/mental_health/prevention/genderwomen/en/)). While pharmacology and behavior therapy are treatment options, pharmacological treatments are only helpful for approximately 41% of individuals ([www.nimh.nih.gov](http://www.nimh.nih.gov), 2001). Additionally, studies have found that 82% of the drug response can be duplicated by a placebo. This leaves much to be desired in the treatment options of this disorder. As with most psychiatric illnesses, MDD affects more than just the individual; caretakers, coworkers, and relationships all suffer.

The symptoms of depressive disorders are varied but can be characterized by feelings of hopelessness, irritability, and anhedonia - a loss of pleasure or rewarding effects of a stimulus. Stress, especially chronic recurrent stress, is a leading cause of the development of depressive disorders (Pittenger & Duman, 2008). Research into stress-induced depressive disorders has identified several contributing factors such as type of

stressor and duration of stress, as well as an individual's own susceptibility to stressors (Krishnan et al., 2007). Understanding these changes will aid in the development of novel antidepressants, the development of which has been virtually stagnant for the last 50 years. Most current medications are based on the monoaminergic theory of depression from the 1950s. The monoaminergic theory suggested a deficit of available norepinephrine in the synaptic cleft. Indeed, this theory of depression resulted in the development of a class of anti-depressant drugs termed monoamine-oxidase-inhibitors (MAO-I) (Yanez et al., 2012). However, it was quickly realized these medications had severe side effects and their use was reduced. The next classes of drugs still target monoamines but more selectively. They consist of tricyclic antidepressants (TCAs), selective serotonin re-uptake inhibitors (SSRIs), and selective serotonin noradrenalin re-uptake inhibitors (SNRIs) (<https://www.ncbi.nlm.nih.gov/pubmedhealth/PMH0087089/>). Despite what seems like several options to treat depression, these antidepressants only work in 40-60% of depressed individuals (<https://www.ncbi.nlm.nih.gov/pubmedhealth/PMH0087089/>). This suggests that the number of treatment resistant individuals could be over half of those who seek the treatment (Kirsch, 2014). In the United States, there has been a shift in medical care trending towards individualized medicine. Indeed, the "one size fits all" approach to medicine is especially problematic when attempting to treat depressive disorders. Individuals suffering from depressive disorders vary greatly in their underlying development and expression of depression, and in their response to depression treatments. For this reason, it is extremely important to elucidate the underlying structural cellular and molecular changes that occur in individuals suffering from MDD.

Accordingly, researchers have established many protocols to model stress and stressful situations using animal models, advancing our understanding of the pathophysiology of MDDs (Bittar & Labonte, 2021; Francis et al., 2015; Krishnan et al., 2007; Qiao et al., 2017). From these pre-clinical studies, several underlying circuit, and molecular changes in response to stress have been identified.

Stress, on its own, is not problematic. Indeed, it can be evolutionarily adaptive to experience short bouts of stress. However, when stress is prolonged, unexpected, or presents as a severe acute stressor, the brain's homeostasis can become unbalanced (McEwen et al., 2012). This can result in difficulties with decision making, increased anxiety, and a self-feeding pattern that serves to strengthen the maladaptive circuit (McEwen et al., 2012; Nestler & Carlezon, 2006). Research has shown a strong link between stress-induced alterations in behavior and dysfunction of a brain circuit involved in reward, the mesocorticolimbic pathway (Knowland & Lim, 2018; Russo & Nestler, 2013). The effects of stress can be observed in this pathway as changes in firing properties of dopaminergic (DA) projections from the ventral tegmental area (VTA) to the medial prefrontal cortex (mPFC), the nucleus accumbens (NAc), amygdala (AMY), and hippocampus (HIPP) (Christoffel, Golden, & Russo, 2011; Russo & Nestler, 2013). Prolonged stress also changes firing patterns in efferent projections from the AMY, PFC, and HIPP to the NAc (Bagot et al., 2015; Lim et al., 2012). In turn, the NAc accordingly exhibits changes in its firing pattern (Christoffel, Golden, Dumitriu, et al., 2011). The mesocorticolimbic pathway is also involved in other reward-related diseases such as drug addiction (Ferguson et al., 2013; Ostroumov & Dani, 2018; Walker et al., 2022). The

maladaptive and enduring behavioral changes observed following stress suggest a functional rewiring within these regions. Structural changes to neurons in response to external stimuli involve synaptic plasticity (Knott et al., 2006).

### **Mesocorticolimbic System**

The mesocorticolimbic system is highly implicated in reward-related diseases, including anxiety and depression (Nestler & Carlezon, 2006). This circuitry involves afferent projections of midbrain neurons to targets located throughout the cortex and limbic area. Projections from the VTA consist of both dopaminergic and GABAergic afferents, the latter which synapses on interneurons within the NAc (Bouarab et al., 2019). VTA afferents innervate many brain regions including the PFC, HIPPOCAMPUS, AMYGDALA, and the NAc (Nestler & Carlezon, 2006). Dysfunction of regulation within this brain circuitry has been implicated in several psychiatric diseases including drug addiction, schizophrenia, anxiety, and depressive disorders (Koob & Bloom, 1988; Nestler et al., 2002; Nestler & Carlezon, 2006). Indeed, the dopaminergic input into the NAc from the VTA is one of the most significant pathways for natural rewards such as social interaction, food, and sex, as well as the rewarding experience from drugs (Nestler & Carlezon, 2006). Animal and human studies have identified a change in the firing properties of VTA neurons to their projection sites in response to both drugs of abuse and different types of stress (Douma & de Kloet, 2020; Lammel et al., 2014). Surprisingly, VTA firing increases following an acute or chronic stress event (Berton et al., 2006; Lodge & Grace, 2006). This is predicted to be due to neurons in a tonic firing state within the VTA being phasically activated by a stimulus (Baik, 2020).



Additionally, all the various brain regions comprising the mesocorticolimbic system all undergo physiological changes in response to stress. The PFC has been reported to have decreased activation in depressed humans (Bittar & Labonte, 2021; Radley et al., 2008) and in animal models immediate early gene (IEG) markers were decreased in stress susceptible mice compared to control (Covington et al., 2010). This effect is also seen in depressed humans, using functional imaging studies researchers confirmed this reduction of activity in the PFC (Radley et al., 2008). Similarly, the HIPP shows a decreased firing response. Following a three-week stress model, *in vivo* recordings in mice show a decrease in basal synaptic transmission in the CA3-CA1 HIPP regions (Qiao et al., 2017). These changes could lead to an overall reduction of glutamate, the brain's excitatory neurotransmitter, being sent to the NAc. Additionally, the AMY has been found to increase its firing rate in the basolateral amygdala (BLA), a result also observed in humans with MDD (Drevets et al., 2008; Guo et al., 2021; Heshmati et al., 2020). Likewise, the NAc displays alterations in the physiological properties of its neuronal population, medium spiny neurons (MSNs), following stress. Interesting, but not surprising, the two different cell-types within the NAc have different outcomes following chronic social defeat stress (CSDS). In past studies it was shown there was an increase in the frequency of excitatory transmission (Christoffel et al., 2010; Francis et al., 2018) When these studies were repeated differentiating between D1-MSNs and D2-MSNS, it was found that stress-susceptible mice had decreased excitatory strength in D1-MSN synapses, while D2-MSN showed an increase in the frequency of excitatory transmission (Francis et al., 2015; Lim et al., 2012). These enduring changes strongly suggest the involvement of synaptic plasticity, or long-term potentiation or long-

term depression (LTP or LTD), the ability of the brain to adjust itself to new conditions or experiences.

### **Nucleus Accumbens**

The NAc is a part of the striatum which consists of the dorsal striatum- caudate/putamen (CP)- and the ventral striatum- NAc- (Salgado & Kaplitt, 2015; Shirayama & Chaki, 2006). It is located ventral and medial to the CP and resides in the region of the anterior commissure (AC) (Salgado & Kaplitt, 2015). The NAc receives dense innervations from the midbrain as well as multiple cortical and limbic brain regions. As such, the NAc is described as the central processing hub for mediating reward and reward-motivated behaviors, processing emotional motivation, and the limbic- motor interaction (Salgado & Kaplitt, 2015; Shirayama & Chaki, 2006). Indeed, research into reward processing has been concentrated on this brain region for decades. As a mediator of reward, the NAc is implicated in many neurological and psychiatric diseases such as Parkinson's disease, Alzheimer's disease, bipolar disorder, obsessive-compulsive disorder, and anxiety disorders (Fasano et al., 2013; Salgado & Kaplitt, 2015; Whittaker et al., 2018). Recently, based on an observed lack of reward-seeking activities (ex: socialization) following stress, the NAc has become increasingly investigated to understand its potential role in the development of depressive disorders.

The NAc is a heterogeneous brain region that functions as an integrating relay station for limbic, executive, and motor functions. The NAc receives glutamatergic input from several cortical regions such as the mPFC, HIPPO, and AMY (Salgado & Kaplitt,

2015). Additionally, accumbal MSNs receive dopaminergic modulation from the VTA (Salgado & Kaplitt, 2015). The NAc has long been implicated as the “brain’s reward center”. Indeed, this brain region has been shown to mediate motivational salience and emotional processes through the limbic-motor interface (Nestler & Carlezon, 2006; Salgado & Kaplitt, 2015) as well as incentivized learning (Salgado & Kaplitt, 2015). The NAc consists of several different, often opposing, cell types. The majority of neurons (~95%), in the NAc are MSNs, with cholinergic interneurons accounting for the remaining 5% (Salgado & Kaplitt, 2015). MSNs in the NAc use gamma-aminobutyric acid (GABA) as their primary neurotransmitter (Salgado & Kaplitt, 2015) and they project to cortical and subcortical nuclei (Nestler & Carlezon, 2006). In addition to the different cell types, the NAc can be divided into two sub-regions: the core and the shell (Campioni et al., 2009). Similarly, to the different cell- types, the core and shell receive specific inputs from various brain regions (Nestler & Carlezon, 2006; Salgado & Kaplitt, 2015).

### **Nucleus Accumbens Core Versus Shell**

The primary output neurons of the NAc are MSNs that project to various areas of the basal ganglia and mesencephalon. The NAc can be divided into two regions, the core and the shell, which can be visualized following staining for various proteins and receptors. Proteins such as substance P, calretinin, DA, serotonin, and serotonin receptors are preferentially found in the shell (Salgado & Kaplitt, 2015). While calbindin, enkephalin, and GABA<sub>A</sub> receptors are more common in the core (Salgado & Kaplitt, 2015). Additionally, the binding of GABA, opioid, and dopamine receptor ligands

display core/shell differences (Meredith, 1999). The shell receives glutamatergic inputs from the medial prefrontal cortex (mPFC), and dopaminergic projections from the VTA (Bossert et al., 2011; Bossert et al., 2012; Gerfen et al., 1987; Salgado & Kaplitt, 2015). The core receives input from the anterior cingulate, dorsal prelimbic cortex, and the substantia nigra (Brog et al., 1993; Salgado & Kaplitt, 2015). The shell projects diffusely through the rostral-caudal extent of the hypothalamus and to the extended AMY, and the ventral pallidum (Heimer et al., 1991; Salgado & Kaplitt, 2015). Core efferents innervate neurons within the dorsolateral ventral pallidum which then project to the subthalamic nucleus and substantia nigra (Salgado & Kaplitt, 2015). The projections through the ventral pallidum signal to the mediodorsal nucleus which sends reciprocal projections to the PFC and VTA (Alexander & Crutcher, 1990; Heimer et al., 1991; Salgado & Kaplitt, 2015; Zahm & Heimer, 1990). The shell projects to the hypothalamus, ventral pallidum (VP), and brainstem (Gangarossa et al., 2013; Zahm & Heimer, 1990). The NAc shell receives dense innervation from the AMY (Christoffel, Golden, Dumitriu, et al., 2011; Meredith, 1999). The shell carries more DA receptors while the core has greater utilization of DA and contains more DA transporters (Jones et al., 1996; Salgado & Kaplitt, 2015). Functionally, it is understood that the NAc shell applies motivational valence and novelty to situations and is responsible for the enhancing effects of drugs of abuse (Ito et al., 2004; Shirayama & Chaki, 2006). The NAc shell responds to both rewarding and aversive stimuli (Christoffel, Golden, Dumitriu, et al., 2011; Meredith, 1999) changes in the structure and function of MSNs may strengthen the association between behaviors rather than driving them (Christoffel, Golden, Dumitriu, et al., 2011). The NAc core is believed to mediate generic motivation, goal-directed behavior, and self-

controlled choice, as is required for the normal preference for a large, delayed reward over a small, immediate reward (think marshmallow experiment) (Bassareo et al., 2002; Cardinal & Cheung, 2005; Shirayama & Chaki, 2006). Morphologically, the dendritic arbor of shell MSNs is reported to be more sparsely distributed and have significantly fewer primary dendrites, terminal segments, branches, and less spiny dendrites than the core (Meredith, 1999).

### **Medium Spiny Neurons**

The neuronal population of the NAc is heterogeneous and consists of approximately 95% dopaminergic MSNs, also known as spiny projection neurons, with the remaining 5% comprised of GABAergic and cholinergic interneurons (Meredith, 1999). The ventral striatum also contains three types of cholinergic interneurons: slow-firing and large; fast-spiking PV-expressing GABA-ergic interneurons; burst-firing somatostatin/ NO expressing interneurons (Nicola et al., 2000). The MSN population itself is not homogenous; two main distinct cell types exist based on their receptor expression, those expressing dopamine-1 receptors (D1Rs, or D1) and dopamine-2 receptors (D2Rs or D2). The variance between the two cell populations can be observed through their unique expression profiles, with D1 neurons expressing dynorphin and D2 neurons enkephalin (Meredith, 1999). These receptors belong to the class known as G-coupled receptors, whose stimulation results in the alteration of adenylyl cyclase activity. D1-MSNs belong to the subclass of G-s proteins (excitatory) while D2 neurons consist of G- i/o proteins, which are inhibitory (Nicola et al., 2000).

Recognizing the different cell populations is critical as the two cell types result in opposing actions. D1-MSNs are a part of the direct pathway of the basal ganglia, the brain's motor movement executor, and it projects to the ventral pallidum, globus pallidum internal, the substantia nigra, and the VTA (Francis et al., 2015; Nicola, 2007; Smith et al., 2013). MSNs that project to the VTA exclusively express D1Rs (Gangarossa et al., 2013). Alternatively, D2-MSNs work within the indirect pathway and project to the ventral pallidum (Nicola et al., 2000; Smith et al., 2013). The indirect pathway is involved in the inhibition of motivated movement. These differing neuronal cell types work together to encourage normal behavior output (Francis et al., 2015). The D1- direct pathway of the basal ganglia initiates motivated movement and plays a role in positive reward and reward prediction (Shirayama & Chaki, 2006). Alternatively, the D2- indirect pathway results in inhibition of movement and aversion (Francis et al., 2015). Likewise, the role of these opposing cell types within the NAc differ following the introduction of dopamine after the application of an external stimulus, such as drugs of abuse or chronic stress (Francis et al., 2015). NAc integration of inputs results in emotionally motivated behaviors through activation of the meso-cortico-thalamic loop (Floresco, 2015; Voorn et al., 2004). Recently, due in large part to advances in transgenic mouse models, dissecting the various outcomes resulting from stimulation of the individual cell populations is now possible. Electrophysiological studies utilizing models of stress-induced depression found that excitatory synaptic transmission enhanced LTD in D1-MSNs but not D2-MSNs in the NAc; these cell-type-specific changes are suggested to mediate anhedonia, a key phenotype of MDD (Lim et al., 2012). Additionally, following chronic social defeat stress (CSDS), a validated stress model (Kim et al., 2016; Krishnan et al., 2007), D1-

MSNs show a reduction in mini excitatory synaptic current (mEPSC) frequency with D2-MSNs having enhanced frequency, in susceptible mice (Francis et al., 2015). Moreover, research utilizing fiber photometry calcium imaging discovered that baseline D1- but not D2 -MSN activity can predict which mice will become susceptible or resilient following CSDS (Muir et al., 2018).

### **Nucleus Accumbens and Dopamine**

Dopamine (DA) is produced in two major midbrain nuclei, the substantia nigra and the VTA. The VTA - NAc pathway has been heavily implicated in psychiatric and mood disorders. DA function within the NAc has been established to be involved in motivation, reward, and hedonia (Koob & Bloom, 1988; Shirayama & Chaki, 2006). Dysfunction of dopaminergic action in the NAc results in anhedonia, a foremost symptom of depressive disorders, and withdrawal from drugs of abuse results in anhedonic symptoms (Barr et al., 2002; McEwen et al., 2012; Shirayama & Chaki, 2006; Willner et al., 1992). Additionally, the mesolimbic DA system is reported to be highly susceptible to perturbations following stress (Kalivas & Duffy, 1995; Shirayama & Chaki, 2006; Tidey & Miczek, 1996). Indeed, fluctuating DA release levels within the NAc have been observed following various types of stress, although these changes are dependent on stress type (Kalivas & Duffy, 1995; Shirayama & Chaki, 2006; Tidey & Miczek, 1996). For example, following acute stress an increase of DA is observed in the NAc (Kalivas & Duffy, 1995; Shirayama & Chaki, 2006; Tidey & Miczek, 1996); following long-term unpredictable stress, decreased levels of DA are observed in the NAc shell (Di Chiara et al., 1999; Di Chiara & Tanda, 1997; Scheggi et al., 2002;

Shirayama & Chaki, 2006). Additionally, these opposing DA levels are observed in mice exposed to escapable foot shock or inescapable foot shock with DA levels increasing and decreasing respectively (Cabib & Puglisi-Allegra, 1994; Shirayama & Chaki, 2006). Further, highlighting the importance of differentiating between cell types, studies have shown that compared to D2Rs, D1Rs have a lower binding affinity for DA making it more sensitive to a reduction of synaptic DA levels (Baik, 2020).

### **Nucleus Accumbens and Stress**

Two major symptoms of depression are anhedonia, the loss of pleasure in once pleasurable things, and learned helplessness. These specific behavioral alterations suggest the brain's motivation and reward pathway, the mesolimbic path, contributes to the pathophysiology of depression (Bessa et al., 2013). Studies show that afferent input to the NAc becomes dysregulated following stressful situations, resulting in cellular and molecular alterations believed to mediate depressive related outcomes (Berton et al., 2006; Chaudhury et al., 2013; Christoffel, Golden, Dumitriu, et al., 2011; Covington et al., 2010; Covington et al., 2009; Francis et al., 2015; Krishnan et al., 2007; Parajuli et al., 2016; Vialou et al., 2010). Further, clinical studies from depressed individuals show a role for disrupted activity in the NAc as high-frequency deep brain stimulation (DBS) has antidepressant effects in treatment-resistant individuals (Bewernick et al., 2012; Francis et al., 2015; Nauczyciel et al., 2013; Schlaepfer et al., 2008). Depressive-like behaviors and their corresponding molecular changes have been observed in mice and rats following chronic stress paradigms.



Several stress models exist for pre-clinical research of depressive disorders. Chronic mild unpredictable stress (CMUS) or chronic variable stress (CVS) are common models employed in stress studies. These types of stressors are variable and can last from days (Hodes et al., 2015) to weeks (Lim et al., 2012; Qiao et al., 2017). Daily, or twice daily, stressors are applied to the subjects. This stress model consists of a rotation of various types of stress such as restraint stress, food intake limits, tail suspension, overcrowded cage, and social isolation (Qiao et al., 2017). Another stress model used is the chronic social defeat stress (CSDS) model. This model is a resident intruder paradigm where the test subjects (intruder) undergo 10-day daily interactions for 10 minutes with a larger retired breeder mouse (resident) (Fox, Figueiredo, et al., 2020; Kim et al., 2016; Krishnan et al., 2007). The CSDS model allows for a unique investigation into the role of stress in the expression of depressive-like behaviors such as social interaction, anxiety-like behaviors, and anhedonia (Kim et al., 2016; Krishnan et al., 2007). This is due to the discovery that 40-60% of the animals that undergo social defeat, become susceptible to depressive-like behaviors while the remainder of the stressed group are resilient (Krishnan et al., 2007). These deviations allow researchers to investigate the effects of stress in a more “human-like” model, as not every person who experiences stress develops depression. Additionally, the opposing outcomes that result from this model enables researchers to identify underlying molecular differences. Further, antidepressant treatment reverses the depressive-like behaviors observed (Watanabe et al., 1992).

The ability of antidepressants to reverse stress-induced depressive-like behaviors has been shown repeatedly and with different drugs. These studies show that

antidepressants not only reverse behavioral aspects of stress-susceptibility but also the underlying molecular changes. Following a 6-weeks long CMS model using rats, it was found that imipramine treatment ameliorated stress-induced anhedonia and helpless-like behaviors (Bessa et al., 2013). Another group used the CSDS model with mice and found that 2-weeks treatment with fluoxetine reversed the stress-induced behavioral and molecular alterations (Berton et al., 2006). Additionally, following CSDS with mice, it was found fluoxetine attenuates depressive-like symptoms through mediation of  $\Delta$ fosB (Vialou et al., 2010). Furthermore, it has been reported that levels of brain-derived neurotrophic factor (BDNF) in the NAc are altered in stress-susceptible animals (Berton et al., 2006; Wook Koo et al., 2016). Indeed, elevated BDNF levels in the NAc are associated with susceptibility as there is no change in resilient animals (Krishnan et al., 2007; Wook Koo et al., 2016). The involvement of BDNF suggests physiological changes have occurred in the mesolimbic pathway.

Changes in the firing properties of NAc MSNs following chronic stress have been reported. Following a round of CSDS it was found there was an increase in spine density which correlated with an increase in the frequency of mEPSCs (Christoffel, Golden, Dumitriu, et al., 2011). Further, it was found there is a reduced frequency of excitatory synaptic input onto D1- MSNs and an increase in D2- MSNs in susceptible mice (Francis et al., 2015). Moreover, electrophysiological recordings in NAc slices from chronically stressed mice showed a decrease in D1-MSN AMPA/NMDAR ratio compared to control (Lim et al., 2012). The variations in firing properties suggest changes in the overall morphology of neurons. Specifically, alterations in dendritic arbors and spines have been

reported in conjunction with physiological modifications (Christoffel, Golden, Dumitriu, et al., 2011; Fox, Figueiredo, et al., 2020).

## **Dendritic Spines**

Since first being identified by Ramon y Cajal in the late 1800s, dendritic spines have experienced an increase in interest in elucidating their possible role in various neurological diseases. Dendritic spines appear early in development, often as long dynamic filopodia-like protrusions. However, in later development, as synapses are made, the filopodia number is reduced while the number of stable mature spines increases (Ziv & Smith, 1996). Dendritic spines, or spines, are small (0.5~ 2  $\mu\text{m}$  in length; total volume < 0.01  $\mu\text{m}^3$ - 0.8  $\mu\text{m}^3$ ) (Hering & Sheng, 2001; Sala et al., 2008) protrusions extending from the dendritic shaft of most neurons. Dendritic spines are the site for most of the brain's excitatory synapses allowing communication between neurons (Pettrak et al., 2005; Zuo et al., 2005). It is estimated that approximately 90% of excitatory brain synapses terminate on dendritic spines (Ferguson et al., 2013; Knott et al., 2006; Nimchinsky et al., 2002). Dendritic spines respond to glutamatergic transmission through a series of biochemical events (Alimohamadi et al., 2021).

Dendritic spines' function allows for synaptic plasticity, a physiological and morphological event that occurs in response to external events. Spines are extremely dynamic and motile, representing a high degree of morphological plasticity (Tada & Sheng, 2006). The dynamic nature of dendritic spines has implicated them as underlying the structural changes observed following LTP or LTD (Petralia et al., 1999). This

understanding has led to these sites being investigated for their possible role in neuro-related disorders such as autism spectrum disorder (Varghese et al., 2017), and neurodegeneration, such as Alzheimer's (Dorostkar et al., 2015). While the debate around the characterization and classification of spines continues, there are two recognized groups 1) mature dendritic spines, and 2) immature spines (Zuo et al., 2005). Mature spines include mushroom spines, while stubby and thin are considered immature, due to their plasticity (Runge et al., 2020). Another immature spine type are dendritic filopodium, or filopodia (Runge et al., 2020; Ziv & Smith, 1996).

A dendritic spine is considered mature when they develop a PSD which contains many stabilizing proteins, AMPA receptor (AMPA) insertion, and they receive glutamatergic input (Chidambaram et al., 2019). Mature spines consist of three distinct compartments, the spine head, neck, and a base attached to the dendritic shaft (Tada & Sheng, 2006). Larger spine heads allow for the insertion of more AMPARs (Tada & Sheng, 2006) resulting in stronger connections. The volume of dendritic spines is proportional to the area of the postsynaptic density (PSD), AMPA receptor (AMAPR) content, and pre-synapse size (Harris et al., 1992; Knott et al., 2006; Nusser et al., 1998; Takumi et al., 1999). Spine neck length and diameter influence postsynaptic levels of  $Ca^{2+}$  elevation that are mediated by NMDAR activation (Tada & Sheng, 2006). Acting as calcium compartments, spines can restrict biochemical signaling to a single input (Araya et al., 2006). Indeed, it has been established that the spine neck filters membrane potentials and spines are able to isolate inputs electrically (Araya et al., 2006). Spines with long necks can be essentially silent at the soma because of kinetic decay (Hering &

Sheng, 2001; Korkotian & Segal, 2011; Volfovsky et al., 1999). To further establish the effect of the spine neck on synaptic communication, Araya et al., 2006, reported that a strong negative correlation was observed in spines and spines with longer necks having more modulatory properties (Araya et al., 2006).

Understanding the development of dendritic spines has become paramount in the exploration of many neurological disorders such as Parkinson's, Alzheimer's, epilepsy, autism spectrum disorder, and in response to stress and depression (Lai et al., 2016). During post-natal development humans, and animals, experience an event known as synaptogenesis (Hering & Sheng, 2001; Petrak et al., 2005). During this time, early spines present as long, thin, hair-like protrusions called filopodium (Sala et al., 2008).

Dendritic filopodia are thin hair-like structures ( $> 0.2 \mu\text{m}$ ) with no discernable head. Filopodia constitute the most motile, dynamic, and immature state of all dendritic protrusions. In the developing brain, the dendritic arbor consists of long, motile protrusions which sample the extracellular space to instigate axo-dendritic synapses (Sala et al., 2008). These protoplasmic protrusions continuously extend and retract into the dendritic shaft (Nimchinsky et al., 2002). Consequently, due to their unstable behavior, they are often excluded from counts of spine densities and left uncategorized (Fasano et al., 2013). However, this could be problematic when considering recent studies reporting that filopodia may be contributing to silent synapses, which allow for mediation of signals from spines to the soma (Berton et al., 2006; Petralia et al., 1999). Indeed, it has been reported that low concentrations of transmitters could reach these receptors resulting from neurotransmitter spillover from a nearby synapse (Kullmann & Asztely, 1998;

Petralia et al., 1999). While the role of filopodia in post-natal development is well characterized (Hering & Sheng, 2001), the presence of these structures later in life, and in many neurological diseases, is unestablished. Dendritic filopodia have been observed to contain numerous NMDA receptors, suggesting they can affect the outcome of an incoming signal or initiate the transformation into a spine through LTP (Mattison et al., 2014; Ziv & Smith, 1996). It is understood that low-level activation of NMDARs results in LTD (Lim et al., 2012). There are three main schools of thought for the function of filopodia on mature dendrites: 1) filopodia are the precursors to more mature spines, they extend sampling the extracellular space and if contact is made with an axon, they form a connection, called a synapse, retract back towards the dendrite and develop into spines; 2) they arise from dendritic shaft synapses where the synapse is instigated by axonal filopodia, when the axonal filopodia retract a spine is “drawn” out of the dendritic shaft (Bourne & Harris, 2007; Ethell & Pasquale, 2005; Fiala et al., 1998). Filopodia continue to be present throughout the lifespan to provide malleability in cases of enhanced or continued spine turnover during occasions of high plasticity (Ethell & Pasquale, 2005; Lendvai et al., 2000).

Stubby spines predominate the dendritic shaft around post-natal day 15 and are believed to represent an immature spine type, as they are less prominent in adulthood (Helm et al., 2021; Petrak et al., 2005). Morphologically, these spines are as tall as they are wide and have no discernable neck (Berton et al., 2006). This lack of a neck is believed to make stubby spines less efficient in processing and adapting to external stimuli in an adult brain (Helm et al., 2021). This could be due to the lack of local

organelles and proteins, rendering them less fit for function. Indeed, it was recently found that the proteome of stubby spines is less well-associated with synaptic strength; a lack of trafficking proteins suggests stubby spines have a slower response to changes in synaptic transmission (Helm et al., 2021). This spine type has strong calcium signaling coupling with the dendritic shaft but also regulates spino-dendritic crosstalk (Christoffel, Golden, Dumitriu, et al., 2011; Schmidt & Eilers, 2009). It is believed that stubby spines, lacking the organelles readily available to mushroom spines, would not be as efficient at responding to experienced-based plasticity (Helm et al., 2021).

Thin spines mimic the morphology of mushroom spines on a smaller, more motile scale. Thin spines have neck lengths that are much longer than the diameter of their heads (Knott et al., 2006). Often referred to as “learning spines” (Bourne & Harris, 2007) thin spines are believed to be the precursor to mushroom spines following induction of LTP (Bourne & Harris, 2007).

Mushroom spines are recognized as the most stable spine type, lasting months or even years (Bourne & Harris, 2007; Ferguson et al., 2013). These mature spines could function as a mechanism to store and transmit information derived from learning experiences (Bello-Medina et al., 2016). Morphologically, mushroom spines consist of a bulbous head formed by PSD proteins, smooth endoplasmic reticulum (SER), a spine apparatus, polyribosomes, and endosomal components (Chidambaram et al., 2019; Ferguson et al., 2013); a narrow neck composed of various actin-binding proteins (ABPs), which can prevent  $\text{Ca}^{2+}$  exchange between spine head and dendritic shaft (Ferguson et al., 2013; Tada & Sheng, 2006; van der Kooij et al., 2016), and the spine

base which has recently been shown to possess its own unique molecular profile (Schatzle et al., 2018). The presence of a spine neck can impact synaptic function as it allows for compartmentalization in the receptor filled head (Helm et al., 2021). The head of mushroom spines has large, complex PSDs expressing a level of glutamate receptors positively correlated to PSD size (Maiti et al., 2015; Sala et al., 2008). Found at the head of spines, the PSD is an electron-dense membrane sitting opposite of the presynaptic bouton (Runge et al., 2020; Sala et al., 2008). The PSD is a complex structure composed of hundreds of proteins including scaffolding proteins, signaling proteins, trafficking proteins, and glutamatergic receptors (Helm et al., 2021; Sala et al., 2008). Stimulation of excitable synapses results in an enlargement of the spine head and an accumulation of AMPARs at the postsynaptic surface, indicators that suggest LTP has occurred (Park, 2018; Sala et al., 2008). These changes are dependent on the activation of either AMPA or NMDARs as it has been shown that activation of these receptors results in an inhibition of spine actin dynamics resulting in rounder, regular shaped spines (Halpain et al., 1998; Hering & Sheng, 2001; Sala et al., 2008). The process of spine enlargement requires the synthesis of new proteins (Lai et al., 2016). The recruitment of many mRNA-binding proteins enables local protein synthesis that contributes to enhanced synaptic strength in a manner that is synapse-specific (Lai et al., 2016). The presence of these organelles and proteins correlates more strongly with synaptic strength and allows for rapid response to frequent changes in synaptic demand (Helm et al., 2021).

### **Stress and Dendritic Morphology**



Dendritic arbor extension or atrophy has been noted in several brain regions following stress (Guo et al., 2021; Lei et al., 2020). Dendrites allow space for the development of specialized compartments that receive incoming signals from other neurons, dendritic spines. The addition of these spines enhances the overall surface area of a neuron. Stress induced effects on the structure of the arbor such as reduced total dendritic length, reduced or increased number of dendritic branch points, or an overall reduction of average branch length would alter the ability to respond to incoming transmissions (Abe-Higuchi et al., 2016; Fox, Figueiredo, et al., 2020). In the prefrontal cortex a sexual dimorphism is seen between male and female animals. In males stress reduced the dendritic branching and total length of pyramidal neurons, but an increase was seen in females (Leuner & Shors, 2013). Cohen et al., following a predator scent stress model looked at dentate gyrus granule neurons and found the total dendritic length and total dendrite number were significantly reduced in stressed animals (Cohen et al., 2014). In the Sholl analysis- a measurement of dendritic complexity- the number of intersections was reduced (Cohen et al., 2014).

Alterations in spine density- the number of spines per a length of dendrite- have been observed in animals following stress. These changes occur in brain regions such as the mPFC, BLA, HIPPO, NAc. As stated previously, different types of stress can elicit different, even opposing results. These differences are often due to acute versus chronic stress models. In addition to these opposing outcomes, stress effects in different brain regions do not produce the same alterations, each region seems to have its own unique response to stress. In the PFC it has been observed that stressed males lead to a decrease

in spine density (Leuner & Shors, 2013; Radley et al., 2008). Indeed Radley et al., found an 11% decrease in spine density in basal and apical dendrites in the dorsal mPFC layers II/III (Radley et al., 2008). Similarly, in the HIPP of stressed animals, dentate granule cells had significantly reduced spine density on a 10  $\mu\text{m}$  dendritic segment, compared to non-stressed controls (Cohen et al., 2014). Additionally, Iniguez et al., using a social defeat stress model found a decrease in the number of stubby spines and an increase in thin spine types in stressed animals (Iniguez et al., 2016). Further, following a bout of intense stress, a reduced spine density on CA3 neurons was seen, compared to control (Leuner & Shors, 2013). Conversely, in an acute animal stress of a brief restraint and tail shocks found an increased spine density in the CA1 region of HIPP (Leuner & Shors, 2013). In the AMY, a brain region associated with fear and anxiety undergoes morphological alterations following stress. Specifically, in the basolateral amygdala (BLA), a significant increase in the number of spines on pyramidal neurons was reported in stressed animals (Guo et al., 2021). This contrasts with what we've seen in the PFC and HIPP which both display atrophied dendritic arbors (Leuner & Shors, 2013).

### **Beyond Monoamines**

The treatment of MDDs began serendipitously in the 1950s. In 1953 Dr. Fox and Dr. Gibas synthesized iproniazid to treat patients with tuberculosis. A doctor prescribing this medication for tuberculosis noticed a lifting of spirits and mood in his patients including euphoria, increased appetite, and improved sleep (Hillhouse & Porter, 2015). This discovery opened the door for exploration into treatments and the development of the first class of antidepressants, monoamines. The 'monoamine' hypothesis posits that a

decrease in monoamine function or availability could underlie depressive symptoms (Krishnan & Nestler, 2008). They work by inhibiting reuptake or degradation of monoamines, resulting in an increased amount of time spent in synaptic cleft (Krishnan & Nestler, 2008). While these medications did help for some, it is estimated that up to two-thirds of patients do not respond and it can take weeks to notice the effects (Kirsch, I., 2014). The former statement briefly highlights the urgency that is needed to address this crisis.

Traditionally, the mesolimbic dopamine circuit has been researched in drugs of abuse. However, within the last three decades, researchers have been investigating this circuit to understand its role in MDD. As mentioned, monoamines are the primary target of most current antidepressant pharmacological treatments (Krishnan & Nestler, 2008). These include serotonin, glutamate, epinephrine, norepinephrine, and dopamine. Dopamine plays a pivotal role in various cognitive, neuroendocrine, motor, and motivational functions (Carlsson, 2001; Greengard, 2001; Yao et al., 2008). It is a regulator of reward and reward-processing. Indeed, aberrant levels of DA have been observed in the NAc following a variety of stressors (Quessy et al., 2021; Wook Koo et al., 2016). In addition to possible changes in neurotransmitters, there have been reports of increased brain-derived-neurotrophic-factor (BDNF) in the NAc of stress susceptible mice (Berton et al., 2006; Krishnan & Nestler, 2008), and knocking out BDNF selectively in VTA to NAc projections results in a pro-resilient phenotype (Berton et al., 2006). While neurotransmission remains an active research avenue, other maladaptations in processes such as those involving protein function and availability are being

researched. An area of study is investigating the role of epigenetics, modifications to histones that are permissive or restrictive to DNA transcription, in the progression of MDD. One form of epigenetic modification is histone deacetylation which results in the tightening of chromatin around histones while acetylation is related to transcriptional activation (Krishnan & Nestler, 2008). One such histone deacetylase (HDAC) is sirtuin-1 or SIRT1.

### **Sirtuin-1**

The *silent regulator of transcription* or sirtuin-1 (SIRT1) is a molecule downstream from DA activation sites (Guarente, 2000; Libert et al., 2011). SIRT1 is the human homolog of yeast sir-2, which was found to extend the budding life of yeast (Guarente, 2000). SIRT1 is a class III histone deacetylase (HDAC), which regulates the acetylation of histones and non-histone proteins and relies on nicotinamide-adenine dinucleotide (NAD<sup>+</sup>) to catalyze a deacetylate reaction (Gao et al., 2010; Guarente, 2000; Libert et al., 2011; McBurney et al., 2013). There are seven individual sirtuins, SIRT1-7, each with distinct cellular locations and participating in a range of physiological processes including, cellular differentiation, inflammation, mitochondrial biogenesis, metabolism, aging, cell death, axonal elongation, apoptosis, development, circadian rhythms (D'Angelo et al., 2021; McBurney et al., 2013). SIRT1 specifically is expressed in tissue throughout the body and is nuclear but can become cytoplasmic in response to physiological stimuli (D'Angelo et al., 2021). SIRT1's regulation of epigenetic and non-epigenetic targets modulates the activity of target proteins through removal of functional acetyl groups (D'Angelo et al., 2021). SIRT1 has been found to be involved in endocrine

regulation, insulin secretion, fatty acid oxidation, and lipogenesis (Haigis & Sinclair, 2010). Recently, it has been discovered that SIRT1 plays an important role in higher-order brain function. SIRT1 has a role in synaptic plasticity from learning and memory (Libert et al., 2011), has been shown to alter dendritic and spine morphology (Abe-Higuchi et al., 2016; Codocedo et al., 2012; Guo et al., 2021), and SIRT1 dysfunction in neuropsychiatric disease states such as addiction and depression have been reported (D'Angelo et al., 2021; Ferguson et al., 2013). Additionally, manipulation of SIRT1 activity has been shown to alter cellular migration (Zhang et al., 2009), nerve growth factor-induced neuritogenesis, and outgrowth of axons and dendrites (D'Angelo et al., 2021). Indeed, SIRT1 in hippocampal CA1 pyramidal neurons enhances dendritic arbor complexity (Codocedo et al., 2012; D'Angelo et al., 2021; Ng et al., 2015). Conversely, when the HIPP is deficient of SIRT1 there is a reduced level of neurotrophins that mediate synaptic function, such as BDNF in mice (Codocedo et al., 2012; D'Angelo et al., 2021; Ng et al., 2015; Zocchi & Sassone-Corsi, 2012). The relationship of SIRT1 and BDNF may result from SIRT1-mediated deacetylation of MeCP2. In SIRT1- KO mice there was an increased recruitment of MeCP2 to the BDNF exon 4 promoter resulting in a decrease of both protein and mRNA levels (Zocchi & Sassone-Corsi, 2012).

In 2015, the CONVERGE (China, Oxford, and Virginia Commonwealth University Experimental Research on Genetic Epidemiology) Consortium collected data from just under 12,000 Han Chinese women who suffer from depression (CONVERGE Consortium, 2015). Following a genome-wide association study (GWAS) they reported two loci contributing to the risk of developing MDD on chromosome 10, one of which is

close to the *Sirt1* gene (Consortium, 2015). Another study from Japan showed that one short nucleotide polymorphism [SNP (rs 10997875)] in the *Sirt1* gene may play a role in the pathophysiology of MDD (Kishi et al., 2010). Moreover, in patients with MDD, peripheral blood draws show a downregulation of SIRT1 as compared to control groups (Luo & Zhang, 2016). From these human studies, it is apparent that SIRT1 may play a role in the pathophysiology of MDD. This highlights the importance and relevance of revealing a more complete understanding of SIRT1.

Research utilizing animal models of depression have also looked at SIRT1 dysfunction as a modulator of stress-related synaptic changes and the development of depressive-like behaviors. A study using a chronic-ultra mild stress (CUMS) protocol, expression levels of SIRT1 were measured in the HIPPO, AMY, and mPFC, brain regions implicated in MDD (Abe-Higuchi et al., 2016). Following the CUMS protocol, levels of SIRT1 mRNA expression were significantly reduced in the HIPPO (Abe-Higuchi et al., 2016). Conversely, they observed increased SIRT1 mRNA in the AMY, and no significant changes in the mPFC (Abe-Higuchi et al., 2016). In another study, also using the CUMS protocol, SIRT1 expression levels in the BLA following stress were measured (Guo et al., 2021). In mice susceptible to the stressors, it was found there was a significant increase of SIRT1, and this increase was accompanied by depressive-like behaviors, such as anhedonia, hopelessness, and despair (Guo et al., 2021). Additionally, it has been shown that selective deletion of SIRT1 in forebrain excitatory neurons results in a depression-like phenotype in male, but not female mice (Lei et al., 2020).

Research from our laboratory has discovered behavioral changes that occur resulting from social, viral, pharmacological, and genetic manipulation of SIRT1 in the NAc (Kim et al., 2016). Following a round of chronic social defeat (CSDS) we found a significant increase of SIRT1 protein and mRNA in mice susceptible to the stressors (Kim et al., 2016). These changes occur within days and are sustained for up to 10 days following cessation of the stressor. This change in expression levels was accompanied by an increase in anti-social behavior as measured by the social interaction test. Further, we showed that we could alter these behavioral outcomes through overexpression (OVEXP) or knock-out (KO) of SIRT1, resulting in increased or decreased anxiety-like behaviors, respectively. In an additional study, we looked at the cell-type specific action of SIRT1 in mice. We virally OVEXP SIRT1 in D1- or D2- MSNs. OVEXP SIRT1 in D1- MSNs resulted in an increase of depressive-like behaviors such as learned helplessness, anhedonia, and anxiety-like behaviors. No changes were seen when SIRT1 is OVEXP in D2-MSNs. These rapid, sustained changes suggest a morphological and neurophysiological role for the SIRT1. However, any SIRT1 driven changes have yet to be quantified within the NAc, specifically in a cell-type-specific manner.

From these studies investigating SIRT1 expression in multiple brain regions, we suspect that these changes in SIRT1 play a role in the behavioral differences we see in stress-susceptible mice and rats. These resulting behavioral changes suggest an underlying change within the morphological and electrophysiological properties of neurons. While changes in morphology and firing rates have been reported following stress, the nature of SIRT1 in these changes has not been established in the NAc.

## **Stress And Females**

Women experience depression at rates almost double that of men and current research suggests that depression may be the most common mental health problem for women (www.who.int, 2016). Globally, the prevalence of depression in females in 2010 was 5.5%, with the prevalence of men closer to 3.2%. This represents a 1.7- fold greater incidence in women. The sexual dimorphism in the prevalence of depression in males and females is stark. Women and men respond to stressors differently and therefore their stress vulnerability- the expression of the disease- is markedly different. While men tend to externalize their symptoms (bouts of anger, physical aggression) women more commonly internalize (guilt and shame) their symptoms. Depressive disorders are responsible for approximately 41.9% of disabilities from neuropsychiatric disorders in women (www.who.int, 2016), yet almost all clinical and preclinical research focuses on males.

Despite the limited research utilizing female animal models, the neurophysiological changes that occur in females following the use of pre-clinical stress models have not been investigated. A quantitative analysis of NAc MSNs in male and female stress naïve Sprague-Dawley rats shows that females have a baseline 22% increase in spine head size and number on distal portions of second- and third- degree dendrites, with no difference in dendritic branching or length (Hodes et al., 2015). This finding is extremely important as stress has been found to alter dendritic branching and spine number and size in the NAc; having a higher baseline prevalence of dendritic spines may account for the increase of incidence of depression in females in response to



stressors. However, the cell-type specificity of these differences was not investigated. Wissman et al., 2011 performed a second set of studies looking at spines on the whole dendrite (vs distal only) as well as regional specificity. They found females have a greater density of spine synapses than males specifically in the caudal region of the NAc core (Wissman et al., 2012). This is intriguing as the regional location of these differences may result from different cell types that populate these regions. Furthermore, unpublished data from our laboratory utilizing male and female mice in a chronic unpredictable stress model showed females display stress susceptibility to this stress paradigm, but not males. Interestingly, female mice display changes in SIRT1, however, SIRT1 is decreased in female mice with this stress model. This is thought-provoking because our data discussed above, in males, shows that SIRT1 is increased following chronic social defeat stress. These dichotomous findings highlight the importance of including both sexes, as well as differentiating between the cell types, in future research into depressive disorders.

## CHAPTER 2

### MATERIALS AND METHODS

#### **Experimental Design**

To determine the cell-type-specific effects of SIRT1 we conducted DiOlistic labeling on transgenic mouse models expressing a Cre activated Ai6- expressing, SIRT knock-out or OVEXP, in D1- or D2- *Cre* MSNs.

#### **Development of Transgenic Mouse Models**

Male and female C57BL/6J mice (7–9 weeks old) were obtained from The Jackson Laboratory. They were housed max 5 to a cage in a climate-controlled facility with a normal 12 / 12-hour light- dark cycle (lights on at 7:00 AM) with *ad libitum* access to food and water. To develop the transgenic mouse model, mice were bred at the University of Arizona Principal Animal Facility (Phoenix, AZ), offspring were tagged and genotyped at 2 weeks, and weaned at 3 weeks. D1-Cre hemizygote (line FK150) or D2-Cre hemizygote (line ER44) BAC transgenic mice from GENSAT (Gerfen et al., 2013; Gong et al., 2007) on a C57BL/6J background were used for the morphological experiments. To induce deletion of the Sirt1 transcript in the NAc, we used mutant mice homozygous for a floxed Sirt1 allele, which are fully backcrossed onto C57BL/6J and have been described in detail previously (Li et al., 2013). To label D1- and D2- neurons for morphological analysis and electrophysiological recordings, Ai6 mice were crossed with D1-/ D2- Cre mice (Ai6; D1-/ D2- Cre). Ai6; D1-/ D2- Cre mice were then bred with Sirt1 floxed or Sirt1 OVEXP D1-/ D2- Cre mice resulting in our triple transgenic cell-type specific, KO or OVEXP SIRT1. For all morphological studies, mice between the ages of 8 and 12 weeks were used. All animal procedures were approved by the University of Arizona Medical School Institutional Animal Care and Use Committees.

### **DiOListic Labeling**

Visualizing neuronal microarchitecture in a cell-type specific manner requires the use of fluorescent dyes. These studies utilized the use of 1, 1'-dioctadecyl-3, 3', 3'-tetramethylindocarbocyanine (DiI), a lipophilic dye which, when incorporated within the neuronal membrane, diffuses laterally across the cell illuminating the microarchitecture.

This is accomplished by coating tungsten particles with the lipophilic DiI, applying those particles to the inside of Tefzel tubing to create “bullets”, then loading the bullets into a gene gun which uses high pressured Helium to discharge the tungsten particles into the desired tissue (Gipson & Olive, 2017). Use in concert with our cell-type specific Ai6+ mice, we are able to identify neurons for analysis.

### **Tissue Collection**

Mice aged 8-12 weeks were anesthetized with an intraperitoneal (ip) injection of Euthazol (0.1 mL/kg, Virbac) and transcardially perfused sequentially with 1X PB followed by perfusion with ice-cold 1.5 % paraformaldehyde (PFA). Following perfusion, brains were removed and post-fixed for 1 hour in 1.5% PFA. Brains were processed immediately or stored in 30% sucrose. Brains were then sectioned into 300 $\mu$ m coronal brain slices using a Leica V1200S vibratome. Slices are then transferred into individual 3 mL wells filled with 1X PBS.

### **Bullets**

Coating of particles with lipophilic dye, DiI, is done as described (Staffend & Meisel, 2011). Briefly, 2 mg of carbocyanine fluorescent dye, DiI, will be dissolved in 75  $\mu$ L methylene chloride and applied to 90  $\mu$ g of 1.3  $\mu$ m tungsten particles and spread evenly on a glass slide. Following drying, particles will be scraped from the slide onto a secondary slide and chopped finely with a razor. The DiI coated particles are then collected into a 15 mL conical tube and suspended in 10 mL deionized water. Suspension will be sonicated for 10 minutes with intermittent vortexing. Tefzel tubing will be pre-

coated with 10 mg/mL PVP for 5 minutes and dried under 0.4 liters per minute (LPM) nitrogen gas flow. The DiI suspension is quickly drawn into the Tefzel tubing and allowed to settle for 30 minutes with intermittent turning for even coating of tubing. The DiI solution is withdrawn slowly from the tubing so as not to disturb the tungsten. The Tefzel tubing is slowly rotated 360° and dried for 20 min under 0.4 LPM nitrogen gas flow. After drying, the tubing is cut into 1.3 mm segments (bullets) and stored desiccated in the dark at room temperature until use.

### **Tissue Labeling**

Particles are delivered via a Helios Gene Gun (Bio-Rad) with a modified barrel (O'Brien & Lummis, 2006). PBS is aspirated from well; gene gun is positioned above tissue sample and DiI delivered with a 100-120 PSI helium burst. Clean PBS is returned to the well. DiI is allowed to diffuse into tissue for 24 hours in the dark at room temperature. Following incubation, PBS is removed from wells and slices are washed twice in 1X PBS then post-fixed in 4% PFA for 1 hour, at room temperature. Slices are then washed again in PBS 2 times, mounted on a glass slide, cover slipped, and allowed to dry overnight.

### **Imaging**

Z-stack images were collected using a confocal LSM 710 (Carl Zeiss, 20X objective, NA1.4, and 0.6 Z step for whole-cell; 63X objective, NA1.4, 0.2mm Z step for dendritic segments). Whole cells that are identified as co-labeled are imaged at 20X.

Dendritic segments were imaged at radial distances of 25, 50, and 75  $\mu\text{m}$  from the soma and imaged under oil at 63X.

### **Neuron and dendritic reconstruction**

Dendritic reconstruction, Sholl analysis, and spine analysis were done using ImageJ [plugin: simple neurite tracer (SNT)]. For dendritic arbor reconstruction, neurons co-labeled with DiI are traced using ImageJ SNT. In conjunction with the Sholl analysis, we will measure the total dendritic length, average branch length, total branch points, and total number of dendritic tips in D1- or D2- MSNs with SIRT1- KO or OVEXP. For spine analysis in all experiments, we will select dendritic segments 25-50, 50-75, 75+  $\mu\text{m}$  away from the soma of Ai6+ DiI labeled cells. Spines will be further classified as stubby, filopodia, thin, or mushroom. We will reconstruct 1-4 neurons per mouse, 3-4 dendrites from each region (25-50  $\mu\text{m}$ ; 50-75  $\mu\text{m}$ ; 75+  $\mu\text{m}$ ), using 1-4 mice per group.

### **Data Analysis**

Sholl analysis comparisons were analyzed via two-way repeated measures ANOVA. The fixed factors were treatment group and distance from soma with number of intersections dependent. Unpaired two-way t-tests were performed for analysis of total spine length, average branch length, total branch points, and total number of dendritic tips. All dendritic spine density analyses were also performed using the above t-test. Post-Hoc Tukey's, Bonferroni tests were conducted to identify significant group differences. All tests were run at  $p=0.05$  significance using GraphPad Prism version 9.0 and SPSS. All data is represented as  $\pm\text{SEM}$ .

## CHAPTER 3

### EXPERIMENTS 1 - 2

#### **Introduction**

Changes in neuronal morphology following manipulations of SIRT1 have yet to be defined in the nucleus accumbens (NAc). While research has reported changes in neuronal structure following SIRT1 manipulation in brain regions such as the HIPPO (Abe-Higuchi et al., 2016), PFC, and AMY these changes have yet to be quantified in the NAc. Importantly, the *cell-type specificity* of these changes has not been elucidated. To address this gap in the literature, I propose to investigate changes in dendritic branching and spine structure following knockout or overexpression of SIRT1 in D1- expressing neurons in the NAc.

#### **Experiment 1**

*Characterization of D1 male SIRT-1 neurons in which SIRT1 has been knocked out.* Mice were bred, genotyped, and raised until 8- 12 weeks old. Once the appropriate age was reached, mice received a lethal dose of Euthasol (0.1 mL/kg, Virbac) and were perfused with 1X PB (20 mL) followed by perfusion with 1.5% paraformaldehyde (PFA). Following this, the brain is removed and post-fixed in 1.5% PFA for another hour. Brains are then transferred to 30% sucrose until processed.

#### **Results**

Previous studies have shown changes in dendritic complexity following manipulation of SIRT1. To establish a role for SIRT1 in dendritic complexity we used transgenic male mice with SIRT1 KO out in D1-MSNs. Following DiI staining it was revealed that SIRT1-KO in D1-MSNs did not result in a significant change in dendritic complexity compared to controls ( $p=0.897$ ; Fig. 1 B). Total path length ( $t(6)=1.379$ ,  $p=0.217$ ), average branch length ( $t(6)=0.86$ ,  $p=0.419$ ), total number of branch points ( $t(6)=1.31$ ,  $p=0.236$ ), and total number of dendritic tips ( $t(6)=1.24$ ,  $p=0.259$ ) did not change significantly between groups (Fig. 1 C-F).

DiOlistic labeling and microscopy revealed no significant alterations in dendritic spine density or spine type in SIRT1- D1- KO mice. Dendritic segments of DiI stained neurons were imaged at 63X, 25  $\mu\text{m}$  in length and dendrites counted and classified. The dendritic segments, imaged at radial distances of 25, 50, and 75  $\mu\text{m}$ , were reconstructed with ImageJ SNT and dendritic spines classified into four categories: stubby, filopodia, thin, or mushroom. An unpaired t-test showed the overall dendritic spine density of SIRT1-D1- KO mice was not significantly changed ( $t(106)=1.088$ ,  $p=0.27$ ; Fig. 2 A). When the four total spine subpopulations and three dendritic regions are looked at individually, we find no significant changes in either spine-type (Stubby spines,  $t(25)=0.84$ ,  $p=0.406$ ; filopodia  $t(25)=0.43$ ,  $p=0.664$ ; thin spines,  $t(25)=1.04$ ,  $p=0.304$ ; mushroom spines,  $t(25)=1.53$ ,  $p=0.138$ ; (Fig. 2 B-E). There were no significant changes in any other region or spine type (25-50  $\mu\text{m}$ , stubby spines  $t(7)=0.42$ ,  $p=0.680$ ; filopodia,  $t(7)=0.83$ ,  $p=0.431$ ; thin spines,  $t(7)=0.55$ ,  $p=0.599$ ; mushroom spines,  $t(7)=1.33$ ,  $p=0.223$ ; 50-75  $\mu\text{m}$ , stubby spines,  $t(7)=0.02$ ,  $p=0.978$ ; filopodia,  $t(7)=0.22$ ,  $p=0.828$ ;

thin spines,  $t(7)=0.40$ ,  $p=0.696$ ; mushroom spines,  $t(7)=0.32$ ,  $p=0.754$ ;  $75+ \mu\text{m}$ , stubby spines,  $t(7)=0.75$ ,  $p=0.477$ ; filopodia,  $t(7)=0.10$ ,  $p=0.918$ ; thin spines,  $t(7)=0.70$ ,  $p=0.500$ ; mushroom spines,  $t(7)=1.08$ ,  $p=0.313$ ; Fig. SUPP 1 A-C) along the dendritic branch.

## **Experiment 2**

*Characterization of D1 male SIRT-1 neurons in which SIRT1 has been OVEXP.* Mice were bred, genotyped, and raised until 8- 12 weeks old. Once the appropriate age was reached, mice received a lethal dose of Euthasol (0.1 mL/kg, Virbac) and were perfused with 1X PB (20 mL) followed by perfusion with paraformaldehyde (PFA). Following this, the brain is removed and post-fixed in 4% PFA for another hour. Brains were then transferred to 30% sucrose until processed.

## **Results**

Following transgenic cell-type specific overexpression of SIRT1 in D1- MSNs of male mice we found, compared to control, SIRT1- OVEXP- D1 mice had no significant change in Sholl intersections ( $p=1.0$ ; Fig. 3 A), however, there appears to be a trending reduction in intersections between 80-110  $\mu\text{m}$  from the soma. There were no significant changes observed between control and OVEXP-D1 mice in measurements of total path length ( $t(5)=0.10$ ,  $p=0.918$ ; Fig. 3 B), average branch length ( $t(5)=0.29$ ,  $p=0.783$ ; Fig. 3 C), average branch points ( $t(5)=1.35$ ,  $p=0.234$ ; Fig. 3 D), or tip ends ( $t(5)=0.01$ ,  $p=0.985$ ; Fig. 3 E).



We next used DiI labeled neurons for analysis of dendritic spine density and spine-types. An unpaired t-test showed SIRT1- D1- OVEXP mice had no significant change in total spine density ( $t(94)=1.34$ ,  $p=0.180$ ; Fig. 4 A). However, specific spine types did show significant changes. Total spine density was significantly increased in stubby spines ( $t(22)=2.57$ ,  $p=0.017$ ; Fig. 4 B) and significantly decreased in mushroom spines ( $t(22)=5.06$ ,  $p<0.0001$ ; Fig. 4 E). There were no significant differences in filopodia or thin spine types (Filopodia,  $t(22)=1.06$ ,  $p=0.297$ ; thin,  $t(22)=1.57$ ,  $p=0.130$ ; Fig. 4 C-D) compared to control. At radial distances of 25  $\mu\text{m}$  and 50  $\mu\text{m}$  there was a significant decrease of mushroom spines (25-50  $\mu\text{m}$ , mushroom,  $t(7)=3.38$ ,  $p=0.011$ ; 50-75  $\mu\text{m}$ , mushroom  $t(6)=2.80$ ,  $p=0.030$ ; Fig. SUPP 2 A & C) with no significant changes in any other spine type or region (25-50  $\mu\text{m}$ , stubby spines,  $t(7)=1.98$ ,  $p=0.087$ ; filopodia,  $t(7)=1.009$ ,  $p=0.346$ ; thin spines,  $t(7)=0.78$ ,  $p=0.460$ ; Fig. SUPP 2 A; 50-75  $\mu\text{m}$ , stubby spines,  $t(6)=1.35$ ,  $p=0.224$ ; filopodia,  $t(6)=0.07$ ,  $p=0.941$ ; thin spines,  $t(6)=0.75$ ,  $p=0.479$ ; 75+  $\mu\text{m}$ , stubby spines,  $t(5)=1.03$ ,  $p=0.347$ ; Fig. SUPP 2 B; filopodia,  $t(5)=0.83$ ,  $p=0.442$ ; thin spines,  $t(5)=0.98$ ,  $p=0.371$ ; mushroom spines,  $t(5)=2.16$ ,  $p=0.082$ ; Fig. SUPP 2 C).

## Discussion

In the above studies, we sought to reveal the role of SIRT1 in the NAc MSNs in a cell-type-specific manner. Following completion of the Sholl analysis, a 2-way repeated-measures ANOVA revealed no significant difference in D1-SIRT1- KO males. While not reaching statistical significance there is a trend toward a reduced number of dendritic intersections between 80-110  $\mu\text{m}$  from the soma. Gao et al., found in hippocampal

dentate gyrus granule cells of SIRT1 KO mice but a significant reduction in Sholl intersections (Gao et al., 2010; Michan et al., 2010). They also found a significant change in the number of branch points (Michan et al., 2010). While our data from the NAc does not completely reflect the findings in the DG, cell type plays a role in how things are expressed. For example, in their same study, they looked at pyramidal neurons in the CA1 region and found no significant changes in dendritic morphology as a result of SIRT1- KO (Michan et al., 2010). Our data from NAc D1-MSNs confirms their findings from CA1 neurons as we found no significant changes in total path length, average branch length, the average number of branch points, or tip ends. Additionally, others have found reduced total dendritic length in granule neurons in the DG (Abe-Higuchi et al., 2016).

For the dendritic spine density analyses, we found no significant changes in overall spine density or spine type in D1- SIRT1- KO mice. These findings are supported by studies in CA1 pyramidal neurons that show no significant change in spine densities or type following transgenic SIRT1- KO, nor were there significant changes in DG granule cells (Abe-Higuchi et al., 2016). However, using the SIRT1 inactivator Sirtinol, a significant reduction in total dendritic length and spine density in DG granule neurons was observed (Abe-Higuchi et al., 2016). These discrepancies in findings not only highlight the participation of SIRT1 in dendritic and spine morphology but also the significance of considering the animal models used. With transgenic mouse models, there exists the possibility of compensatory takeover in animals lacking SIRT1 from conception.

SIRT1 overexpression in NAc D1- MSNs showed no significant change in Sholl analysis compared to control animals. In cultured hippocampal neurons, SIRT1 activation with wtSIRT1 resulted in an increased growth of neurites and when SIRT1 activity was blocked with SRT1720, the outgrowth reversed (Abe-Higuchi et al., 2016). The inconsistency of models used between these studies are many; cultured neurons with pharmacological manipulation versus a genetic OVEXP that has had time to either compensate for dendritic growth over its lifetime or is showing results from a sustained SIRT1- OVEXP. At this point it is difficult to determine an exact reason for these differences. When we looked at changes in spine density and spine type, we found no significant change in spine density. However, we did find that OVEXP SIRT1 in D1- MSNs resulted in an increase of stubby spines and a decrease in mushroom spines. The changes in these two spine types specifically are interesting as stubby spine-types are considered immature and mushroom spines as mature and stable.

## CHAPTER 4

### EXPERIMENTS 3 - 4

#### **Introduction**

The sexual dimorphism in the prevalence of depression in males and females is stark. Women and men respond to stressors differently and therefore their stress vulnerability- expression of the disease- is markedly different. While men tend to externalize their symptoms (bouts of anger, physical aggression) women more commonly internalize (guilt and shame) their symptoms (Albert, 2015). Women experience

depression at rates almost double that of men and current research suggests that depression may be the most common mental health problem for women (www.who.int, 2020). Globally, the prevalence of depression in females in 2010 was 5.5%, with the prevalence of men closer to 3.2% (Floresco, 2015). This represents a 1.7- fold greater incidence in women (Albert, 2015). Over the last 5 years, depression rates in women in the United States have soared from roughly 8.7% in 2017 to 10.5% in 2022 (www.who.int, 2020). While depressive disorders are responsible for approximately 41.9% of disability from neuropsychiatric disorders in women (www.who.int, 2020), almost all clinical and preclinical research focuses on males. Unsurprisingly, the limited research employing female animal models demonstrates that the neurological changes that occur following stress have not been widely investigated.

Past stress research using female mice is limited due to the inability of earlier researchers to delineate possible behavioral changes from hormonal changes. Therefore, female animal models are grossly underrepresented in literature. With the development of novel stress models that can utilize CSDS on females, some data is beginning to emerge. From these studies, which often use male mouse urine sprayed on the female to initiate aggression, differences in the molecular and behavioral profiles are beginning to be understood. Similarities in stress outcomes include a sustained decrease in the amount of time spent interacting with a novel mouse, decreased sucrose consumption, and fewer entries into the open arms of the EPM (Harris et al., 2018). Often however, results between males and females present as contradictory. For example, it has been reported using a BDNF- KO in forebrain mouse model, male mice exhibited normal anxiety-like

behavior while female mice showed a trend towards less anxiety-like behavior (Monteggia et al., 2007). Additionally, in the Porsolt forced swim test female BDNF- KO mice exhibited an increased immobility time while males showed no difference to control (Monteggia et al., 2007). Further, sexually dimorphic effects of stress have been reported in forebrain excitatory neurons. Following KO of SIRT1 in the mPFC of male and female mice, there was an increase of depressive-like behaviors in only male mice (Bittar & Labonte, 2021). Furthermore, unpublished data from our laboratory utilizing male and female mice in a chronic unpredictable stress model showed females display stress susceptibility to this stress paradigm, but not males. Interestingly, while female mice do present with changes in SIRT1, it is decreased in female mice using this stress model. This is interesting especially because our previous data, in males, shows that SIRT1 is increased following chronic social defeat stress (Kim et al., 2016). These dichotomous findings highlight the importance of including both sexes, as well as differentiating between the cell types, in future research into depressive disorders.

Quantitative analysis of NAc MSNs in male and female stress naïve animals is beginning to shine a light on the mechanics underlying female depression. An analysis of MSNs in the NAc with male and female Sprague-Dawley rats shows that females have a baseline 22% increase in spine density on distal portions of second- and third- degree dendrites, with no difference in dendritic branching or length (Wissman et al., 2012). Additionally, it was found that females have significantly more large and giant spines (thin and mushroom respectively) compared to males (Forlano & Woolley, 2010). These findings are important as stress has been found to alter dendritic branching and spine

number and size in the NAc (Sholl, 1953; Zampa et al., 2018). Therefore, having an increased baseline prevalence of dendritic spines may account for the increased incidence of depression in females in response to stressors. However, the previous study did not look at the cell-type specificity of these differences. Wissman et al, 2012 performed a second set of studies looking at spines on whole dendrite (vs distal only) as well as regional specificity (Wissman et al., 2012). They found females have a greater density of spine synapses than males specifically in the caudal region of the NAc core (Wissman et al., 2012).

### **Experiment 3:**

*Characterization of D1 female SIRT-1 neurons in which SIRT1 has been knocked out.*

Mice were bred, genotyped, and raised until 8- 12 weeks old. Once the appropriate age was reached, mice received a lethal dose of Euthasol (0.1 mL/kg, Virbac) and were perfused with 1X PB (20 mL) followed by perfusion with 1.5% paraformaldehyde (PFA). Following this, the brain is removed and post-fixed in 1.5% PFA for another hour. Brains are then transferred to 30% sucrose until processed.

### **Results**

Female mice with SIRT1 KO in D1- MSNs showed a significant increase in the number of Sholl intersections ( $p=1.0$ ; Fig. 3 A) at 110-120  $\mu\text{m}$  from the soma compared to controls. We then measured total path length, average branch length, total branch points, and total tip numbers. Compared to controls there was no significant change in total path length ( $t(8)=1.70$ ,  $p=0.126$ ; Fig. 3 B) or average branch length ( $t(8)=0.61$ ,

p=0.555; Fig. 3 C). There was a significant decrease in the total number of branch points (t(8)=2.33, p=0.047; Fig. 3 D) and the total number of tips (t(8)= 3.079, p=0.015; Fig. 3 E).

We next looked at possible changes in dendritic spine density and the spine types represented along the dendritic branch. We observed no overall significant change in total spine density (t(106)=1.56, p=0.120; Fig. 4 A) compared to control. There are, however, spine-type specific alterations. The overall spine densities of thin (t(25)=2.08, p=0.047; Fig. 4 D) and mushroom (t(25)=2.17, p=0.039; Fig. 4 E) spines were significantly increased as compared to controls. There was no significant change in the density of either stubby spine (t(25)=1.26, p=0.217; Fig. 4 B) or filopodia (t(25)=0.58, p=0.565; Fig. 4 C). There was a significant, region-specific increase in thin spines (50-75  $\mu\text{m}$ , thin spines, t(7)=19.81, p=<0.0001; Fig. SUPP 3 B). There were no significant changes for any other spine type (25-50  $\mu\text{m}$ , stubby spines, t(7)=0.09, p=0.929; filopodia, t(7)=0.42, p=0.682; thin spines, t(7)=0.36, p=0.726; mushroom spines, t(7)=0.99, p=0.350; Fig. SUPP 3 A; 50-75  $\mu\text{m}$ , stubby spines, t(7)=0.55, p=0.595; filopodia, t(7)=0.20, p=0.842; mushroom spines, t(7)=1.73, p=0.127; Fig. SUPP 3 B; 75+  $\mu\text{m}$ , stubby spines, t(7)=2.09, p=0.074; filopodia, t(7)=0.34, p=0.742; thin spines, t(7)=0.61, p=0.560; mushroom spines, t(7)=0.80, p=0.446; Fig. SUPP 3 C) compared to control.

#### **Experiment 4:**

*Characterization of female DI- SIRT-1 neurons in which Sirt-1 has been OVEXP.* Mice were bred, genotyped, and raised until 8- 12 weeks old. Once the appropriate age was

reached, mice received a lethal dose of Euthasol (0.1 mL/kg, Virbac) and were perfused with 1X PB (20 mL) followed by perfusion with paraformaldehyde (PFA). Following this, the brain is removed and post-fixed in 4% PFA for another hour. Brains were then transferred to 30% sucrose until processed.

## Results

We looked at morphological changes following overexpression of SIRT1 in D1-MSNs in female mice. In SIRT1 OVEXP mice we found no significant change in Sholl intersections ( $p=0.98$ ; Fig. 5 A) compared to controls. It does seem that between 90-150 $\mu\text{m}$  from the soma there is a trend in decreased Sholl intersections, however, no intersection reached statistical. When the total path length, average branch length, total branch points, and total tip numbers were measured we found no significant changes in any other parameter (Total path length,  $t(6)=1.93$ ,  $p=0.101$ ; average branch length,  $t(6)=2.02$ ,  $p=0.089$ ; total number of branch points,  $t(6)=1.40$ ,  $p=0.208$ , and the total number of tips,  $t(6)=1.20$ ,  $p=0.272$ ; Fig. 5 B-E).

We next looked at the dendritic spine and spine type densities. In SIRT1- D1- OVEXP female mice there was no significant difference in total spine density ( $t(94)=0.84$ ,  $p=0.397$ ; Fig. 6 A) compared to control. Overall spine type densities show a significant decrease in stubby spines ( $t(22)=3.46$ ,  $p=0.002$ ; Fig. 6 B), a significant increase in filopodia ( $t(22)=3.96$ ,  $p=0.0007$ ; Fig. 6 C), and a significant increase in mushroom spines ( $t(22)=3.87$ ,  $p=0.039$ ; Fig. 6 E). There are no significant changes in total thin spine density ( $t(22)=0.05$ ,  $p=0.955$ ; Fig. 6 D) compared to controls. There were



significant regional changes in thin spines ( $t(6)=9.58$ ,  $p=0.0001$ ; Fig. SUPP 4 B) at 50-75 $\mu\text{m}$  from soma compared to controls. There was also a significant increase of filopodia ( $t(6)=2.99$ ,  $p=0.024$ ; Fig. SUPP 4 C) and mushroom spines ( $t(6)=2.62$ ,  $p=0.039$  Fig. SUPP 4 C) on the distal regions (75+  $\mu\text{m}$ ) of the dendritic arbor. No significance was found for the other spine types or regions (25-50  $\mu\text{m}$ , stubby spines,  $t(6)=2.19$ ,  $p=0.071$ ; filopodia,  $t(6)=1.83$ ,  $p=0.116$ ; thin spines,  $t(6)=0.75$ ,  $p=0.476$ ; mushroom spines,  $t(6)=1.97$ ,  $p=0.096$ ; Fig. SUPP 4 A; 50-75  $\mu\text{m}$ , stubby spines,  $t(6)=1.67$ ,  $p=0.145$ ; filopodia,  $t(6)=1.75$ ,  $p=0.129$ ; mushroom spines,  $t(6)=1.87$ ,  $p=0.110$ ; Fig. SUPP 4 B; 75+  $\mu\text{m}$ , stubby spines,  $t(6)=0.12$ ,  $p=0.127$ ; thin spines,  $t(6)=1.04$ ,  $p=0.335$ ; Fig. SUPP 4 C).

## Discussion

The above study is the first, to our knowledge, to look at the cell-type-specific action of SIRT1 in dendritic and spine morphology in NAc MSNs of female mice. Following the KO of SIRT1 in D1- MSNs we found a significant increase in the number of Sholl intersections at 110-120 $\mu\text{m}$  from the soma. This finding is opposite of what we observed in male D1- SIRT1- KO mice, which had a trending decrease of intersections. Interestingly, the increase of intersections is accompanied by a decrease in branch points and tip number. A decrease in tip points agrees with the finding of decreased branch points, however how this relates to an increase in Sholl intersections is perplexing. One possibility for this is an increase of primary dendrites, which could result in more dendritic intersections without relying on bifurcation of dendrites. There was no overall change in the total spine density in SIRT1- KO- D1 female mice. However, when divided

into spine-type we see a significant increase in both thin and mushroom spines. The increase of these spine type suggests a strengthening of synapses.

When SIRT1 is OVEXP in female D1- MSNs we saw a trend towards a reduction of Sholl intersections, however it did not reach statistical significance. This is interesting as, although also not reaching significance, the trend in female OVEXP mice is again opposite of the trend we see in male OVEXP mice. There was no significant change in the remaining morphological measurements, although average branch length may be affected to a point.

Again, the total spine density did not change significantly in SIRT1- OVEXP- D1 female mice. There were, however, significant changes in spine type. We found a significant decrease in stubby spines, and a significant increase in both filopodia and mushroom spines. Again, this is interesting as the decrease in stubby and increase in mushroom spines in female mice is opposite of what we see in male mice. Additionally, the increase of filopodia may promote destabilization of synaptic connectivity resulting from an increase in plasticity. Increases in density and length of filopodia and spine density may be a compensatory outcome to form functional synapses; increased filopodia may represent an increase chance of forming functional synapses (Kanjhan et al., 2016).

## CHAPTER 5

### EXPERIMENT 5 – 6

#### **Experiment 5:**

*Characterization of D2 male SIRT1 neurons in which Sirt-1 has been knocked out.* Mice were bred, genotyped, and raised until 8- 12 weeks old. Once the appropriate age was reached, mice received a lethal dose of Euthasol (0.1 mL/kg, Virbac) and were perfused with 1X PB (20 mL) followed by perfusion with paraformaldehyde (PFA). Following this, the brain is removed and post-fixed in 4% PFA for another hour. Brains were then transferred to 30% sucrose until processed.

#### **Results**

Changes in the number of intersections have been observed in D1-MSNs of both male and female mice. We sought to investigate the SIRT1-induced morphological changes in D2 mice. We first KO'd SIRT1 in male D2- MSNs. We found no significant changes in the number of Sholl intersections ( $p=1.0$ ; Fig. 9 A) compared to controls. We next measured the total path length, average branch length, total branch points, and total tip numbers. There were no significant changes in any measurement (Total path length,  $t(7)=0.02$ ,  $p=0.981$ ; average branch length,  $t(7)=0.81$ ,  $p=0.440$ ; total number of branch points,  $t(7)=0.41$ ,  $p=0.688$ ; and total number of tips,  $t(7)=0.35$ ,  $p=0.731$ ; Fig. 9 B-E).

We next sought to quantify any alterations in dendritic spine density. We found a significant increase in total spine density ( $t(94)=4.75$ ,  $p<0.0001$ ; Fig. 10 A) compared to

controls. For total spine- type densities, there was a significant increase of stubby spines ( $t(22)=4.69$ ,  $p=0.0001$ ; Fig. 10 B), filopodia ( $t(22)=2.96$ ,  $p=0.007$ ; Fig. 10 C), and thin spines ( $t(22)=3.46$ ,  $p=0.002$ ; Fig. 10 D) and no significant change in mushroom spines ( $t(22)=0.44$ ,  $p=0.663$ ). There were regional changes as well: in all regions there was a significant increase of stubby spines at 25-50  $\mu\text{m}$  ( $t(6)= 3.05$ ,  $p=0.002$ ; Fig. SUPP 5 A), 50-75  $\mu\text{m}$  ( $t(6)=2.95$ ,  $p=0.025$ ; Fig. SUPP 5 B), and 75+  $\mu\text{m}$  ( $t(6)=3.26$ ,  $p=0.017$ ; Fig. SUPP 3 C) from soma. There were no significant changes in the other spine types (25-50  $\mu\text{m}$ , filopodia,  $t(6)=1.23$ ,  $p=0.253$ ; thin spines,  $t(6)=1.16$ ,  $p=0.289$ ; mushroom spines,  $t(6)=0.92$ ,  $p=0.390$ ; 50-75  $\mu\text{m}$ , filopodia,  $t(6)=2.34$ ,  $p=0.057$ ; thin spines,  $t(6)=0.93$ ,  $p=0.386$ ; mushroom spines,  $t(6)=0.25$ ,  $p=0.257$ ; 75+  $\mu\text{m}$ , filopodia,  $t(6)=1.50$ ,  $p=0.182$ ; thin spines,  $t(6)=2.27$ ,  $p=0.063$ ; mushroom spines,  $t(6)=0.17$ ,  $p=0.863$ ; Fig. SUPP. 5 A-C).

## **Experiment 6:**

*Characterization of D2 male SIRT-1 neurons in which Sirt-1 has been OVEXP.* Mice were bred, genotyped, and raised until 8- 12 weeks old. Once the appropriate age was reached, mice received a lethal dose of Euthasol (0.1 mL/kg, Virbac) and were perfused with 1X PB (20 mL) followed by perfusion with paraformaldehyde (PFA). Following this, the brain is removed and post-fixed in 4% PFA for another hour. Brains were then transferred to 30% sucrose until processed.

## **Results**

We next OVEXP SIRT1 in D2- MSNs of male mice. There was no significant change in the number of intersections ( $p=1.0$  ; Fig. 11 A) compared to controls as measured by Sholl analysis. There were no significant changes in any other morphometric measurements (Total path length,  $t(6)=0.03$ ,  $p=0.973$ ; average branch length,  $t(6)=0.98$ ,  $p=0.364$ ; total number of branch points,  $t(6)=0.15$ ,  $p=0.885$ ; and total number of tips,  $t(6)=0.20$ ,  $p=0.844$ ; Fig. 11 B-E).

We then looked at changes in spine density in SIRT1- OVEXP in D2 male mice. We observed a significant increase in total spine density ( $t(94)=5.04$ ,  $p<0.0001$ ; Fig. 12 A) compared to controls. We observed significant changes in several spine types: stubby ( $t(22)=5.31$ ,  $p<0.0001$ ; Fig. 12 B), filopodia ( $t(22)=4.77$ ,  $p<0.0001$ ; Fig. 12 C), and thin spines ( $t(22)=5.35$ ,  $p<0.0001$ ; Fig. 12 D) with no significant change in total mushroom spine density ( $t(22)=0.16$ ,  $p=0.869$ ; Fig. 12 E). There were also regional changes in most spine types; notably there was a significant increase in stubby spines across all regions (25-50  $\mu\text{m}$ , stubby spines,  $t(6)=0.97$ ,  $p=0.024$ ; filopodia,  $t(6)=1.79$ ,  $p=0.123$ ; thin spines,  $t(6)=2.73$ ,  $p=0.034$ ; mushroom spines,  $t(6)=1.41$ ,  $p=0.207$ ; 50-75  $\mu\text{m}$ , stubby spines,  $t(6)=2.70$ ,  $p=0.035$ ; filopodia,  $t(6)=3.80$ ,  $p=0.008$ ; thin spines,  $t(6)=3.25$ ,  $p=0.017$ ; mushroom spines,  $t(6)=1.03$ ,  $p=0.339$ ; 75+  $\mu\text{m}$ , stubby spines,  $t(6)=2.82$ ,  $p=0.030$ ; filopodia,  $t(6)=2.63$ ,  $p=0.039$ ; thin spines,  $t(6)=1.72$ ,  $p=0.135$ ; mushroom spines,  $t(6)=0.82$ ,  $p=0.443$ ; Fig. SUPP 6 A-C).

## **Discussion**

Following the manipulation of SIRT1 in D1-MSNs of male and female mice, we chose to also investigate its action in D2- MSNs. After collecting tissue from our male KO-D2 mice, we did not observe any significant changes in Sholl intersections or in the other measured parameters. There was a significant increase in spine density in SIRT1-KO- D2 male mice. This change was accompanied by significant increases in stubby spines, filopodia, and thin spines. The increase in these spine types suggests a more plastic brain and the possibility of weaker synapses that respond poorly to activation.

SIRT1- OVEXP in D2 males resulted in no significant change in Sholl intersections or other morphological measurements. This finding is consistent with male D1- OVEXP data which show no change in Sholl analysis. When SIRT1 was OVEXP in male D2- MSNs we again found a significant increase in total spine density. This overall increase was accompanied by an increase in the total stubby spine, filopodia, and thin spine density. Again, this would suggest a less stable synapse. However, the transient nature of immature spines could suggest these are spines primed to strengthen. As for the almost identical outcome resulting from knocking out and overexpressing SIRT1 in male D2- MSNs, it is known and not uncommon for proteins to have cell-type specific actions. Perhaps SIRT1 in D2-MSNs has deacetylase actions not yet established.

## CHAPTER 6

### EXPERIMENTS 7 – 8

#### **Experiment 7:**

*Characterization of D2 female SIRT-1 neurons in which Sirt-1 has been knocked out.*

Mice were bred, genotyped, and raised until 8- 12 weeks old. Once the appropriate age was reached, mice received a lethal dose of Euthasol (0.1 mL/kg, Virbac) and were perfused with 1X PB (20 mL) followed by perfusion with paraformaldehyde (PFA). Following this, the brain is removed and post-fixed in 4% PFA for another hour. Brains were then transferred to 30% sucrose until processed.

#### **Results**

To complement the D1 female data, we KO SIRT1 in female D2- MSNs. No significant changes were seen in the number of intersections ( $p=0.98$  Fig. 13 A). We then performed measurements on the total path length, average branch length, total branch points, and total tip numbers and we found no significant changes (Total path length,  $t(3)=0.44$ ,  $p=0.687$ ; average branch length,  $t(3)=0.63$ ,  $p=0.569$ ; total number of branch points,  $t(3)=0.28$ ,  $p=0.795$ , and the total number of tips,  $t(3)=0.20$ ,  $p=0.847$ ; Fig. 13 B-E).

In SIRT1- D2- KO female mice we found no significant difference in total spine density ( $t(70)=1.07$ ,  $p=0.287$ ; Fig. 14 A). We did see significant changes in total density of filopodia ( $t(16)=2.56$ ,  $p=0.020$ ; Fig. 14 C) and thin spines ( $t(16)=2.79$ ,  $p=0.012$ ; Fig. 14 D) but no significant change in stubby ( $t(16)=0.77$ ,  $p=0.452$ ; Fig. 14 B) or mushroom

spines ( $t(16)=1.96$ ,  $p=0.067$ ; Fig. 14 E). When we looked at regional differences, we found a significant decrease of filopodia ( $t(4)=2.84$ ,  $p=0.046$ ; Fig. SUPP 7 A) at 25-50  $\mu\text{m}$  from soma as well as a significant increase in stubby spines ( $t(4)=3.84$ ,  $p=0.018$ ; Fig. SUPP 7 C) at 75+  $\mu\text{m}$  from soma. While there are trends for alteration in other spine types, none reached statistical significance (25-50  $\mu\text{m}$ , stubby spines,  $t(4)=1.04$ ,  $p=0.356$ ; thin spines,  $t(4)=1.97$ ,  $p=0.119$ ; mushroom spines,  $t(4)=1.51$ ,  $p=0.205$ ; 50-75  $\mu\text{m}$ , stubby spines,  $t(4)=1.62$ ,  $p=0.178$ ; filopodia,  $t(4)=1.24$ ,  $p=0.282$ ; thin spines,  $t(4)=0.79$ ,  $p=0.473$ ; mushroom spines,  $t(4)=0.50$ ,  $p=0.64$ ; 75+  $\mu\text{m}$ , filopodia,  $t(4)=0.70$ ,  $p=0.520$ ; thin spines,  $t(4)=2.06$ ,  $p=0.108$ ; mushroom spines  $t(4)=0.91$ ,  $p=0.411$ ; Fig. SUPP 7 A-C).

### **Experiment 8:**

*Characterization of D2 female SIRT-1 neurons in which Sirt-1 has been OVEXP.* Mice were bred, genotyped, and raised until 8- 12 weeks old. Once the appropriate age was reached, mice received a lethal dose of Euthasol (0.1 mL/kg, Virbac) and were perfused with 1X PB (20 mL) followed by perfusion with paraformaldehyde (PFA). Following this, the brain is removed and post-fixed in 4% PFA for another hour. Brains were then transferred to 30% sucrose until processed.

### **Results**

We found a significant decrease ( $p=0.57$ ; Fig. 15 A) in the number of intersections in the Sholl analysis of SIRT1- OVEXP- D2 females compared to controls. When the total path length, average branch length, total branch points, and total tip numbers were measured we found no significant changes in any other parameter (Total



path length,  $t(3)=1.15$ ,  $p=0.333$ ; average branch length,  $t(3)=0.11$ ,  $p=0.916$ ; total number of branch points,  $t(3)=0.80$ ,  $p=0.479$ , and the total number of tips,  $t(3)=0.85$ ,  $p=0.454$ ; Fig. 15 B-E).

Following DiI processing we looked at total spine density. We found no significant change in total spine density ( $t(70)=0.04$ ,  $p=0.960$ ; Fig. 16 A). When we looked at specific spine types, we did observe a significant decrease in stubby spine density ( $t(16)=2.71$ ,  $p=0.015$ ; Fig. 16 B). There were no significant changes for the other spine types (Total spine density: filopodia,  $t(16)=1.01$ ,  $p=0.324$ ; thin,  $t(16)=0.67$ ,  $p=0.508$ ; mushroom,  $t(16)=1.23$ ,  $p=0.236$ ; Fig. 16 C-E). When observed by regional sections there was a significant increase in stubby spines ( $t(4)=3.46$ ,  $p=0.025$ ; Fig. SUPP 8 C) at 75+  $\mu\text{m}$  from soma with no significant changes in any other spine type (25-50  $\mu\text{m}$ , stubby spines,  $t(4)=0.93$ ,  $p=0.404$ ; filopodia,  $t(4)=0.03$ ,  $p=0.970$ ; thin spines,  $t(4)=0.20$ ,  $p=0.851$ ; mushroom spines,  $t(4)=0.99$ ,  $p=0.378$ ; 50-75  $\mu\text{m}$ , stubby spines,  $t(4)=1.41$ ,  $p=0.228$ ; filopodia,  $t(4)=0.67$ ,  $p=0.537$ ; thin spines,  $t(4)=0.19$ ,  $p=0.852$ ; mushroom spines,  $t(4)=0.52$ ,  $p=0.627$ ; 75+  $\mu\text{m}$ , filopodia,  $t(4)=0.955$ ,  $p=0.393$ ; thin spines,  $t(4)=1.42$ ,  $p=0.226$ ; mushroom spines,  $t(4)=0.91$ ,  $p=0.412$ ; Fig. SUPP 8 A-C).

## CHAPTER 7

### FINAL DISCUSSION

The experiments conducted above sought to reveal the role of SIRT1- KO or OVEXP in dendritic and spine morphology in D1- and D2- MSNs of the NAc. We used both male and female mice for these studies. To our knowledge, this is the first time the

role of SIRT1 expression in the NAc has investigated changes in dendritic and spine morphology. Moreover, this is the first inclusion of female groups in a morphological study of SIRT1-driven, cell-type-specific changes in the NAc. Here, we uncovered a probable role for SIRT1 regulation of dendritic complexity and spine-type density (Table 1). While neither D1- male treatment group reached significance, there is a trend in D1-KO males towards a decrease in number of intersections in the Sholl analysis, with no change in D1-OVEXP males. Notwithstanding reports of significant alterations in dendritic complexity and length following manipulation of SIRT1, different methodologies were employed. For example, Abe-Higuchi et al., used cultured hippocampal neurons for their Sholl and spine analysis, manipulating SIRT1 pharmacologically with a SIRT1 activator (wtSirt1) or a deactivator (SIRT1720, 0.5um) (Abe-Higuchi et al., 2016). Similarly, Codocedo et al., 2012, found in cultured hippocampal neurons there was a significant increase of Sholl intersections following application of SIRT1 activators (RSV, NAD) and a significant decrease when an inhibitor was applied (nicotinamide) (Codocedo et al., 2012). For our studies, we employed the use of transgenic mouse models which allow us to investigate these changes in connected working brains. In our model, there is a chance of unknown compensatory mechanisms that may have developed over a timespan not suitable for culture studies. In our studies, the lack of any significant changes in dendritic length may also result from methodological differences. For example, a bilateral osmotic mini-pump injection of a SIRT1 inhibitor (Sirtinol) for two weeks resulted in a reduction of dendritic length and spine density (Abe-Higuchi et al., 2016). Conversely, following stress in mice, SIRT1 activation (RSV) blocked these stress-induced changes (Abe-Higuchi et al., 2016).

The data from D1-KO females show a significant increase of dendritic intersections from approximately 100-120  $\mu\text{m}$  from soma. There is no significance seen in D1-OVEXP females, however there is a strong trend toward a decrease in Sholl intersections approximately 90-140  $\mu\text{m}$  from soma. The opposing conclusions from the Sholl analysis between male and female D1-targeted mice is intriguing. Although not statistically significant, D1- male SIRT1-KO mice show a trend towards a reduction in dendritic intersections while their female counterparts show a significant increase of intersections, with a corresponding decrease of intersections in D1- female SIRT1-OVEXP. The opposing results are not totally unexpected as sexual dimorphisms are common. For example, following a Cre- mediated SIRT1- KO in the forebrain, it was found only the male mice demonstrated depressive-like behaviors with no change in female mice (Lei et al., 2020). These sexually dimorphic responses have also been reported in the NAc shell. Following 6 days of a sub-chronic variable stress (SCVS) model only female stressed mice show a significant decrease of VGLUT1 and an increase in VGLUT2, a marker of glutamatergic presynaptic axon terminals (Brancato et al., 2017).

We next repeated these morphological experiments in D2 male and female mice. We saw no significant difference in D2 males for either treatment group on the Sholl analysis. Minimal, but significant changes were seen in the number of Sholl intersections in D2- SIRT1-OVEXP females. Specifically, these changes occur between 80- 140  $\mu\text{m}$  from soma. There was no significant change seen in D2-KO females.

We also established a role for SIRT1 in the regulation of dendritic spines. Specifically, it seems SIRT1 may affect the ability of dendritic spines to mature into mushroom spines in D1- OVEXP males, with the opposite effect seen in D1- OVEXP females. While SIRT1-KO-D1 males show no significant change in any spine type, this finding seems to be an exception as significant changes are seen in several dendritic regions as well as whole-cell for the other groups, in our studies. SIRT1-KO-D1 females show a significant increase in both thin and mushroom spines. SIRT1-KO-D2 males also show a significant increase in thin spines, as well as filopodia and stubby spines. Female SIRT1-KO-D2 mice show a significant decrease in both filopodia and thin spines with a trend towards a reduction of mushroom spines. Interestingly, while in whole-cell there was no statistical significance, in the distal regions of the dendritic arbor (75+ um) there is a significant increase of stubby spines.

The morphological analyses conducted here show various and often opposing outcomes between the sexes and cell-types. The results observed from the Sholl analysis that often show opposite trends by sex and cell-type, seem to translate to dendritic spine-type density as well. For example, in stubby spines SIRT1-OVEXP-D1 males show an increase while D1-KO females show a decrease in density. Additionally, SIRT1-OVEXP-D1 males show a significant decrease in mature mushroom spines, while female counterpart shows an increase in mushroom spines. In SIRT1-KO-D2 females we see the opposite of that seen in D1 female and similar to SIRT1-OVEXP-D1 males; in D2-KO females there is a significant increase of stubby spines and a trending decrease of

mushroom spines. Further, SIRT1-D2-KO males show an increase in stubby, filopodia, and thin spines while SIRT1-D2-KO females have a decrease in filopodia and thin spines.

The shift in spine type we observe in our female SIRT1-OVEXP-D1 mice, which is opposite of what we observe in the male counterparts, could be reflective of sex-differences in the expression of synaptic proteins. For example, following an acute administration of ketamine, there was a rescue of isolation-induced changes to synaptic proteins and spine density in male, but not female, rats (Sarkar & Kabbaj, 2016). However, despite the female rats showing no adjustment to the isolation stress-induced decline of synaptic proteins and spine density, they did experience the same anti-depressant effects as male rats (Sarkar & Kabbaj, 2016). This suggests that the molecular pathways involved in the executive processing of emotionally driven stimuli are different between male and female rats in the PFC. Further, following CVS, NAc-projecting pyramidal neurons showed a significant decrease in dendritic arborization in females but not males; the opposite was seen in VTA-projecting neurons, with males showing a retraction of dendrites (Bittar & Labonte, 2021).

Prior studies have shown that the same molecule can have opposing- or no-effects depending on the brain region and cell-type in which it is expressed. Blockade of NMDA receptors in the NAc core impaired spatial learning while having no effect on learning in the shell (Shirayama & Chaki, 2006; Smith-Roe & Kelley, 2000). Stress has been shown to have various effects on protein expression in different brain regions. Following a CSDS model, it was found that levels of proBDNF were significantly increased in the BLA of stressed animals while the PFC of these same animals had no

change in proBDNF (Colyn et al., 2019). Additionally, when SIRT1 was activated with SIRT1 activator 3, mice spent more time in the center of an open field while mice with SIRT1 inhibited in the DG spent less time in the center compared to controls (Yu et al., 2018). More specifically, following stress SIRT1 increased in the BLA and NAc but decreased in the PFC and HIPP. Moreover, when SIRT1 is increased in D1-MSNs but not D2-MSNs, pro-depressant behaviors are observed (Kim et al., 2016).

Not only do molecules perform differently depending on their location, but the physiological properties of cells and how they fire can function differently depending on brain region. For example, it has been shown that the frequency of excitatory input is increased on D2-MSNs but decreased in D1-MSNs following stress (Francis et al., 2015). Additionally, Lim et al. found, following repeated restraint stress, there was long-term depression in D1-MSNs but not D2-MSNs (Lim et al., 2012). Further, following CSDS, artificially increasing the activity of D1-MSNs results in pro-resilient behaviors, while inhibition induces depressive behaviors, and modulation of D2-MSNs in either direction has no behavioral response to CSDS (Francis et al., 2015). Moreover, a cell-type specific analysis of thin and mushroom spine-types revealed enhanced synaptic strength of D1-MSN mushroom spines from resilient animals and reduced strength in D2-MSN mushroom spines.

The collected data from our D1 males, in conjunction with previously collected data from our stressed mice, allow for some predictions about what might be happening. Previously we found elevated levels of SIRT1 in the NAc of stress-susceptible mice (Kim et al., 2016). When we virally OVEXP SIRT1 in the NAc of either D1- or D2-MSNs we

found a significant increase in depressive-like behaviors only in the SIRT1-OVEXP- D1 mice (Kim et al., 2016). Unfortunately, there is no data from past studies that would inform us if the resulting increase of SIRT1 following the CSDS model occurs in D1- or D2-MSNs. However, as demonstrated in our viral study, elevated levels of SIRT1 in D2-MSNs had no significant effect on behavior. Therefore, it seems likely that elevated levels of SIRT1 in D1-MSNs of male mice underlies the expression of pro-depressive behaviors. For example, SIRT1- OVEXP in male D1-MSNs resulted in a decrease in time spent crossing the center of an open field, an increase in float time on the FST, and a significant decrease in sucrose consumption, measures of anxiety, learned helplessness, and anhedonia respectively (Kim et al., 2016).

It is difficult to draw direct lines from molecule to function, however there are some interesting avenues of interpretation. It has been widely noted that mice susceptible to stress show an increase of stubby spines in the NAc (Christoffel, Golden, Dumitriu, et al., 2011; Fox, Chandra, et al., 2020). However, in the HIPp of stress-susceptible mice there is a decrease of stubby spines (Iniguez et al., 2016). This increase and decrease accompany the expression levels of SIRT1 in these regions following stress. Specifically, SIRT1 in the HIPp is decreased and this is accompanied by a decrease in stubby spines. Meanwhile, SIRT1 is increased in the NAc resulting in an increase of stubby spines. Here we show that SIRT1- OVEXP in D1-MSNs in the NAc of male mice results in a significant increase of stubby spines and a subsequent decrease in mushroom spines despite no change in overall spine density.

The common reports of insignificant changes in overall spine density in D1-MSNs following CSDS may be overlooking important deviations that have occurred in the type of spine (Christoffel, Golden, Dumitriu, et al., 2011). Additionally, a significant decrease in mushroom spines of stress-susceptible mice has not been reported. This may represent an important difference highlighting changes that occur in concert with external factors (stress) versus a transgenic mouse model that OVEXP SIRT1 from conception. The data here strongly support the notion that SIRT1 may be responsible for developmental stagnation of stubby spines in a way that is more permissive or receptive to stress. Indeed, a significant decrease in the number of mushroom spines of transgenic SIRT1- D1- OVEXP mice may suggest that SIRT1 levels correspond to expression of stubby spines, or it is repressing an important molecule needed to mature stubby spines to mushroom. SIRT1 itself likely doesn't reduce mushroom spines because no decrease in stressed mice has been reported. It seems most likely that SIRT1 prevents spines from developing to mature forms.

The effects of SIRT1 activation or deactivation may very well be specific to the cell type. SIRT1 appears to have a more predictable role in D1-MSNs as seen by the spine type changes (stubby and mushroom) and the almost complete reversal of these spine differences seen in female OVEXP-D1 mice. The observation that there is a significant switch between stubby spine and mushroom spines but with no change in overall spine density suggests a dysfunction in the development of stubby spines into thin or mushroom spines. This finding supports a role for SIRT1 in the function of spine maturation. For a spine to mature the necessary scaffolding proteins, microtubules, and



actin-binding proteins (ABP) must be available. One such ABP is cortactin. Cortactin is a F-actin binding protein involved in the stabilization and branching of actin filaments (Hering & Sheng, 2003). Cortactin is essential for the maintenance of dendritic spine structure in neurons (Hering & Sheng, 2003) and it stabilizes F-actin through binding with its central tandem repeat region (Weed et al., 2000). Dysfunction of cortactin acetylation results in alterations of dendritic spine type and density (Zhang et al., 2009). Studies have discovered that the class III HDAC inhibitor nicotinamide enhances acetylation of cortactin (Zhang et al., 2009) and it has been established that nicotinamide is an inhibitor of SIRT1 (Codocedo et al., 2012). To determine the precise sirtuin that interacts with cortactin, Zhang et al. used cultured 293T cells with bead-bound glutathione S-transferase (GST)-cortactin that was transfected with Flag-SIRT1-7. The GST-cortactin-sirtuin complexes were pulled down and ran through a western blot and only Flag-SIRT1 was associated within GST-cortactin (Zhang et al., 2009). It has been shown that SIRT1 directly deacetylates cortactin on its tandem repeat section, the same region that binds to actin to stabilize it (Zhang et al., 2009).

It is difficult to say with any strong certainty what role cortactin may have on spine maturation on MSNs of the NAc. While some have reported that increased SIRT1-driven deacetylation of cortactin results in longer spines with thinner heads (Zhang et al., 2009), it is difficult to compare results from our developmental-like transgenic mouse models to these 293T cell cultures. It is intriguing to speculate on what other scaffolding proteins, or ABPs may be affected in our SIRT1 mice. Overexpression of SIRT1 would result in an increase of deacetylase activity. As acetyl groups help stabilize proteins an imbalance

may result from excess deacetylated proteins involved in synaptic plasticity. Elevated SIRT1 would theoretically result in an increase of deacetylated cortactin (. However, as cortactin needs its acetyl groups to bind f-actin, having less SIRT1 may not necessarily affect this, as reflected in our findings. The resulting inability of cortactin to bind to F-actin would result in failure of the cytoarchitecture to support itself and grow. In our SIRT1-OVEXP-D1 male mice, deacetylase activity towards cortactin could be a reason for these spines to not mature. Though, cortactin has been noted to specifically lead to longer spines (Zhang et al., 2009). It is possible, specifically in our male SIRT1-OVEXP-D1 mice, that the elevated levels of SIRT1 interact with many other proteins during development. SIRT1 has been shown to interact with Ying-Yang 1 (YY1) to repress miR-134 transcription (Gao et al., 2010). Endogenous miR-134 works to inhibit LIMK1 mRNA translation by binding to its 3' binding site (Schratt et al., 2006). Further, LIMK1 regulates actin dynamics through phosphorylation of ADP/cofilin which prevents ADP/cofilin from severing F-actin resulting in the accumulation of actin microfilaments (Gao et al., 2010). Therefore, one might conclude that elevated levels of SIRT1 leads to a repression of miR-134 which would usually act to inhibit LIMK1. Elevated LIMK1 phosphorylates ADP/cofilin which results in ADF/cofilin being unable to sever F-actin allowing accumulation of actin filaments (Gao et al., 2010).

Following chronic stress there is an increase of BDNF (Monteggia et al., 2007; Wook Koo et al., 2016) and an increase of SIRT1 in the NAc(Kim et al., 2016). Building from this I will describe parallel pathways resulting in an increase of LIMK1, subsequent hyper-phosphorylation of ADF/cofilin and SIRT1 deacetylating cortactin. While elevated

levels of LIMK1- or any protein- are being theorized in our stress susceptible mice, we will propose a possibility based on the evidence presented above. Elevated levels of BDNF starts a chain of events, through the recruitment of the RHO- family GTPase, leading to an increase of LIMK1. At the same time, there is an increase of SIRT1 in susceptible mice. SIRT1, bound with YY1 represses miR-134. This results in miR-134 being unable to repress LIMK1, resulting in even more LIMK1. So, we have elevated levels of LIMK1 from separate pathways resulting in hypoacetylation of ADF/cofilin which inhibits its ability to sever actin filaments. BDNF also recruits cortactin to post-synaptic sites where it binds Apr2/3 to stabilize the spine. However, SIRT1 is deacetylating cortactin, possibly resulting in the inability of actin to formally organize and support itself. This results in an increase of stubby spines and decrease in mushroom. As for observing the exact opposite in female mice, we have seen many instances of the same protein acting differently in not only specific cell types, but between the sexes as well. More research is needed to dissect the delicate dance between these proteins.

The above studies sought to elucidate changes to the dendritic arbor and spines following overexpression or knock-out of SIRT1. Although variable by sex and cell-type, we have established a role for SIRT1 in the development of spines. Our data show an increase in the number of stubby spines in SIRT1-OVEXP-D1 male mice. These findings reflect similar changes observed in stubby spine density following chronic stress. There are several follow-up studies that could help advance our understanding of how these divergent cell-types react in response to stress. Conducting in-depth study of synaptic proteins altered in our stress-susceptible mice, where SIRT1 is elevated, would help

guide more of this discussion. Additionally, establishing if SIRT1 is increased in one cell type or the other or even globally in the NAc following stress. Building on the material studied and experiments conducted, I have made educated speculations into how SIRT1 maybe involved in the maturation of dendritic spines and how SIRT1 and stress result in excess stubby spines and subsequent stress-susceptibility.

## REFERENCES

- Abe-Higuchi, N., Uchida, S., Yamagata, H., Higuchi, F., Hobara, T., Hara, K., Kobayashi, A., & Watanabe, Y. (2016). Hippocampal Sirtuin 1 Signaling Mediates Depression-like Behavior. *Biol Psychiatry*, *80*(11), 815-826. <https://doi.org/10.1016/j.biopsych.2016.01.009>
- Albert, P. R. (2015). Why is depression more prevalent in women? *J Psychiatry Neurosci*, *40*(4), 219-221. <https://doi.org/10.1503/jpn.150205>
- Alexander, G. E., & Crutcher, M. D. (1990). Functional architecture of basal ganglia circuits: neural substrates of parallel processing. *Trends Neurosci*, *13*(7), 266-271. [https://doi.org/10.1016/0166-2236\(90\)90107-1](https://doi.org/10.1016/0166-2236(90)90107-1)
- Alimohamadi, H., Bell, M. K., Halpain, S., & Rangamani, P. (2021). Mechanical Principles Governing the Shapes of Dendritic Spines. *Front Physiol*, *12*, 657074. <https://doi.org/10.3389/fphys.2021.657074>
- Araya, R., Jiang, J., Eisenthal, K. B., & Yuste, R. (2006). The spine neck filters membrane potentials. *Proc Natl Acad Sci U S A*, *103*(47), 17961-17966. <https://doi.org/10.1073/pnas.0608755103>
- Bagot, R. C., Parise, E. M., Pena, C. J., Zhang, H. X., Maze, I., Chaudhury, D., Persaud, B., Cachope, R., Bolanos-Guzman, C. A., Cheer, J. F., Deisseroth, K., Han, M. H., & Nestler, E. J. (2015). Ventral hippocampal afferents to the nucleus accumbens regulate susceptibility to depression. *Nat Commun*, *6*, 7062. <https://doi.org/10.1038/ncomms8062>
- Baik, J. H. (2020). Stress and the dopaminergic reward system. *Exp Mol Med*, *52*(12), 1879-1890. <https://doi.org/10.1038/s12276-020-00532-4>
- Barr, A. M., Markou, A., & Phillips, A. G. (2002). A 'crash' course on psychostimulant withdrawal as a model of depression. *Trends Pharmacol Sci*, *23*(10), 475-482. [https://doi.org/10.1016/s0165-6147\(02\)02086-2](https://doi.org/10.1016/s0165-6147(02)02086-2)
- Bassareo, V., De Luca, M. A., & Di Chiara, G. (2002). Differential Expression of Motivational Stimulus Properties by Dopamine in Nucleus Accumbens Shell versus Core and Prefrontal Cortex. *J Neurosci*, *22*(11), 4709-4719. <https://doi.org/20026445>
- Bello-Medina, P. C., Flores, G., Quirarte, G. L., McGaugh, J. L., & Prado Alcala, R. A. (2016). Mushroom spine dynamics in medium spiny neurons of dorsal striatum

- associated with memory of moderate and intense training. *Proc Natl Acad Sci U S A*, 113(42), E6516-E6525. <https://doi.org/10.1073/pnas.1613680113>
- Berton, O., McClung, C. A., Dileone, R. J., Krishnan, V., Renthal, W., Russo, S. J., Graham, D., Tsankova, N. M., Bolanos, C. A., Rios, M., Monteggia, L. M., Self, D. W., & Nestler, E. J. (2006). Essential role of BDNF in the mesolimbic dopamine pathway in social defeat stress. *Science*, 311(5762), 864-868. <https://doi.org/10.1126/science.1120972>
- Bessa, J. M., Morais, M., Marques, F., Pinto, L., Palha, J. A., Almeida, O. F., & Sousa, N. (2013). Stress-induced anhedonia is associated with hypertrophy of medium spiny neurons of the nucleus accumbens. *Transl Psychiatry*, 3, e266. <https://doi.org/10.1038/tp.2013.39>
- Bewernick, B. H., Kayser, S., Sturm, V., & Schlaepfer, T. E. (2012). Long-term effects of nucleus accumbens deep brain stimulation in treatment-resistant depression: evidence for sustained efficacy. *Neuropsychopharmacology*, 37(9), 1975-1985. <https://doi.org/10.1038/npp.2012.44>
- Bittar, T. P., & Labonte, B. (2021). Functional Contribution of the Medial Prefrontal Circuitry in Major Depressive Disorder and Stress-Induced Depressive-Like Behaviors. *Front Behav Neurosci*, 15, 699592. <https://doi.org/10.3389/fnbeh.2021.699592>
- Bossert, J. M., Stern, A. L., Theberge, F. R., Cifani, C., Koya, E., Hope, B. T., & Shaham, Y. (2011). Ventral medial prefrontal cortex neuronal ensembles mediate context-induced relapse to heroin. *Nat Neurosci*, 14(4), 420-422. <https://doi.org/10.1038/nn.2758>
- Bossert, J. M., Stern, A. L., Theberge, F. R., Marchant, N. J., Wang, H. L., Morales, M., & Shaham, Y. (2012). Role of projections from ventral medial prefrontal cortex to nucleus accumbens shell in context-induced reinstatement of heroin seeking. *J Neurosci*, 32(14), 4982-4991. <https://doi.org/10.1523/JNEUROSCI.0005-12.2012>
- Bouarab, C., Thompson, B., & Polter, A. M. (2019). VTA GABA Neurons at the Interface of Stress and Reward [Review]. *Frontiers in Neural Circuits*, 13. <https://doi.org/10.3389/fncir.2019.00078>
- Bourne, J., & Harris, K. M. (2007). Do thin spines learn to be mushroom spines that remember? *Curr Opin Neurobiol*, 17(3), 381-386. <https://doi.org/10.1016/j.conb.2007.04.009>
- Brancato, A., Bregman, D., Ahn, H. F., Pfau, M. L., Menard, C., Cannizzaro, C., Russo, S. J., & Hodes, G. E. (2017). Sub-chronic variable stress induces sex-specific effects on glutamatergic synapses in the nucleus accumbens. *Neuroscience*, 350, 180-189. <https://doi.org/10.1016/j.neuroscience.2017.03.014>

- Brog, J. S., Salyapongse, A., Deutch, A. Y., & Zahm, D. S. (1993). The patterns of afferent innervation of the core and shell in the "accumbens" part of the rat ventral striatum: immunohistochemical detection of retrogradely transported fluoro-gold. *J Comp Neurol*, 338(2), 255-278. <https://doi.org/10.1002/cne.903380209>
- Cabib, S., & Puglisi-Allegra, S. (1994). Opposite responses of mesolimbic dopamine system to controllable and uncontrollable aversive experiences. *J Neurosci*, 14(5 Pt 2), 3333-3340. <https://www.ncbi.nlm.nih.gov/pubmed/8182476>
- Campioni, M. R., Xu, M., & McGehee, D. S. (2009). Stress-induced changes in nucleus accumbens glutamate synaptic plasticity. *J Neurophysiol*, 101(6), 3192-3198. <https://doi.org/10.1152/jn.91111.2008>
- Cardinal, R. N., & Cheung, T. H. (2005). Nucleus accumbens core lesions retard instrumental learning and performance with delayed reinforcement in the rat. *BMC Neurosci*, 6, 9. <https://doi.org/10.1186/1471-2202-6-9>
- Carlsson, A. (2001). A half-century of neurotransmitter research: impact on neurology and psychiatry (Nobel lecture). *Chembiochem*, 2(7-8), 484-493. [https://doi.org/10.1002/1439-7633\(20010803\)2:7/8<484::AID-CBIC484>3.0.CO;2-5](https://doi.org/10.1002/1439-7633(20010803)2:7/8<484::AID-CBIC484>3.0.CO;2-5)
- Chaudhury, D., Walsh, J. J., Friedman, A. K., Juarez, B., Ku, S. M., Koo, J. W., Ferguson, D., Tsai, H. C., Pomeranz, L., Christoffel, D. J., Nectow, A. R., Ekstrand, M., Domingos, A., Mazei-Robison, M. S., Mouzon, E., Lobo, M. K., Neve, R. L., Friedman, J. M., Russo, S. J., . . . Han, M. H. (2013). Rapid regulation of depression-related behaviours by control of midbrain dopamine neurons. *Nature*, 493(7433), 532-536. <https://doi.org/10.1038/nature11713>
- Chidambaram, S. B., Rathipriya, A. G., Bolla, S. R., Bhat, A., Ray, B., Mahalakshmi, A. M., Manivasagam, T., Thenmozhi, A. J., Essa, M. M., Guillemin, G. J., Chandra, R., & Sakharkar, M. K. (2019). Dendritic spines: Revisiting the physiological role. *Prog Neuropsychopharmacol Biol Psychiatry*, 92, 161-193. <https://doi.org/10.1016/j.pnpbp.2019.01.005>
- Christoffel, D. J., Golden, S. A., Dumitriu, D., Robison, A. J., Janssen, W. G., Ahn, H. F., Krishnan, V., Reyes, C. M., Han, M. H., Ables, J. L., Eisch, A. J., Dietz, D. M., Ferguson, D., Neve, R. L., Greengard, P., Kim, Y., Morrison, J. H., & Russo, S. J. (2011). IkappaB kinase regulates social defeat stress-induced synaptic and behavioral plasticity. *J Neurosci*, 31(1), 314-321. <https://doi.org/10.1523/JNEUROSCI.4763-10.2011>
- Christoffel, D. J., Golden, S. A., & Russo, S. J. (2011). Structural and synaptic plasticity in stress-related disorders. *Rev Neurosci*, 22(5), 535-549. <https://doi.org/10.1515/RNS.2011.044>

- Codocedo, J. F., Allard, C., Godoy, J. A., Varela-Nallar, L., & Inestrosa, N. C. (2012). SIRT1 regulates dendritic development in hippocampal neurons. *PLoS One*, 7(10), e47073. <https://doi.org/10.1371/journal.pone.0047073>
- Cohen, H., Kozlovsky, N., Matar, M. A., Zohar, J., & Kaplan, Z. (2014). Distinctive hippocampal and amygdalar cytoarchitectural changes underlie specific patterns of behavioral disruption following stress exposure in an animal model of PTSD. *Eur Neuropsychopharmacol*, 24(12), 1925-1944. <https://doi.org/10.1016/j.euroneuro.2014.09.009>
- Colyn, L., Venzala, E., Marco, S., Perez-Otano, I., & Tordera, R. M. (2019). Chronic social defeat stress induces sustained synaptic structural changes in the prefrontal cortex and amygdala. *Behav Brain Res*, 373, 112079. <https://doi.org/10.1016/j.bbr.2019.112079>
- consortium, C. (2015). Sparse whole-genome sequencing identifies two loci for major depressive disorder. *Nature*, 523(7562), 588-591. <https://doi.org/10.1038/nature14659>
- Covington, H. E., 3rd, Lobo, M. K., Maze, I., Vialou, V., Hyman, J. M., Zaman, S., LaPlant, Q., Mouzon, E., Ghose, S., Tamminga, C. A., Neve, R. L., Deisseroth, K., & Nestler, E. J. (2010). Antidepressant effect of optogenetic stimulation of the medial prefrontal cortex. *J Neurosci*, 30(48), 16082-16090. <https://doi.org/10.1523/JNEUROSCI.1731-10.2010>
- Covington, H. E., 3rd, Maze, I., LaPlant, Q. C., Vialou, V. F., Ohnishi, Y. N., Berton, O., Fass, D. M., Renthal, W., Rush, A. J., 3rd, Wu, E. Y., Ghose, S., Krishnan, V., Russo, S. J., Tamminga, C., Haggarty, S. J., & Nestler, E. J. (2009). Antidepressant actions of histone deacetylase inhibitors. *J Neurosci*, 29(37), 11451-11460. <https://doi.org/10.1523/JNEUROSCI.1758-09.2009>
- D'Angelo, S., Mele, E., Di Filippo, F., Viggiano, A., & Meccariello, R. (2021). Sirt1 Activity in the Brain: Simultaneous Effects on Energy Homeostasis and Reproduction. *Int J Environ Res Public Health*, 18(3). <https://doi.org/10.3390/ijerph18031243>
- Di Chiara, G., Loddo, P., & Tanda, G. (1999). Reciprocal changes in prefrontal and limbic dopamine responsiveness to aversive and rewarding stimuli after chronic mild stress: implications for the psychobiology of depression. *Biol Psychiatry*, 46(12), 1624-1633. [https://doi.org/10.1016/s0006-3223\(99\)00236-x](https://doi.org/10.1016/s0006-3223(99)00236-x)
- Di Chiara, G., & Tanda, G. (1997). Blunting of reactivity of dopamine transmission to palatable food: a biochemical marker of anhedonia in the CMS model?



- Psychopharmacology (Berl)*, 134(4), 351-353; discussion 371-357.  
<https://doi.org/10.1007/s002130050465>
- Dorostkar, M. M., Zou, C., Blazquez-Llorca, L., & Herms, J. (2015). Analyzing dendritic spine pathology in Alzheimer's disease: problems and opportunities. *Acta Neuropathol*, 130(1), 1-19. <https://doi.org/10.1007/s00401-015-1449-5>
- Douma, E. H., & de Kloet, E. R. (2020). Stress-induced plasticity and functioning of ventral tegmental dopamine neurons. *Neurosci Biobehav Rev*, 108, 48-77. <https://doi.org/10.1016/j.neubiorev.2019.10.015>
- Drevets, W. C., Price, J. L., & Furey, M. L. (2008). Brain structural and functional abnormalities in mood disorders: implications for neurocircuitry models of depression. *Brain Struct Funct*, 213(1-2), 93-118. <https://doi.org/10.1007/s00429-008-0189-x>
- Ethell, I. M., & Pasquale, E. B. (2005). Molecular mechanisms of dendritic spine development and remodeling. *Prog Neurobiol*, 75(3), 161-205. <https://doi.org/10.1016/j.pneurobio.2005.02.003>
- Fasano, C., Bourque, M. J., Lapointe, G., Leo, D., Thibault, D., Haber, M., Kortleven, C., Desgroseillers, L., Murai, K. K., & Trudeau, L. E. (2013). Dopamine facilitates dendritic spine formation by cultured striatal medium spiny neurons through both D1 and D2 dopamine receptors. *Neuropharmacology*, 67, 432-443. <https://doi.org/10.1016/j.neuropharm.2012.11.030>
- Ferguson, D., Koo, J. W., Feng, J., Heller, E., Rabkin, J., Heshmati, M., Renthal, W., Neve, R., Liu, X., Shao, N., Sartorelli, V., Shen, L., & Nestler, E. J. (2013). Essential role of SIRT1 signaling in the nucleus accumbens in cocaine and morphine action. *J Neurosci*, 33(41), 16088-16098. <https://doi.org/10.1523/JNEUROSCI.1284-13.2013>
- Fiala, J. C., Feinberg, M., Popov, V., & Harris, K. M. (1998). Synaptogenesis via dendritic filopodia in developing hippocampal area CA1. *J Neurosci*, 18(21), 8900-8911. <https://www.ncbi.nlm.nih.gov/pubmed/9786995>
- Floresco, S. B. (2015). The nucleus accumbens: an interface between cognition, emotion, and action. *Annu Rev Psychol*, 66, 25-52. <https://doi.org/10.1146/annurev-psych-010213-115159>
- Forlano, P. M., & Woolley, C. S. (2010). Quantitative analysis of pre- and postsynaptic sex differences in the nucleus accumbens. *J Comp Neurol*, 518(8), 1330-1348. <https://doi.org/10.1002/cne.22279>

- Fox, M. E., Chandra, R., Menken, M. S., Larkin, E. J., Nam, H., Engeln, M., Francis, T. C., & Lobo, M. K. (2020). Dendritic remodeling of D1 neurons by RhoA/Rho-kinase mediates depression-like behavior. *Mol Psychiatry*, 25(5), 1022-1034. <https://doi.org/10.1038/s41380-018-0211-5>
- Fox, M. E., Figueiredo, A., Menken, M. S., & Lobo, M. K. (2020). Dendritic spine density is increased on nucleus accumbens D2 neurons after chronic social defeat. *Sci Rep*, 10(1), 12393. <https://doi.org/10.1038/s41598-020-69339-7>
- Francis, T. C., Chandra, R., Friend, D. M., Finkel, E., Dayrit, G., Miranda, J., Brooks, J. M., Iniguez, S. D., O'Donnell, P., Kravitz, A., & Lobo, M. K. (2015). Nucleus accumbens medium spiny neuron subtypes mediate depression-related outcomes to social defeat stress. *Biol Psychiatry*, 77(3), 212-222. <https://doi.org/10.1016/j.biopsych.2014.07.021>
- Gangarossa, G., Espallergues, J., de Kerchove d'Exaerde, A., El Mestikawy, S., Gerfen, C. R., Herve, D., Girault, J. A., & Valjent, E. (2013). Distribution and compartmental organization of GABAergic medium-sized spiny neurons in the mouse nucleus accumbens. *Front Neural Circuits*, 7, 22. <https://doi.org/10.3389/fncir.2013.00022>
- Gao, J., Wang, W. Y., Mao, Y. W., Graff, J., Guan, J. S., Pan, L., Mak, G., Kim, D., Su, S. C., & Tsai, L. H. (2010). A novel pathway regulates memory and plasticity via SIRT1 and miR-134. *Nature*, 466(7310), 1105-1109. <https://doi.org/10.1038/nature09271>
- Gerfen, C. R., Herkenham, M., & Thibault, J. (1987). The neostriatal mosaic: II. Patch- and matrix-directed mesostriatal dopaminergic and non-dopaminergic systems. *J Neurosci*, 7(12), 3915-3934. <https://www.ncbi.nlm.nih.gov/pubmed/2891799>
- Gerfen, C. R., Paletzki, R., & Heintz, N. (2013). GENSAT BAC cre-recombinase driver lines to study the functional organization of cerebral cortical and basal ganglia circuits. *Neuron*, 80(6), 1368-1383. <https://doi.org/10.1016/j.neuron.2013.10.016>
- Gipson, C. D., & Olive, M. F. (2017). Structural and functional plasticity of dendritic spines - root or result of behavior? *Genes Brain Behav*, 16(1), 101-117. <https://doi.org/10.1111/gbb.12324>
- Gong, S., Doughty, M., Harbaugh, C. R., Cummins, A., Hatten, M. E., Heintz, N., & Gerfen, C. R. (2007). Targeting Cre recombinase to specific neuron populations with bacterial artificial chromosome constructs. *J Neurosci*, 27(37), 9817-9823. <https://doi.org/10.1523/JNEUROSCI.2707-07.2007>
- Greengard, P. (2001). The neurobiology of slow synaptic transmission. *Science*, 294(5544), 1024-1030. <https://doi.org/10.1126/science.294.5544.1024>

- Guarente, L. (2000). Sir2 links chromatin silencing, metabolism, and aging. *Genes Dev*, 14(9), 1021-1026. <https://www.ncbi.nlm.nih.gov/pubmed/10809662>
- Guo, H., Deji, C., Peng, H., Zhang, J., Chen, Y., Zhang, Y., & Wang, Y. (2021). The role of SIRT1 in the basolateral amygdala in depression-like behaviors in mice. *Genes Brain Behav*, 20(8), e12765. <https://doi.org/10.1111/gbb.12765>
- Haigis, M. C., & Sinclair, D. A. (2010). Mammalian sirtuins: biological insights and disease relevance. *Annu Rev Pathol*, 5, 253-295. <https://doi.org/10.1146/annurev.pathol.4.110807.092250>
- Halpain, S., Hipolito, A., & Saffer, L. (1998). Regulation of F-actin stability in dendritic spines by glutamate receptors and calcineurin. *J Neurosci*, 18(23), 9835-9844. <https://www.ncbi.nlm.nih.gov/pubmed/9822742>
- Harris, A. Z., Atsak, P., Bretton, Z. H., Holt, E. S., Alam, R., Morton, M. P., Abbas, A. I., Leonardo, E. D., Bolkan, S. S., Hen, R., & Gordon, J. A. (2018). A Novel Method for Chronic Social Defeat Stress in Female Mice. *Neuropsychopharmacology*, 43(6), 1276-1283. <https://doi.org/10.1038/npp.2017.259>
- Harris, K. M., Jensen, F. E., & Tsao, B. (1992). Three-dimensional structure of dendritic spines and synapses in rat hippocampus (CA1) at postnatal day 15 and adult ages: implications for the maturation of synaptic physiology and long-term potentiation. *J Neurosci*, 12(7), 2685-2705. <https://www.ncbi.nlm.nih.gov/pubmed/1613552>
- Heimer, L., Zahm, D. S., Churchill, L., Kalivas, P. W., & Wohltmann, C. (1991). Specificity in the projection patterns of accumbal core and shell in the rat. *Neuroscience*, 41(1), 89-125. [https://doi.org/10.1016/0306-4522\(91\)90202-y](https://doi.org/10.1016/0306-4522(91)90202-y)
- Helm, M. S., Dankovich, T. M., Mandad, S., Rammner, B., Jahne, S., Salimi, V., Koerbs, C., Leibrandt, R., Urlaub, H., Schikorski, T., & Rizzoli, S. O. (2021). A large-scale nanoscopy and biochemistry analysis of postsynaptic dendritic spines. *Nat Neurosci*, 24(8), 1151-1162. <https://doi.org/10.1038/s41593-021-00874-w>
- Hering, H., & Sheng, M. (2001). Dendritic spines: structure, dynamics and regulation. *Nat Rev Neurosci*, 2(12), 880-888. <https://doi.org/10.1038/35104061>
- Hering, H., & Sheng, M. (2003). Activity-dependent redistribution and essential role of cortactin in dendritic spine morphogenesis. *J Neurosci*, 23(37), 11759-11769. <https://www.ncbi.nlm.nih.gov/pubmed/14684878>
- Heshmati, M., Christoffel, D. J., LeClair, K., Cathomas, F., Golden, S. A., Aleyasin, H., Turecki, G., Friedman, A. K., Han, M. H., Menard, C., & Russo, S. J. (2020). Depression and Social Defeat Stress Are Associated with Inhibitory Synaptic

- Changes in the Nucleus Accumbens. *J Neurosci*, 40(32), 6228-6233.  
<https://doi.org/10.1523/JNEUROSCI.2568-19.2020>
- Hillhouse, T. M., & Porter, J. H. (2015). A brief history of the development of antidepressant drugs: from monoamines to glutamate. *Exp Clin Psychopharmacol*, 23(1), 1-21. <https://doi.org/10.1037/a0038550>
- Hodes, G. E., Pfau, M. L., Purushothaman, I., Ahn, H. F., Golden, S. A., Christoffel, D. J., Magida, J., Brancato, A., Takahashi, A., Flanigan, M. E., Menard, C., Aleyasin, H., Koo, J. W., Lorsch, Z. S., Feng, J., Heshmati, M., Wang, M., Turecki, G., Neve, R., . . . Russo, S. J. (2015). Sex Differences in Nucleus Accumbens Transcriptome Profiles Associated with Susceptibility versus Resilience to Subchronic Variable Stress. *J Neurosci*, 35(50), 16362-16376.  
<https://doi.org/10.1523/JNEUROSCI.1392-15.2015>
- Iniguez, S. D., Aubry, A., Riggs, L. M., Alipio, J. B., Zanca, R. M., Flores-Ramirez, F. J., Hernandez, M. A., Nieto, S. J., Musheyev, D., & Serrano, P. A. (2016). Social defeat stress induces depression-like behavior and alters spine morphology in the hippocampus of adolescent male C57BL/6 mice. *Neurobiol Stress*, 5, 54-64.  
<https://doi.org/10.1016/j.ynstr.2016.07.001>
- Ito, R., Robbins, T. W., & Everitt, B. J. (2004). Differential control over cocaine-seeking behavior by nucleus accumbens core and shell. *Nat Neurosci*, 7(4), 389-397.  
<https://doi.org/10.1038/nn1217>
- Jones, S. R., O'Dell, S. J., Marshall, J. F., & Wightman, R. M. (1996). Functional and anatomical evidence for different dopamine dynamics in the core and shell of the nucleus accumbens in slices of rat brain. *Synapse*, 23(3), 224-231.  
[https://doi.org/10.1002/\(SICI\)1098-2396\(199607\)23:3<224::AID-SYN12>3.0.CO;2-Z](https://doi.org/10.1002/(SICI)1098-2396(199607)23:3<224::AID-SYN12>3.0.CO;2-Z)
- Kalivas, P. W., & Duffy, P. (1995). Selective activation of dopamine transmission in the shell of the nucleus accumbens by stress. *Brain Res*, 675(1-2), 325-328.  
[https://doi.org/10.1016/0006-8993\(95\)00013-g](https://doi.org/10.1016/0006-8993(95)00013-g)
- Kanjhan, R., Noakes, P. G., & Bellingham, M. C. (2016). Emerging Roles of Filopodia and Dendritic Spines in Motoneuron Plasticity during Development and Disease. *Neural Plast*, 2016, 3423267. <https://doi.org/10.1155/2016/3423267>
- Kim, H. D., Hesterman, J., Call, T., Magazu, S., Keeley, E., Armenta, K., Kronman, H., Neve, R. L., Nestler, E. J., & Ferguson, D. (2016). SIRT1 Mediates Depression-Like Behaviors in the Nucleus Accumbens. *J Neurosci*, 36(32), 8441-8452.  
<https://doi.org/10.1523/JNEUROSCI.0212-16.2016>

- Kirsch, I. (2014). Antidepressants and the Placebo Effect. *Z Psychol*, 222(3), 128-134. <https://doi.org/10.1027/2151-2604/a000176>
- Kishi, T., Yoshimura, R., Kitajima, T., Okochi, T., Okumura, T., Tsunoka, T., Yamanouchi, Y., Kinoshita, Y., Kawashima, K., Fukuo, Y., Naitoh, H., Umene-Nakano, W., Inada, T., Nakamura, J., Ozaki, N., & Iwata, N. (2010). SIRT1 gene is associated with major depressive disorder in the Japanese population. *J Affect Disord*, 126(1-2), 167-173. <https://doi.org/10.1016/j.jad.2010.04.003>
- Knott, G. W., Holtmaat, A., Wilbrecht, L., Welker, E., & Svoboda, K. (2006). Spine growth precedes synapse formation in the adult neocortex in vivo. *Nat Neurosci*, 9(9), 1117-1124. <https://doi.org/10.1038/nn1747>
- Knowland, D., & Lim, B. K. (2018). Circuit-based frameworks of depressive behaviors: The role of reward circuitry and beyond. *Pharmacol Biochem Behav*, 174, 42-52. <https://doi.org/10.1016/j.pbb.2017.12.010>
- Koob, G. F., & Bloom, F. E. (1988). Cellular and molecular mechanisms of drug dependence. *Science*, 242(4879), 715-723. <https://doi.org/10.1126/science.2903550>
- Korkotian, E., & Segal, M. (2011). Synaptopodin regulates release of calcium from stores in dendritic spines of cultured hippocampal neurons. *J Physiol*, 589(Pt 24), 5987-5995. <https://doi.org/10.1113/jphysiol.2011.217315>
- Krishnan, V., Han, M. H., Graham, D. L., Berton, O., Renthal, W., Russo, S. J., Laplant, Q., Graham, A., Lutter, M., Lagace, D. C., Ghose, S., Reister, R., Tannous, P., Green, T. A., Neve, R. L., Chakravarty, S., Kumar, A., Eisch, A. J., Self, D. W., . . . Nestler, E. J. (2007). Molecular adaptations underlying susceptibility and resistance to social defeat in brain reward regions. *Cell*, 131(2), 391-404. <https://doi.org/10.1016/j.cell.2007.09.018>
- Krishnan, V., & Nestler, E. J. (2008). The molecular neurobiology of depression. *Nature*, 455(7215), 894-902. <https://doi.org/10.1038/nature07455>
- Kullmann, D. M., & Asztely, F. (1998). Extrasynaptic glutamate spillover in the hippocampus: evidence and implications. *Trends Neurosci*, 21(1), 8-14. [https://doi.org/10.1016/s0166-2236\(97\)01150-8](https://doi.org/10.1016/s0166-2236(97)01150-8)
- Lai, K. O., Jordan, B. A., Ma, X. M., Srivastava, D. P., & Tolia, K. F. (2016). Molecular Mechanisms of Dendritic Spine Development and Plasticity. *Neural Plast*, 2016, 2078121. <https://doi.org/10.1155/2016/2078121>

- Lammel, S., Lim, B. K., & Malenka, R. C. (2014). Reward and aversion in a heterogeneous midbrain dopamine system. *Neuropharmacology*, *76 Pt B*, 351-359. <https://doi.org/10.1016/j.neuropharm.2013.03.019>
- Lei, Y., Wang, J., Wang, D., Li, C., Liu, B., Fang, X., You, J., Guo, M., & Lu, X. Y. (2020). SIRT1 in forebrain excitatory neurons produces sexually dimorphic effects on depression-related behaviors and modulates neuronal excitability and synaptic transmission in the medial prefrontal cortex. *Mol Psychiatry*, *25*(5), 1094-1111. <https://doi.org/10.1038/s41380-019-0352-1>
- Lendvai, B., Stern, E. A., Chen, B., & Svoboda, K. (2000). Experience-dependent plasticity of dendritic spines in the developing rat barrel cortex in vivo. *Nature*, *404*(6780), 876-881. <https://doi.org/10.1038/35009107>
- Leuner, B., & Shors, T. J. (2013). Stress, anxiety, and dendritic spines: what are the connections? *Neuroscience*, *251*, 108-119. <https://doi.org/10.1016/j.neuroscience.2012.04.021>
- Li, X. H., Chen, C., Tu, Y., Sun, H. T., Zhao, M. L., Cheng, S. X., Qu, Y., & Zhang, S. (2013). Sirt1 promotes axonogenesis by deacetylation of Akt and inactivation of GSK3. *Mol Neurobiol*, *48*(3), 490-499. <https://doi.org/10.1007/s12035-013-8437-3>
- Libert, S., Pointer, K., Bell, E. L., Das, A., Cohen, D. E., Asara, J. M., Kapur, K., Bergmann, S., Preisig, M., Otowa, T., Kendler, K. S., Chen, X., Hettema, J. M., van den Oord, E. J., Rubio, J. P., & Guarente, L. (2011). SIRT1 activates MAO-A in the brain to mediate anxiety and exploratory drive. *Cell*, *147*(7), 1459-1472. <https://doi.org/10.1016/j.cell.2011.10.054>
- Lim, B. K., Huang, K. W., Grueter, B. A., Rothwell, P. E., & Malenka, R. C. (2012). Anhedonia requires MC4R-mediated synaptic adaptations in nucleus accumbens. *Nature*, *487*(7406), 183-189. <https://doi.org/10.1038/nature11160>
- Lodge, D. J., & Grace, A. A. (2006). The hippocampus modulates dopamine neuron responsivity by regulating the intensity of phasic neuron activation. *Neuropsychopharmacology*, *31*(7), 1356-1361. <https://doi.org/10.1038/sj.npp.1300963>
- Luo, X. J., & Zhang, C. (2016). Down-Regulation of SIRT1 Gene Expression in Major Depressive Disorder. *Am J Psychiatry*, *173*(10), 1046. <https://doi.org/10.1176/appi.ajp.2016.16040394>
- Maiti, P., Manna, J., Ilavazhagan, G., Rossignol, J., & Dunbar, G. L. (2015). Molecular regulation of dendritic spine dynamics and their potential impact on synaptic

- plasticity and neurological diseases. *Neurosci Biobehav Rev*, 59, 208-237.  
<https://doi.org/10.1016/j.neubiorev.2015.09.020>
- Mattison, H. A., Popovkina, D., Kao, J. P., & Thompson, S. M. (2014). The role of glutamate in the morphological and physiological development of dendritic spines. *Eur J Neurosci*, 39(11), 1761-1770. <https://doi.org/10.1111/ejn.12536>
- McBurney, M. W., Clark-Knowles, K. V., Caron, A. Z., & Gray, D. A. (2013). SIRT1 is a Highly Networked Protein That Mediates the Adaptation to Chronic Physiological Stress. *Genes Cancer*, 4(3-4), 125-134.  
<https://doi.org/10.1177/1947601912474893>
- McEwen, B. S., Eiland, L., Hunter, R. G., & Miller, M. M. (2012). Stress and anxiety: structural plasticity and epigenetic regulation as a consequence of stress. *Neuropharmacology*, 62(1), 3-12.  
<https://doi.org/10.1016/j.neuropharm.2011.07.014>
- Meredith, G. E. (1999). The synaptic framework for chemical signaling in nucleus accumbens. *Ann N Y Acad Sci*, 877, 140-156. <https://doi.org/10.1111/j.1749-6632.1999.tb09266.x>
- Michan, S., Li, Y., Chou, M. M., Parrella, E., Ge, H., Long, J. M., Allard, J. S., Lewis, K., Miller, M., Xu, W., Mervis, R. F., Chen, J., Guerin, K. I., Smith, L. E., McBurney, M. W., Sinclair, D. A., Baudry, M., de Cabo, R., & Longo, V. D. (2010). SIRT1 is essential for normal cognitive function and synaptic plasticity. *J Neurosci*, 30(29), 9695-9707. <https://doi.org/10.1523/JNEUROSCI.0027-10.2010>
- Monteggia, L. M., Luikart, B., Barrot, M., Theobald, D., Malkovska, I., Nef, S., Parada, L. F., & Nestler, E. J. (2007). Brain-derived neurotrophic factor conditional knockouts show gender differences in depression-related behaviors. *Biol Psychiatry*, 61(2), 187-197. <https://doi.org/10.1016/j.biopsych.2006.03.021>
- Muir, J., Lorsch, Z. S., Ramakrishnan, C., Deisseroth, K., Nestler, E. J., Calipari, E. S., & Bagot, R. C. (2018). In Vivo Fiber Photometry Reveals Signature of Future Stress Susceptibility in Nucleus Accumbens. *Neuropsychopharmacology*, 43(2), 255-263. <https://doi.org/10.1038/npp.2017.122>
- Nauczyciel, C., Robic, S., Dondaine, T., Verin, M., Robert, G., Drapier, D., Naudet, F., & Millet, B. (2013). The nucleus accumbens: a target for deep brain stimulation in resistant major depressive disorder. *J Mol Psychiatry*, 1, 17.  
<https://doi.org/10.1186/2049-9256-1-17>
- Nestler, E. J., Barrot, M., DiLeone, R. J., Eisch, A. J., Gold, S. J., & Monteggia, L. M. (2002). Neurobiology of depression. *Neuron*, 34(1), 13-25.  
[https://doi.org/10.1016/s0896-6273\(02\)00653-0](https://doi.org/10.1016/s0896-6273(02)00653-0)

- Nestler, E. J., & Carlezon, W. A., Jr. (2006). The mesolimbic dopamine reward circuit in depression. *Biol Psychiatry*, *59*(12), 1151-1159.  
<https://doi.org/10.1016/j.biopsych.2005.09.018>
- Ng, F., Wijaya, L., & Tang, B. L. (2015). SIRT1 in the brain-connections with aging-associated disorders and lifespan. *Front Cell Neurosci*, *9*, 64.  
<https://doi.org/10.3389/fncel.2015.00064>
- Nicola, S. M., Surmeier, J., & Malenka, R. C. (2000). Dopaminergic modulation of neuronal excitability in the striatum and nucleus accumbens. *Annu Rev Neurosci*, *23*, 185-215. <https://doi.org/10.1146/annurev.neuro.23.1.185>
- Nimchinsky, E. A., Sabatini, B. L., & Svoboda, K. (2002). Structure and function of dendritic spines. *Annu Rev Physiol*, *64*, 313-353.  
<https://doi.org/10.1146/annurev.physiol.64.081501.160008>
- Nusser, Z., Lujan, R., Laube, G., Roberts, J. D., Molnar, E., & Somogyi, P. (1998). Cell type and pathway dependence of synaptic AMPA receptor number and variability in the hippocampus. *Neuron*, *21*(3), 545-559. [https://doi.org/10.1016/s0896-6273\(00\)80565-6](https://doi.org/10.1016/s0896-6273(00)80565-6)
- O'Brien, J. A., & Lummis, S. C. (2006). Diolistic labeling of neuronal cultures and intact tissue using a hand-held gene gun. *Nat Protoc*, *1*(3), 1517-1521.  
<https://doi.org/10.1038/nprot.2006.258>
- Ostroumov, A., & Dani, J. A. (2018). Inhibitory Plasticity of Mesocorticolimbic Circuits in Addiction and Mental Illness. *Trends Neurosci*, *41*(12), 898-910.  
<https://doi.org/10.1016/j.tins.2018.07.014>
- Parajuli, L. K., Ageta-Ishihara, N., Ageta, H., Fukazawa, Y., & Kinoshita, M. (2016). Methods for immunoblot detection and electron microscopic localization of septin subunits in mammalian nervous systems. *Methods Cell Biol*, *136*, 285-294.  
<https://doi.org/10.1016/bs.mcb.2016.04.021>
- Park, M. (2018). AMPA Receptor Trafficking for Postsynaptic Potentiation. *Front Cell Neurosci*, *12*, 361. <https://doi.org/10.3389/fncel.2018.00361>
- Petrak, L. J., Harris, K. M., & Kirov, S. A. (2005). Synaptogenesis on mature hippocampal dendrites occurs via filopodia and immature spines during blocked synaptic transmission. *J Comp Neurol*, *484*(2), 183-190.  
<https://doi.org/10.1002/cne.20468>
- Petralia, R. S., Esteban, J. A., Wang, Y. X., Partridge, J. G., Zhao, H. M., Wenthold, R. J., & Malinow, R. (1999). Selective acquisition of AMPA receptors over postnatal



- development suggests a molecular basis for silent synapses. *Nat Neurosci*, 2(1), 31-36. <https://doi.org/10.1038/4532>
- Pittenger, C., & Duman, R. S. (2008). Stress, depression, and neuroplasticity: a convergence of mechanisms. *Neuropsychopharmacology*, 33(1), 88-109. <https://doi.org/10.1038/sj.npp.1301574>
- Qiao, H., An, S. C., Xu, C., & Ma, X. M. (2017). Role of proBDNF and BDNF in dendritic spine plasticity and depressive-like behaviors induced by an animal model of depression. *Brain Res*, 1663, 29-37. <https://doi.org/10.1016/j.brainres.2017.02.020>
- Quessy, F., Bittar, T., Blanchette, L. J., Levesque, M., & Labonte, B. (2021). Stress-induced alterations of mesocortical and mesolimbic dopaminergic pathways. *Sci Rep*, 11(1), 11000. <https://doi.org/10.1038/s41598-021-90521-y>
- Radley, J. J., Rocher, A. B., Rodriguez, A., Ehlenberger, D. B., Dammann, M., McEwen, B. S., Morrison, J. H., Wearne, S. L., & Hof, P. R. (2008). Repeated stress alters dendritic spine morphology in the rat medial prefrontal cortex. *J Comp Neurol*, 507(1), 1141-1150. <https://doi.org/10.1002/cne.21588>
- Runge, K., Cardoso, C., & de Chevigny, A. (2020). Dendritic Spine Plasticity: Function and Mechanisms. *Front Synaptic Neurosci*, 12, 36. <https://doi.org/10.3389/fnsyn.2020.00036>
- Russo, S. J., & Nestler, E. J. (2013). The brain reward circuitry in mood disorders. *Nat Rev Neurosci*, 14(9), 609-625. <https://doi.org/10.1038/nrn3381>
- Sala, C., Cambianica, I., & Rossi, F. (2008). Molecular mechanisms of dendritic spine development and maintenance. *Acta Neurobiol Exp (Wars)*, 68(2), 289-304. <https://www.ncbi.nlm.nih.gov/pubmed/18511962>
- Salgado, S., & Kaplitt, M. G. (2015). The Nucleus Accumbens: A Comprehensive Review. *Stereotact Funct Neurosurg*, 93(2), 75-93. <https://doi.org/10.1159/000368279>
- Sarkar, A., & Kabbaj, M. (2016). Sex Differences in Effects of Ketamine on Behavior, Spine Density, and Synaptic Proteins in Socially Isolated Rats. *Biol Psychiatry*, 80(6), 448-456. <https://doi.org/10.1016/j.biopsych.2015.12.025>
- Schatzle, P., Esteves da Silva, M., Tas, R. P., Katrukha, E. A., Hu, H. Y., Wierenga, C. J., Kapitein, L. C., & Hoogenraad, C. C. (2018). Activity-Dependent Actin Remodeling at the Base of Dendritic Spines Promotes Microtubule Entry. *Curr Biol*, 28(13), 2081-2093 e2086. <https://doi.org/10.1016/j.cub.2018.05.004>

- Scheggi, S., Leggio, B., Masi, F., Grappi, S., Gambarana, C., Nanni, G., Rauggi, R., & De Montis, M. G. (2002). Selective modifications in the nucleus accumbens of dopamine synaptic transmission in rats exposed to chronic stress. *J Neurochem*, 83(4), 895-903. <https://doi.org/10.1046/j.1471-4159.2002.01193.x>
- Schlaepfer, T. E., Cohen, M. X., Frick, C., Kosel, M., Brodesser, D., Axmacher, N., Joe, A. Y., Kreft, M., Lenartz, D., & Sturm, V. (2008). Deep brain stimulation to reward circuitry alleviates anhedonia in refractory major depression. *Neuropsychopharmacology*, 33(2), 368-377. <https://doi.org/10.1038/sj.npp.1301408>
- Schmidt, H., & Eilers, J. (2009). Spine neck geometry determines spino-dendritic cross-talk in the presence of mobile endogenous calcium binding proteins. *J Comput Neurosci*, 27(2), 229-243. <https://doi.org/10.1007/s10827-009-0139-5>
- Schratt, G. M., Tuebing, F., Nigh, E. A., Kane, C. G., Sabatini, M. E., Kiebler, M., & Greenberg, M. E. (2006). A brain-specific microRNA regulates dendritic spine development. *Nature*, 439(7074), 283-289. <https://doi.org/10.1038/nature04367>
- Shirayama, Y., & Chaki, S. (2006). Neurochemistry of the nucleus accumbens and its relevance to depression and antidepressant action in rodents. *Curr Neuropharmacol*, 4(4), 277-291. <https://doi.org/10.2174/157015906778520773>
- Sholl, D. A. (1953). Dendritic organization in the neurons of the visual and motor cortices of the cat. *J Anat*, 87(4), 387-406. <https://www.ncbi.nlm.nih.gov/pubmed/13117757>
- Smith-Roe, S. L., & Kelley, A. E. (2000). Coincident activation of NMDA and dopamine D1 receptors within the nucleus accumbens core is required for appetitive instrumental learning. *J Neurosci*, 20(20), 7737-7742. <https://www.ncbi.nlm.nih.gov/pubmed/11027236>
- Smith, R. J., Lobo, M. K., Spencer, S., & Kalivas, P. W. (2013). Cocaine-induced adaptations in D1 and D2 accumbens projection neurons (a dichotomy not necessarily synonymous with direct and indirect pathways). *Curr Opin Neurobiol*, 23(4), 546-552. <https://doi.org/10.1016/j.conb.2013.01.026>
- Staffend, N. A., & Meisel, R. L. (2011). DiOlistic labeling in fixed brain slices: phenotype, morphology, and dendritic spines. *Curr Protoc Neurosci*, Chapter 2, Unit 2 13. <https://doi.org/10.1002/0471142301.ns0213s55>
- Tada, T., & Sheng, M. (2006). Molecular mechanisms of dendritic spine morphogenesis. *Curr Opin Neurobiol*, 16(1), 95-101. <https://doi.org/10.1016/j.conb.2005.12.001>

- Takumi, Y., Ramirez-Leon, V., Laake, P., Rinvik, E., & Ottersen, O. P. (1999). Different modes of expression of AMPA and NMDA receptors in hippocampal synapses. *Nat Neurosci*, 2(7), 618-624. <https://doi.org/10.1038/10172>
- Tidey, J. W., & Miczek, K. A. (1996). Social defeat stress selectively alters mesocorticolimbic dopamine release: an in vivo microdialysis study. *Brain Res*, 721(1-2), 140-149. [https://doi.org/10.1016/0006-8993\(96\)00159-x](https://doi.org/10.1016/0006-8993(96)00159-x)
- van der Kooij, M. A., Masana, M., Rust, M. B., & Muller, M. B. (2016). The stressed cytoskeleton: How actin dynamics can shape stress-related consequences on synaptic plasticity and complex behavior. *Neurosci Biobehav Rev*, 62, 69-75. <https://doi.org/10.1016/j.neubiorev.2015.12.001>
- Varghese, M., Keshav, N., Jacot-Descombes, S., Warda, T., Wicinski, B., Dickstein, D. L., Harony-Nicolas, H., De Rubeis, S., Drapeau, E., Buxbaum, J. D., & Hof, P. R. (2017). Autism spectrum disorder: neuropathology and animal models. *Acta Neuropathol*, 134(4), 537-566. <https://doi.org/10.1007/s00401-017-1736-4>
- Vialou, V., Robison, A. J., Laplant, Q. C., Covington, H. E., 3rd, Dietz, D. M., Ohnishi, Y. N., Mouzon, E., Rush, A. J., 3rd, Watts, E. L., Wallace, D. L., Iniguez, S. D., Ohnishi, Y. H., Steiner, M. A., Warren, B. L., Krishnan, V., Bolanos, C. A., Neve, R. L., Ghose, S., Berton, O., . . . Nestler, E. J. (2010). DeltaFosB in brain reward circuits mediates resilience to stress and antidepressant responses. *Nat Neurosci*, 13(6), 745-752. <https://doi.org/10.1038/nn.2551>
- Volfovsky, N., Parnas, H., Segal, M., & Korkotian, E. (1999). Geometry of dendritic spines affects calcium dynamics in hippocampal neurons: theory and experiments. *J Neurophysiol*, 82(1), 450-462. <https://doi.org/10.1152/jn.1999.82.1.450>
- Voorn, P., Vanderschuren, L. J., Groenewegen, H. J., Robbins, T. W., & Pennartz, C. M. (2004). Putting a spin on the dorsal-ventral divide of the striatum. *Trends Neurosci*, 27(8), 468-474. <https://doi.org/10.1016/j.tins.2004.06.006>
- Walker, D. M., Zhou, X., Cunningham, A. M., Lipschultz, A. P., Ramakrishnan, A., Cates, H. M., Bagot, R. C., Shen, L., Zhang, B., & Nestler, E. J. (2022). Sex-Specific Transcriptional Changes in Response to Adolescent Social Stress in the Brain's Reward Circuitry. *Biol Psychiatry*, 91(1), 118-128. <https://doi.org/10.1016/j.biopsych.2021.02.964>
- Watanabe, Y., Gould, E., & McEwen, B. S. (1992). Stress induces atrophy of apical dendrites of hippocampal CA3 pyramidal neurons. *Brain Res*, 588(2), 341-345. [https://doi.org/10.1016/0006-8993\(92\)91597-8](https://doi.org/10.1016/0006-8993(92)91597-8)
- Weed, S. A., Karginov, A. V., Schafer, D. A., Weaver, A. M., Kinley, A. W., Cooper, J. A., & Parsons, J. T. (2000). Cortactin localization to sites of actin assembly in

- lamellipodia requires interactions with F-actin and the Arp2/3 complex. *J Cell Biol*, 151(1), 29-40. <https://doi.org/10.1083/jcb.151.1.29>
- Whittaker, J. R., Foley, S. F., Ackling, E., Murphy, K., & Caseras, X. (2018). The Functional Connectivity Between the Nucleus Accumbens and the Ventromedial Prefrontal Cortex as an Endophenotype for Bipolar Disorder. *Biol Psychiatry*, 84(11), 803-809. <https://doi.org/10.1016/j.biopsych.2018.07.023>
- Willner, P., Muscat, R., & Papp, M. (1992). Chronic mild stress-induced anhedonia: a realistic animal model of depression. *Neurosci Biobehav Rev*, 16(4), 525-534. [https://doi.org/10.1016/s0149-7634\(05\)80194-0](https://doi.org/10.1016/s0149-7634(05)80194-0)
- Wissman, A. M., May, R. M., & Woolley, C. S. (2012). Ultrastructural analysis of sex differences in nucleus accumbens synaptic connectivity. *Brain Struct Funct*, 217(2), 181-190. <https://doi.org/10.1007/s00429-011-0353-6>
- Wook Koo, J., Labonte, B., Engmann, O., Calipari, E. S., Juarez, B., Lorsch, Z., Walsh, J. J., Friedman, A. K., Yorgason, J. T., Han, M. H., & Nestler, E. J. (2016). Essential Role of Mesolimbic Brain-Derived Neurotrophic Factor in Chronic Social Stress-Induced Depressive Behaviors. *Biol Psychiatry*, 80(6), 469-478. <https://doi.org/10.1016/j.biopsych.2015.12.009>
- Yanez, M., Padin, J. F., Arranz-Tagarro, J. A., Camina, M., & Laguna, R. (2012). History and therapeutic use of MAO-A inhibitors: a historical perspective of mao-a inhibitors as antidepressant drug. *Curr Top Med Chem*, 12(20), 2275-2282. <https://doi.org/10.2174/156802612805220011>
- Yao, W. D., Spealman, R. D., & Zhang, J. (2008). Dopaminergic signaling in dendritic spines. *Biochem Pharmacol*, 75(11), 2055-2069. <https://doi.org/10.1016/j.bcp.2008.01.018>
- Yu, D., Homiack, D. R., Sawyer, E. J., & Schrader, L. A. (2018). BK channel deacetylation by SIRT1 in dentate gyrus regulates anxiety and response to stress. *Commun Biol*, 1, 82. <https://doi.org/10.1038/s42003-018-0088-5>
- Zahm, D. S., & Heimer, L. (1990). Two transpallidal pathways originating in the rat nucleus accumbens. *J Comp Neurol*, 302(3), 437-446. <https://doi.org/10.1002/cne.903020302>
- Zampa, F., Bicker, S., & Schratt, G. (2018). Activity-Dependent Pre-miR-134 Dendritic Localization Is Required for Hippocampal Neuron Dendritogenesis. *Front Mol Neurosci*, 11, 171. <https://doi.org/10.3389/fnmol.2018.00171>
- Zhang, Y., Zhang, M., Dong, H., Yong, S., Li, X., Olashaw, N., Kruk, P. A., Cheng, J. Q., Bai, W., Chen, J., Nicosia, S. V., & Zhang, X. (2009). Deacetylation of

- cortactin by SIRT1 promotes cell migration. *Oncogene*, 28(3), 445-460.  
<https://doi.org/10.1038/onc.2008.388>
- Ziv, N. E., & Smith, S. J. (1996). Evidence for a role of dendritic filopodia in synaptogenesis and spine formation. *Neuron*, 17(1), 91-102.  
[https://doi.org/10.1016/s0896-6273\(00\)80283-4](https://doi.org/10.1016/s0896-6273(00)80283-4)
- Zocchi, L., & Sassone-Corsi, P. (2012). SIRT1-mediated deacetylation of MeCP2 contributes to BDNF expression. *Epigenetics*, 7(7), 695-700.  
<https://doi.org/10.4161/epi.20733>
- Zuo, Y., Lin, A., Chang, P., & Gan, W. B. (2005). Development of long-term dendritic spine stability in diverse regions of cerebral cortex. *Neuron*, 46(2), 181-189.  
<https://doi.org/10.1016/j.neuron.2005.04.001>
- [www.mentalhealthamerica.net/suicide](http://www.mentalhealthamerica.net/suicide)
- [www.ncbi.nlm.nih.gov/pubmedhealth/PMH0087089/](http://www.ncbi.nlm.nih.gov/pubmedhealth/PMH0087089/)
- [www.nimh.nih.gov](http://www.nimh.nih.gov), 2001
- [www.who.int](http://www.who.int), 2016
- [www.who.int](http://www.who.int), 2020
- [www.who.int/mental\\_health/prevention/genderwomen/en/](http://www.who.int/mental_health/prevention/genderwomen/en/)

APPENDIX A

TABLES

### Spine Densities

Genotype	Sholl	Whole Cell	Stubby	Filopodia	Thin	Mushroom
SIRT1-KO, D1 M	↔	↔	↔	↔	↔	↔
SIRT1-OVEXP, D1 M	↔	↔	↑	↔	↔	↓
SIRT1-KO, D1 F	↑	↔	↔	↔	↑	↑
SIRT1-OVEXP, D1 F	↔	↔	↓	↑	↔	↑
SIRT1-KO, D2 M	↔	↑	↑	↑	↑	↔
SIRT1-OVEXP, D2 M	↔	↑	↑	↑	↑	↔
SIRT1-KO, D2 F	↔	↔	↔	↓	↓	↓
SIRT1-OVEXP, D2 F	↓	↔	↑	↔	↔	↔

↔	No change
↓	Sig. increase
↑	Sig. decrease

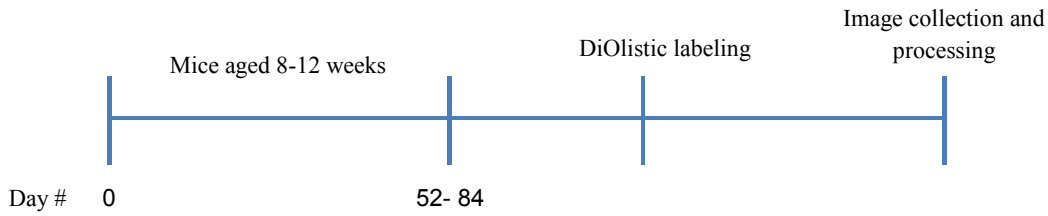
**Table 1.** Comparison of all groups for changes in the following measurements: Total number of Sholl intersections; Whole cell spine density; Whole cell stubby, filopodia, thin and mushroom spines.

## APPENDIX B

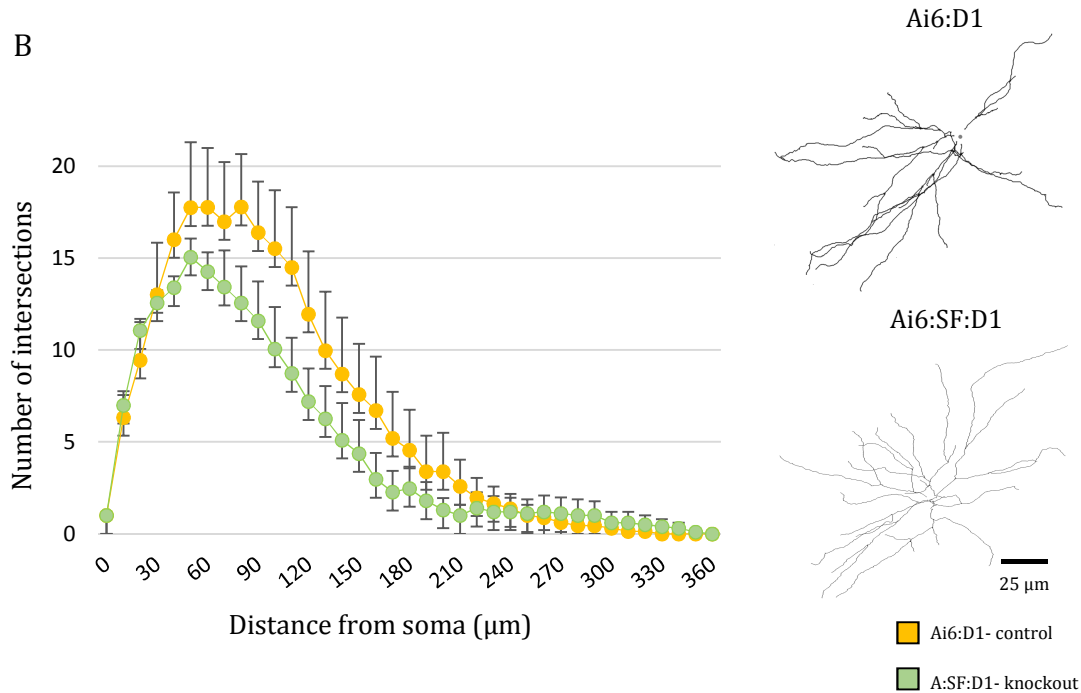
### FIGURES



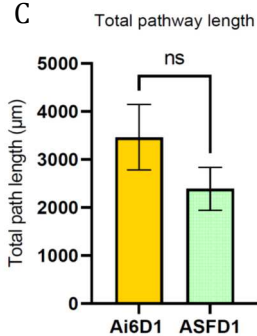
## A Timeline of Experimental Procedures



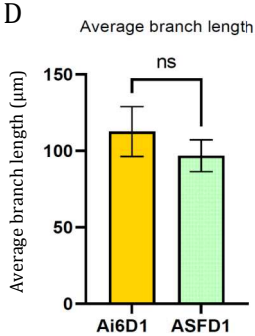
## B



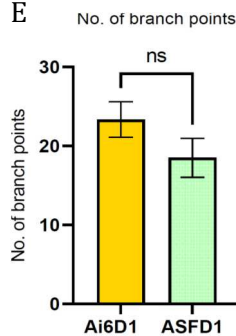
## C



## D



## E



## F

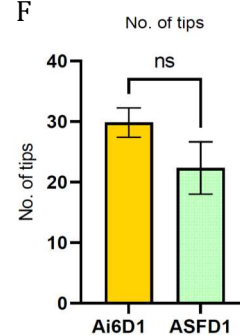


**Figure 1.** Dendritic morphology of male SIRT1- knock-out in D1-MSNs. (A) Timeline of experimental procedures. (B) Sholl analysis of SIRT1-KO-D1 males and representative traces (Sholl analysis: 2-way repeated measures ANOVA,  $p=0.897$ ; Ai6D1,  $n=10$  cells from 4 animals; ASFD1,  $n=11$  cells from 5 mice; ASOD1,  $n=9$  cells from 4 mice). (C) Total dendritic length ( $p=0.217$ ). (D) Average branch length ( $p=0.419$ ). (E) Total number of branch points ( $p=0.236$ ). (F) Total number of tips ( $p=0.259$ ).

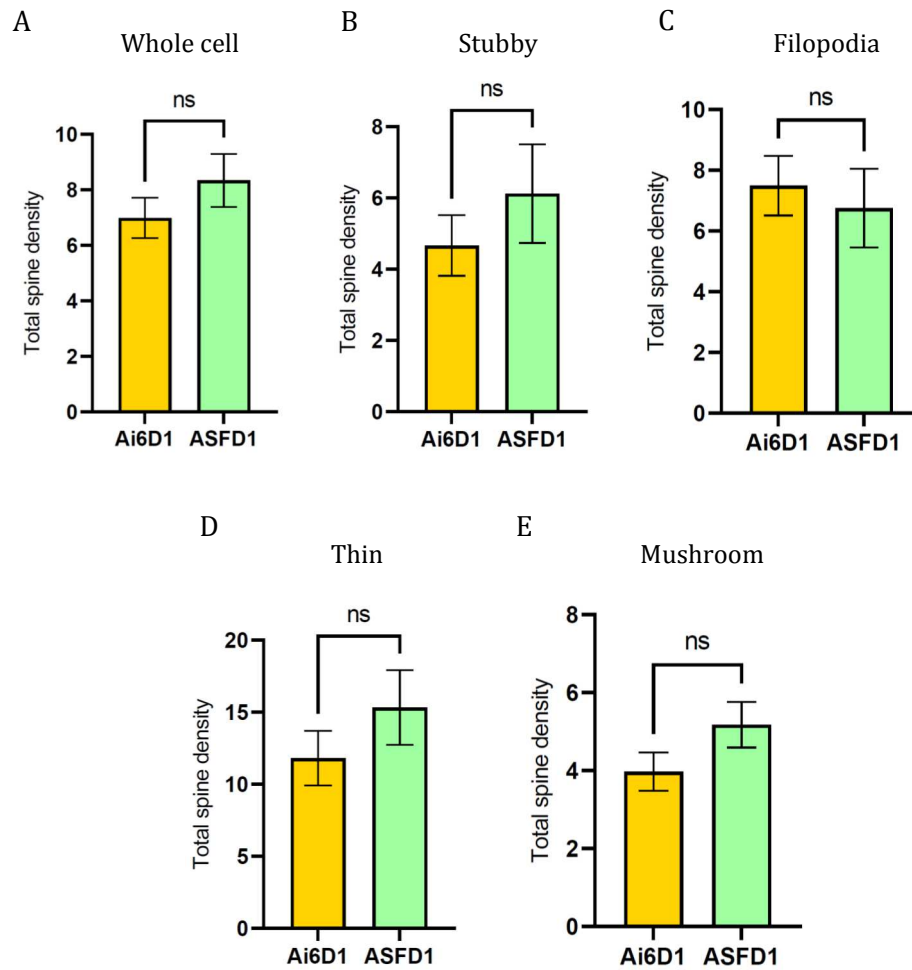


**Figure 2.** Whole cell dendritic spine density of male SIRT1- knock-out in D1-MSNs. (A) Whole cell spine density in male SIRT1-KO-D1 mice ( $p=0.278$ ; Ai6D1,  $n=10$  cells from 4 animals; ASFD1,  $n=11$  cells from 5 mice) (B) Stubby spine density ( $p=0.406$ ). (C) Filopodia density ( $p=0.664$ ). (D) Thin spine density ( $p=0.304$ ). (E) Mushroom spine density ( $p=0.138$ ).

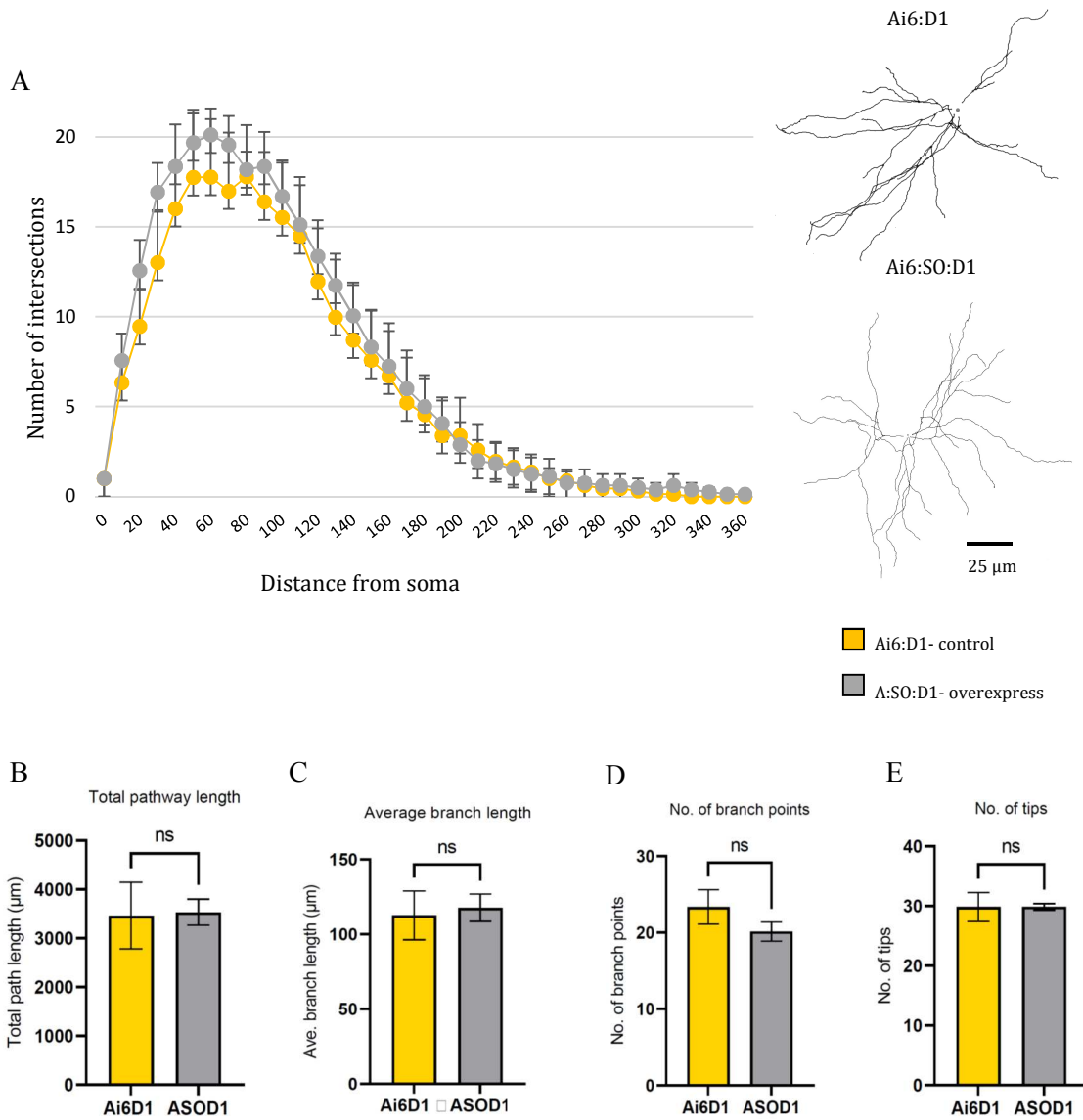


**Figure 3.** Dendritic morphology of male SIRT1- overexpress in D1-MSNs. (A) Sholl analysis of SIRT1-OVEXP-D1 males and representative traces (Sholl analysis: 2-way repeated measures ANOVA,  $p=0.897$ ; Ai6D1,  $n=10$  cells from 4 animals; ASOD1,  $n=9$  cells from 4 mice). (B) Total dendritic length ( $p=0.918$ ). (C) Average branch length ( $p=0.783$ ). (D) Total number of branch points ( $p=0.234$ ). (E) Total number of tips ( $p=0.985$ ).

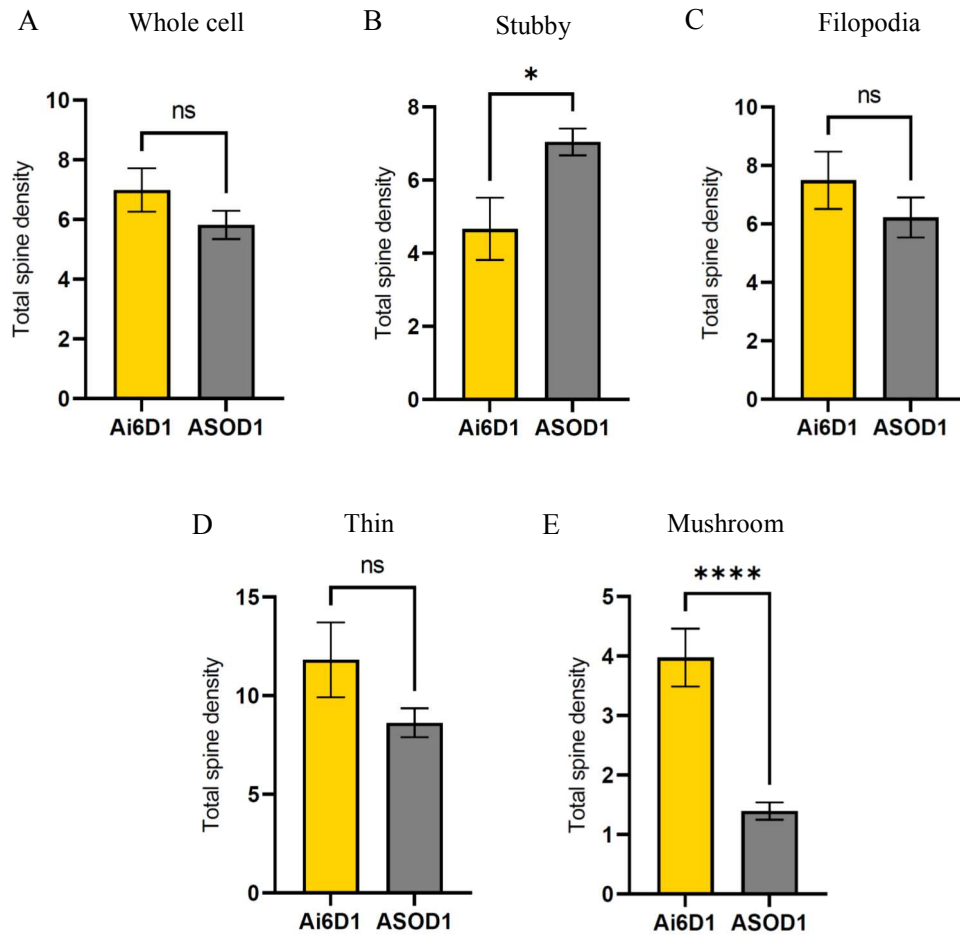


**Figure 4.** Whole cell dendritic spine density of male SIRT1- overexpress in D1-MSNs. (A) Whole cell spine density in male SIRT1-OVEXP-D1 mice ( $p=0.180$ ; ; Ai6D1,  $n=10$  cells from 4 animals; ASOD1,  $n=9$  cells from 4 mice). (B) Stubby spine density ( $p=0.017$ ). (C) Filopodia density ( $p=0.297$ ). (D) Thin spine density ( $p=0.130$ ). (E) Mushroom spine density ( $p<0.0001$ ).

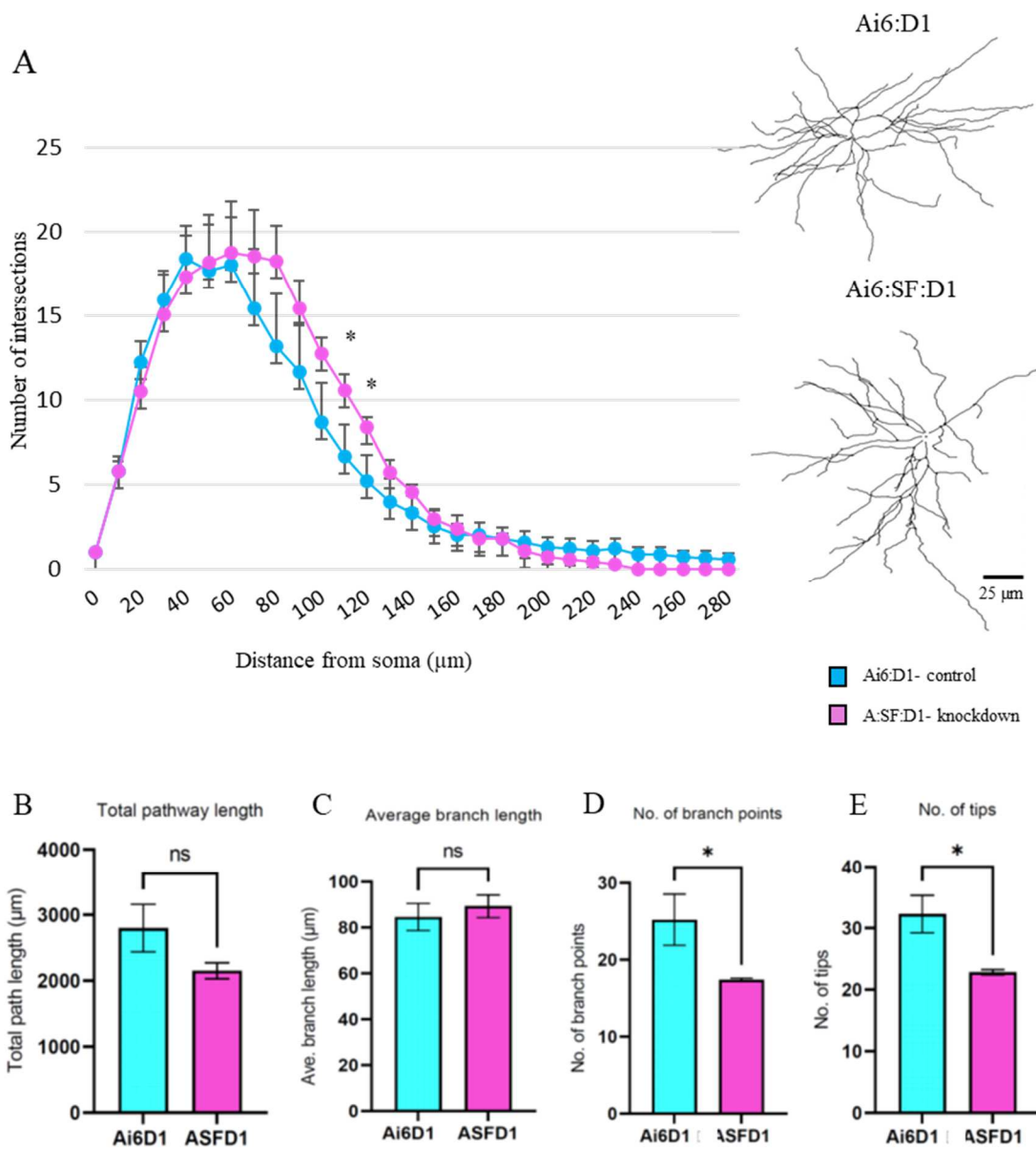


**Figure 5.** Dendritic morphology of female SIRT1- knock-out in D1-MSNs. (A) Sholl analysis of SIRT1-KO-D1 females and representative traces (Sholl analysis: 2-way repeated measures ANOVA,  $p=0.845$ ; Sholl radius 110  $\mu\text{m}$ ,  $p=0.05$ ; 120  $\mu\text{m}$ ,  $p=0.05$ ; Ai6D1,  $n=17$  cells from 6 animals; ASFD1,  $n=13$  cells from 5 mice). (B) Total dendritic length ( $p=0.126$ ). (C) Average branch length ( $p=0.55$ ). (D) Total number of branch points ( $p=0.047$ ). (E) Total number of tips ( $p=0.015$ ).

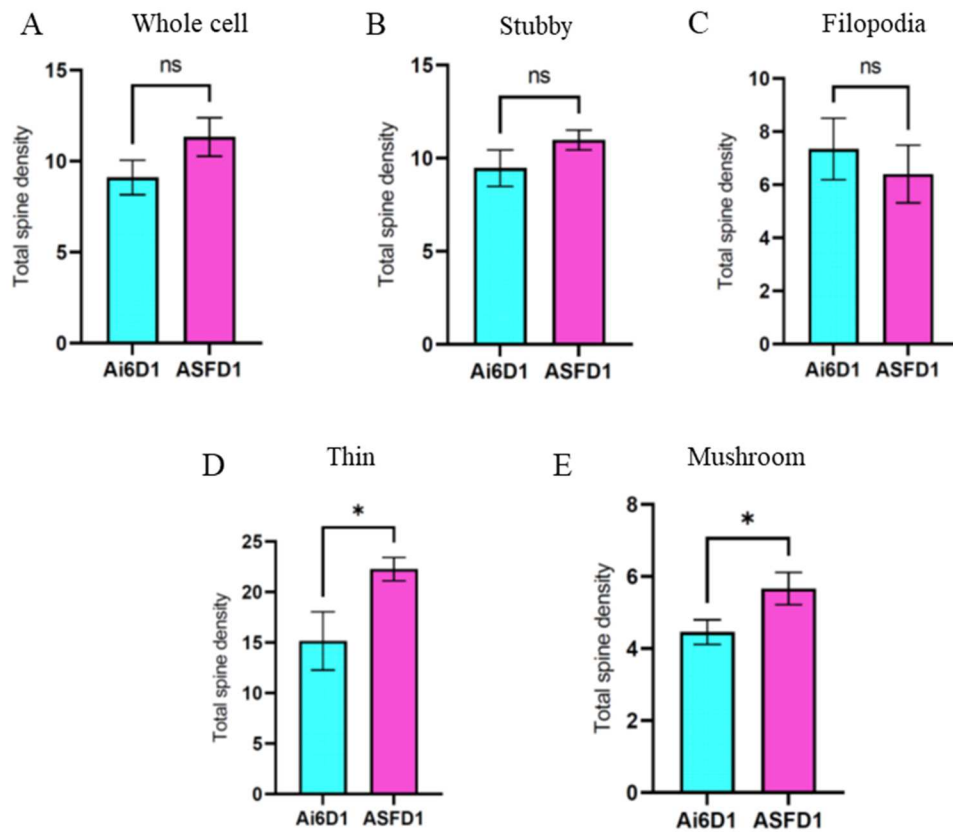


**Figure 6.** Whole cell dendritic spine density of female SIRT1- overexpress in D1-MSNs. (A) Whole cell spine density in female SIRT1-OVEXP-D1 mice ( $p=0.12$ ). (B) Stubby spine density ( $p=0.217$ ). (C) Filopodia density ( $p=0.56$ ). (D) Thin spine density ( $p=0.047$ ). (E) Mushroom spine density ( $p=0.039$ ).

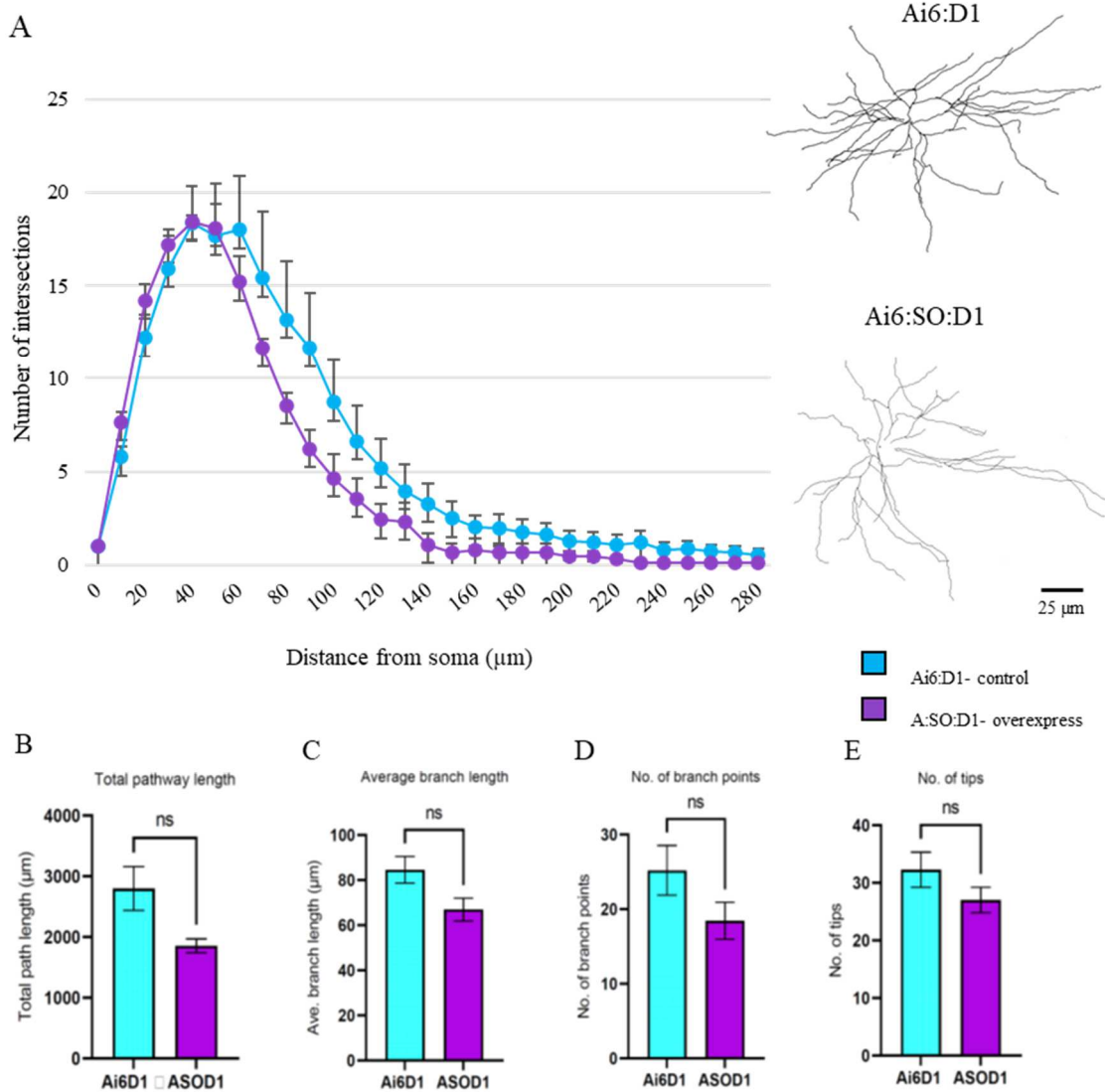


**Figure 7.** Dendritic morphology of female SIRT1- overexpress in D1-MSNs. (A) Sholl analysis of SIRT1-OVEXP-D1 females and representative traces (Sholl analysis: 2-way repeated measures ANOVA,  $p=0.577$ ; Ai6D1,  $n=17$  cells from 6 animals; ASOD1,  $n=9$  cells from 3 mice). (B) Total dendritic length ( $p=0.101$ ) (C) Average branch length ( $p=0.089$ ). (D) Total number of branch points ( $p=0.208$ ). (E) Total number of tips (0.272).

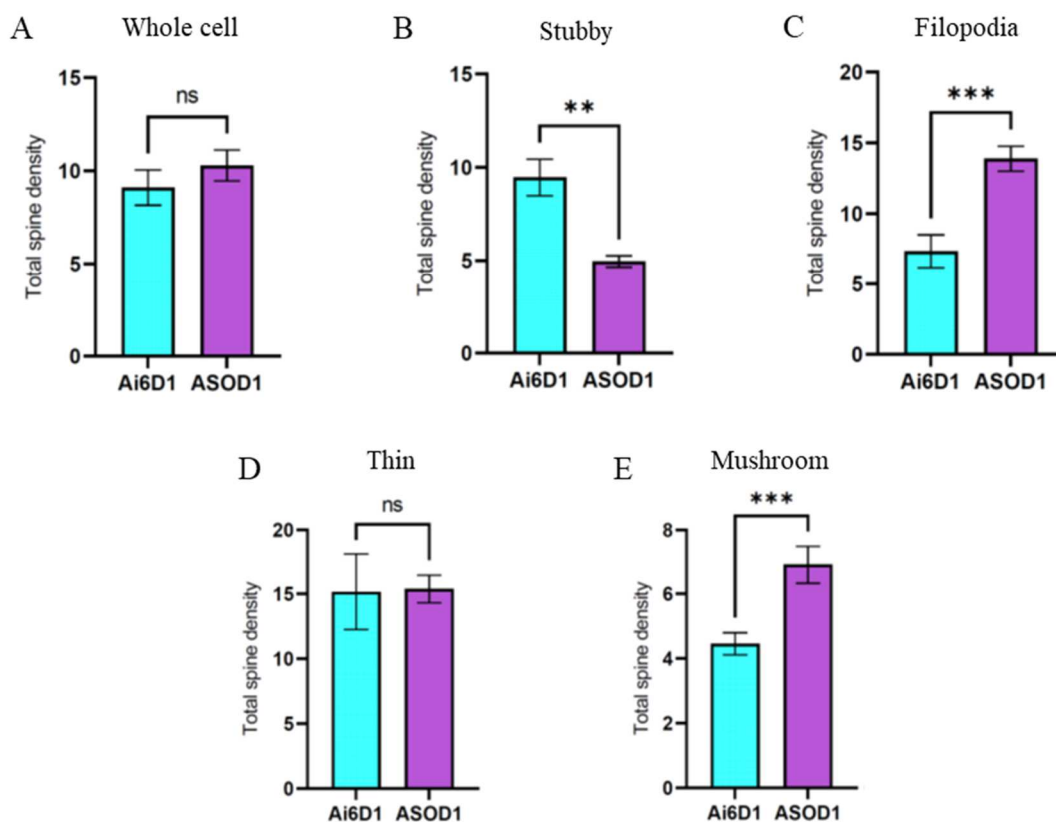


**Figure 8.** Whole cell dendritic spine density of female SIRT1- overexpress in D1-MSNs. (A) Whole cell spine density in female SIRT1-OVEXP-D1 mice ( $p=0.39$ ) (B) Stubby spine density ( $p=0.002$ ). (C) Filopodia density ( $p=0.0007$ ). (D) Thin spine density ( $p=0.955$ ). (E) Mushroom spine density ( $p=0.0008$ ).



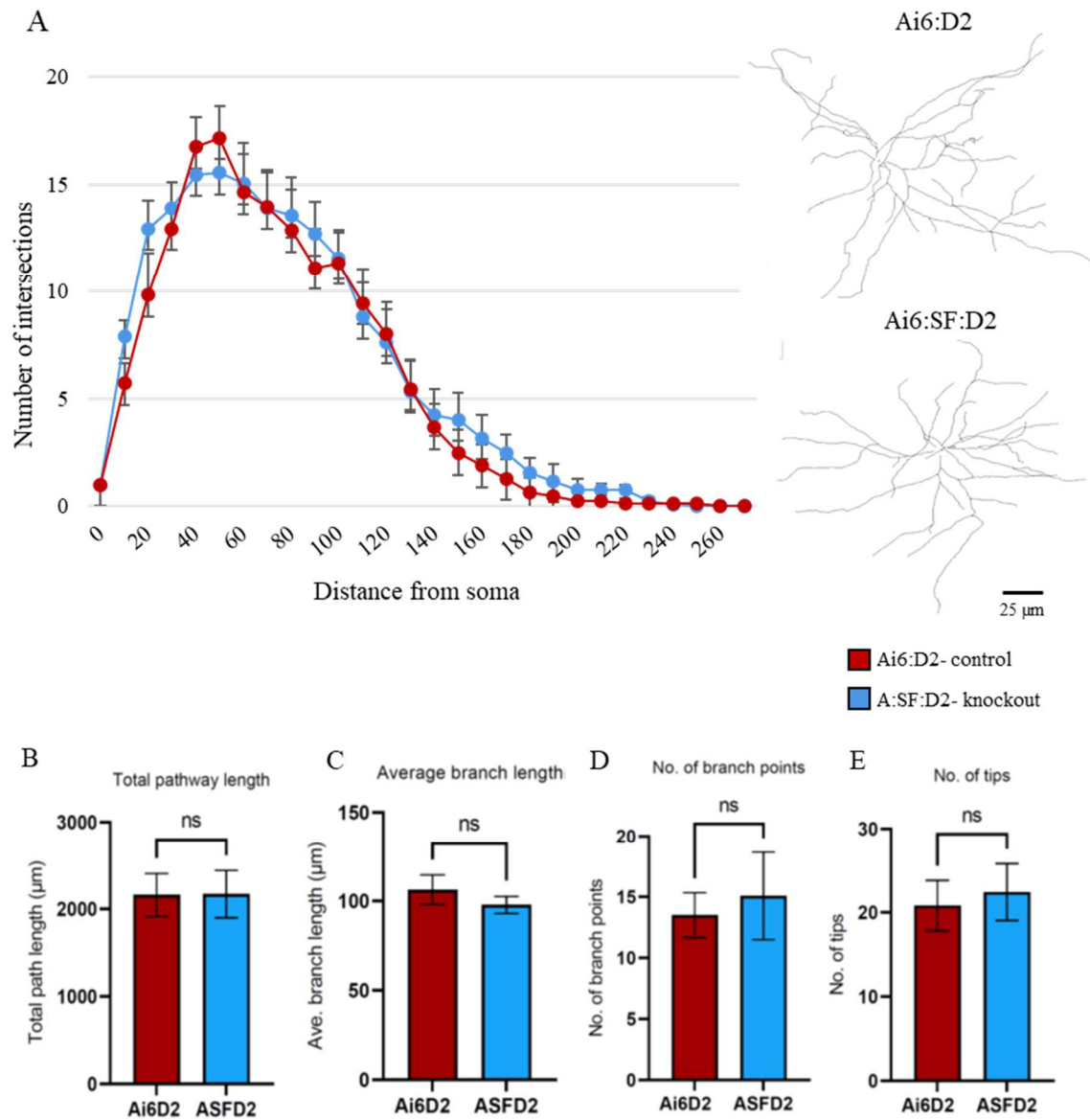


**Figure 9.** Dendritic morphology of male SIRT1- knockout in D2-MSNs. (A) Sholl analysis of SIRT1-KO-D2 males and representative traces (Sholl analysis: 2-way repeated measures ANOVA,  $p=1.00$ ; Ai6D2,  $n=13$  cells from 5 animals; ASFD2,  $n=10$  cells from 5 mice). (B) Total dendritic length ( $p=0.981$ ). (C) Average branch length ( $p=0.440$ ). (D) Total number of branch points ( $p=0.688$ ). (E) Total number of tips ( $p=0.731$ ).

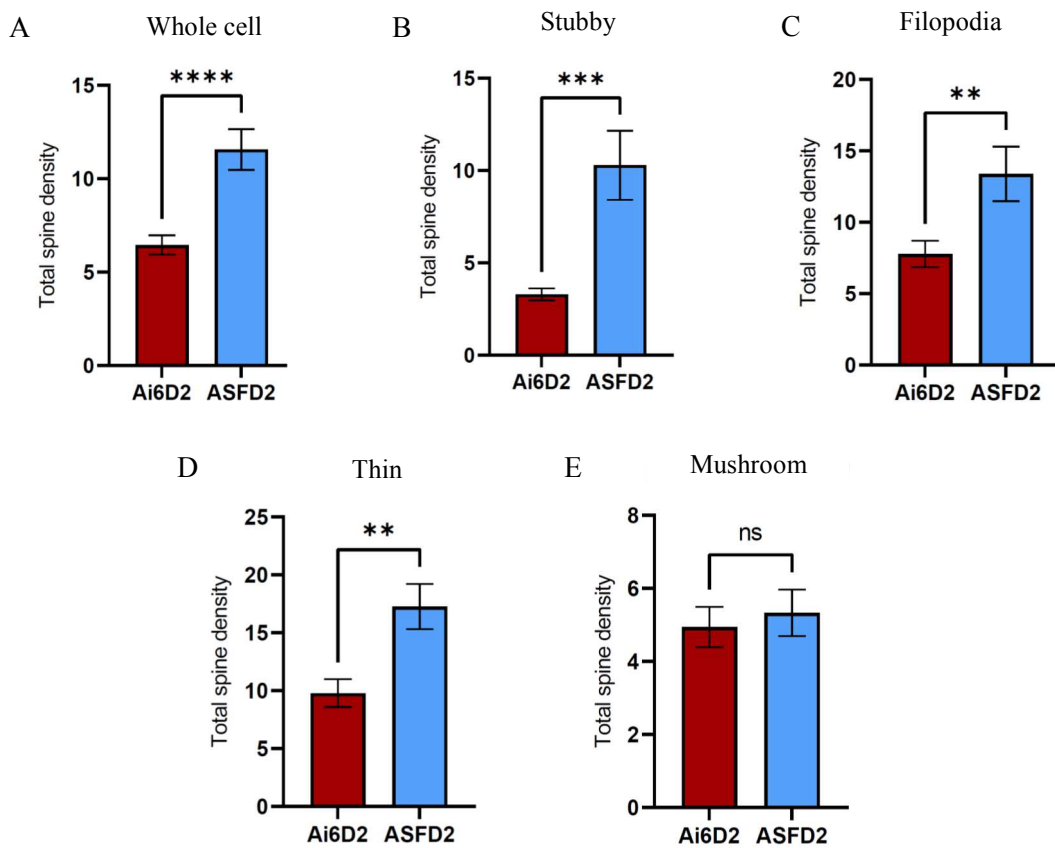


**Figure 10.** Whole cell dendritic spine density of male SIRT1- knock-out in D2-MSNs. (A) Whole cell spine density in male SIRT1-KO-D2 mice ( $p < 0.0001$ ; Ai6D2,  $n = 13$  cells from 5 animals; ASFD2,  $n = 10$  cells from 5 mice) (B) Stubby spine density ( $p = 0.0001$ ). (C) Filopodia density ( $p = 0.007$ ). (D) Thin spine density ( $p = 0.002$ ). (E) Mushroom spine density ( $p = 0.663$ ).

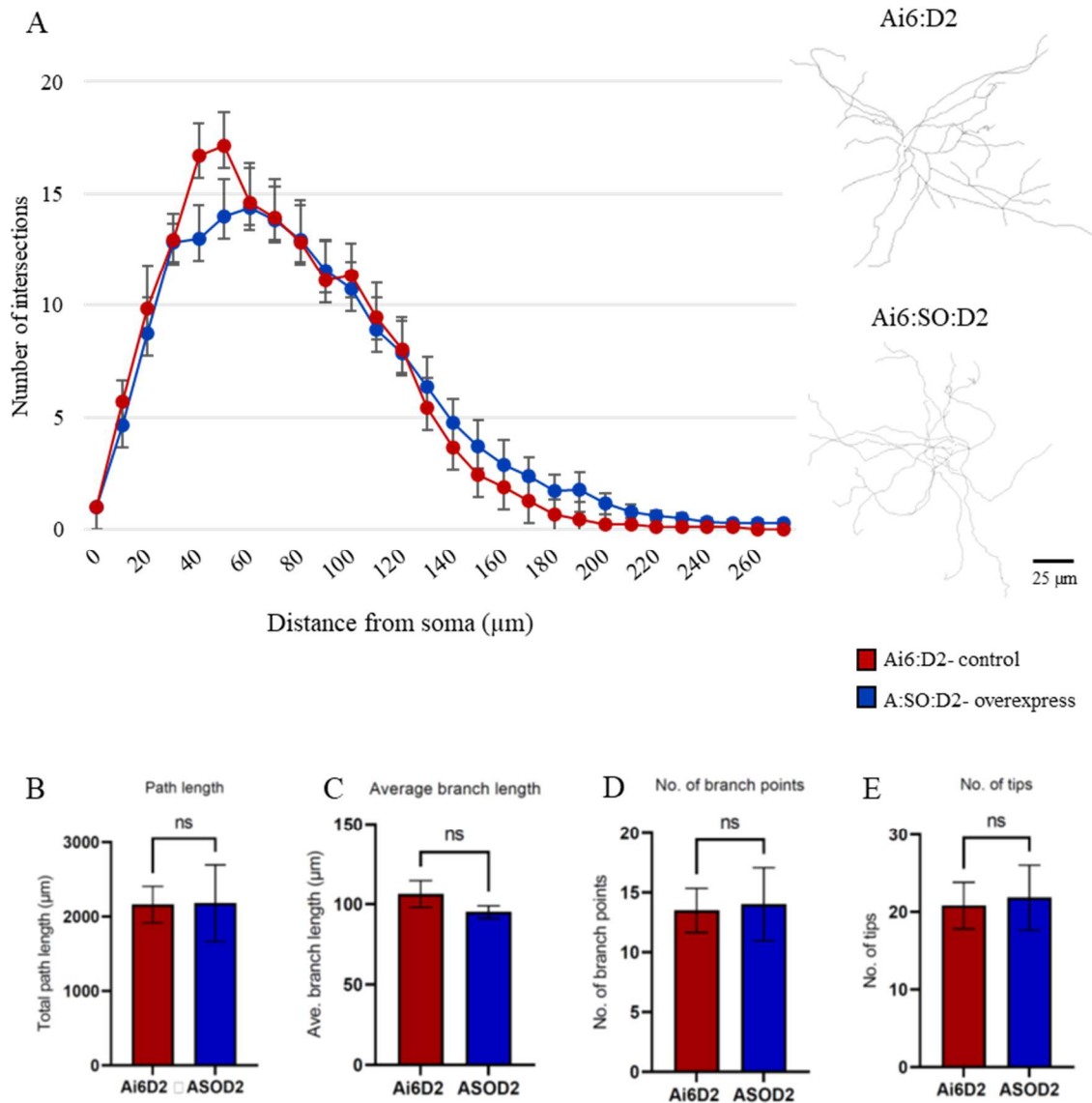


**Figure 11.** Dendritic morphology of male SIRT1- overexpress in D2-MSNs. (A) Sholl analysis of SIRT1-OVEXP-D2 males and representative traces (Sholl analysis: 2-way repeated measures ANOVA,  $p=1.00$ ; Ai6D2,  $n=13$  cells from 5 animals; ASOD2,  $n=8$  cells from 3 mice). (B) Total dendritic length ( $p=0.97$ ). (C) Average branch length ( $p=0.36$ ). (D) Total number of branch points ( $p=0.88$ ). (E) Total number of tips ( $p=0.84$ ).

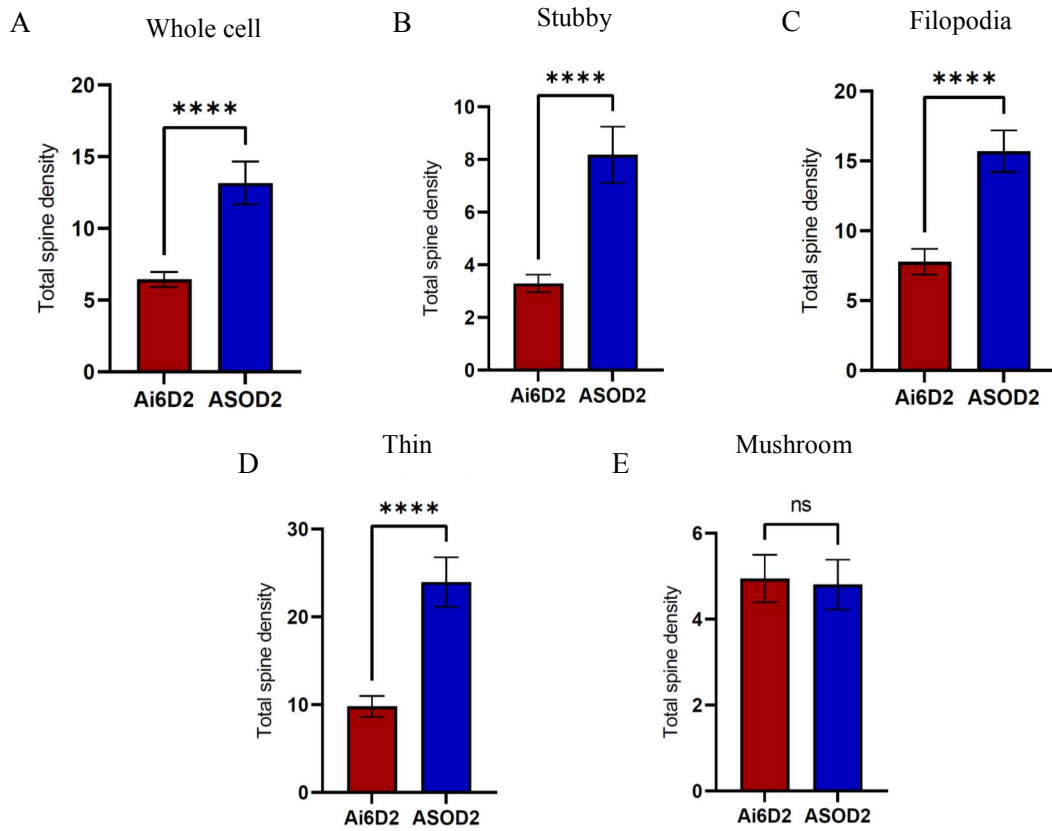


**Figure 12.** Whole cell dendritic spine density of male SIRT1- overexpress in D2-MSNs. (A) Whole cell spine density in male SIRT1-OVEXP-D2 mice ( $p < 0.0001$ ; Ai6D2,  $n = 13$  cells from 5 animals; ASOD2,  $n = 8$  cells from 3 mice) (B) Stubby spine density ( $p = 0.0001$ ). (C) Filopodia density ( $p = 0.007$ ). (D) Thin spine density ( $p = 0.002$ ). (E) Mushroom spine density ( $p = 0.663$ ).

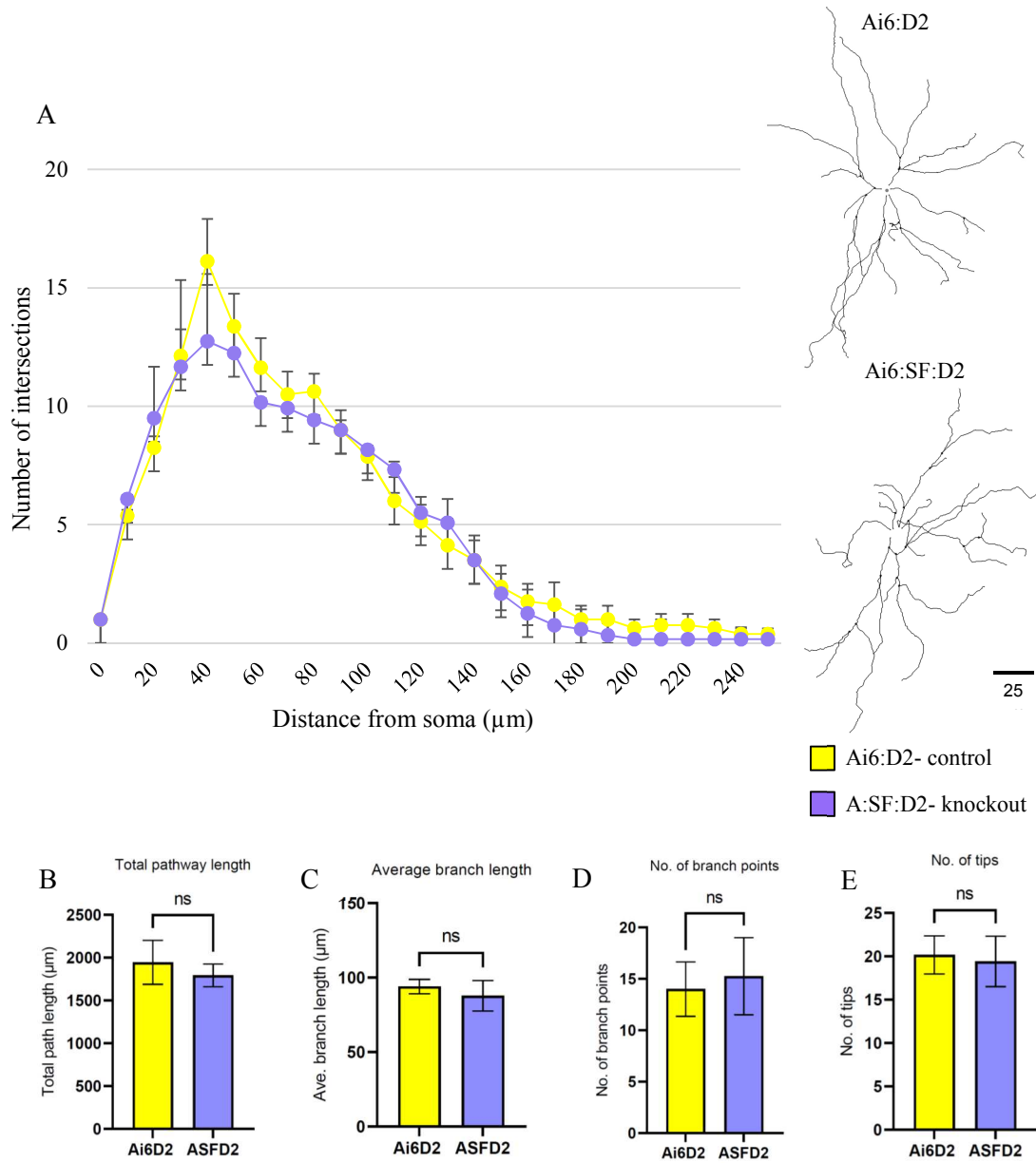


**Figure 13.** Dendritic morphology of female SIRT1- knockout in D2-MSNs. (A) Sholl analysis of SIRT1-KO-D2 females and representative traces (Sholl analysis: 2-way repeated measures ANOVA,  $p=1.00$ ; Ai6D2,  $n=5$  cells from 4 animals; ASFD2,  $n=5$  cells from 2 mice). (B) Total dendritic length ( $p=0.687$ ). (C) Average branch length ( $p=0.569$ ). (D) Total number of branch points ( $p=0.795$ ). (E) Total number of tips ( $p=0.847$ ).

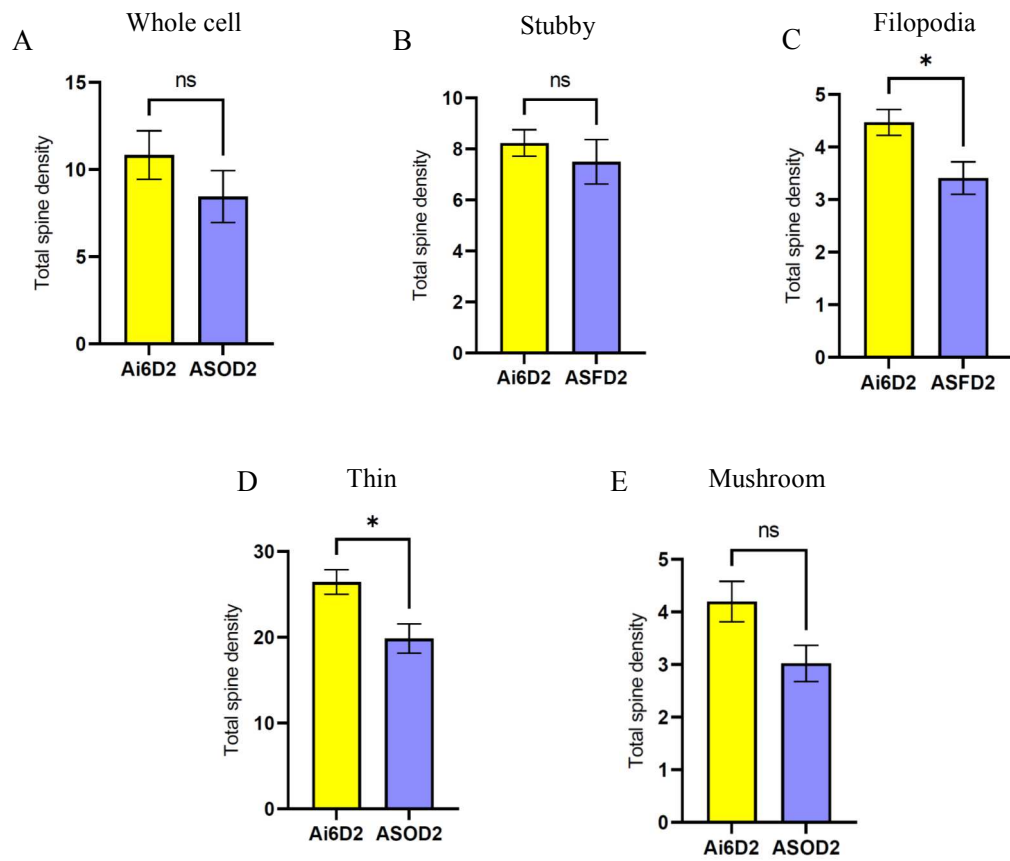


**Figure 14.** Whole cell dendritic spine density of female SIRT1- knock-out in D2-MSNs. (A) Whole cell spine density in female SIRT1-KO-D2 mice (B) Stubby spine density. (C) Filopodia density. (D) Thin spine density. (E) Mushroom spine density.

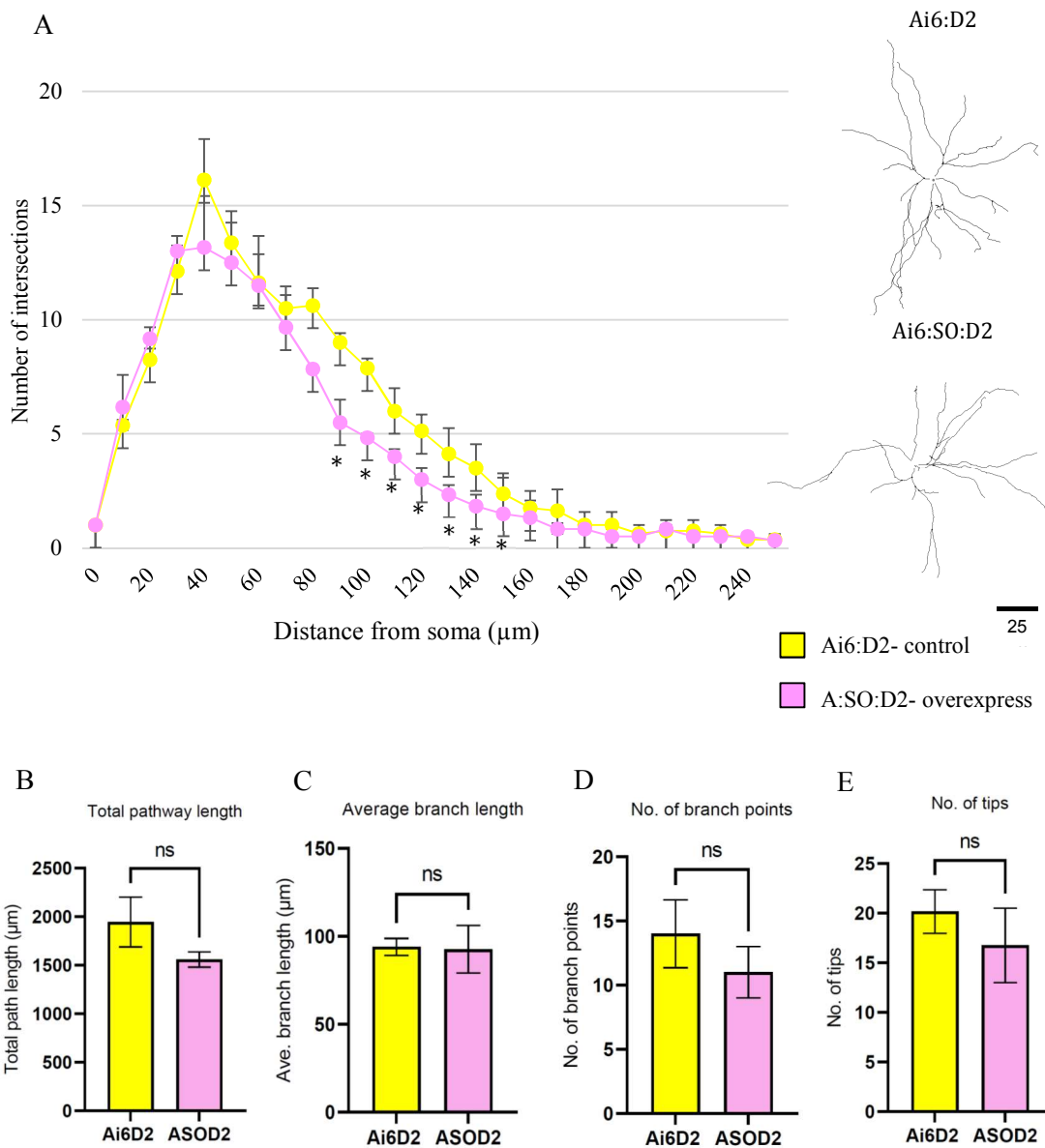


**Figure 15.** Dendritic morphology of female SIRT1- overexpress in D2-MSNs. (A) Sholl analysis of SIRT1-OVEXP-D2 females and representative traces (Sholl analysis: 2-way repeated measures ANOVA,  $p=1.00$ ; Ai6D2,  $n=5$  cells from 4 animals; ASOD2,  $n=6$  cells from 2 mice). (B) Total dendritic length ( $p=0.333$ ). (C) Average branch length ( $p=0.916$ ). (D) Total number of branch points ( $p=0.479$ ). (E) Total number of tips (0.454).

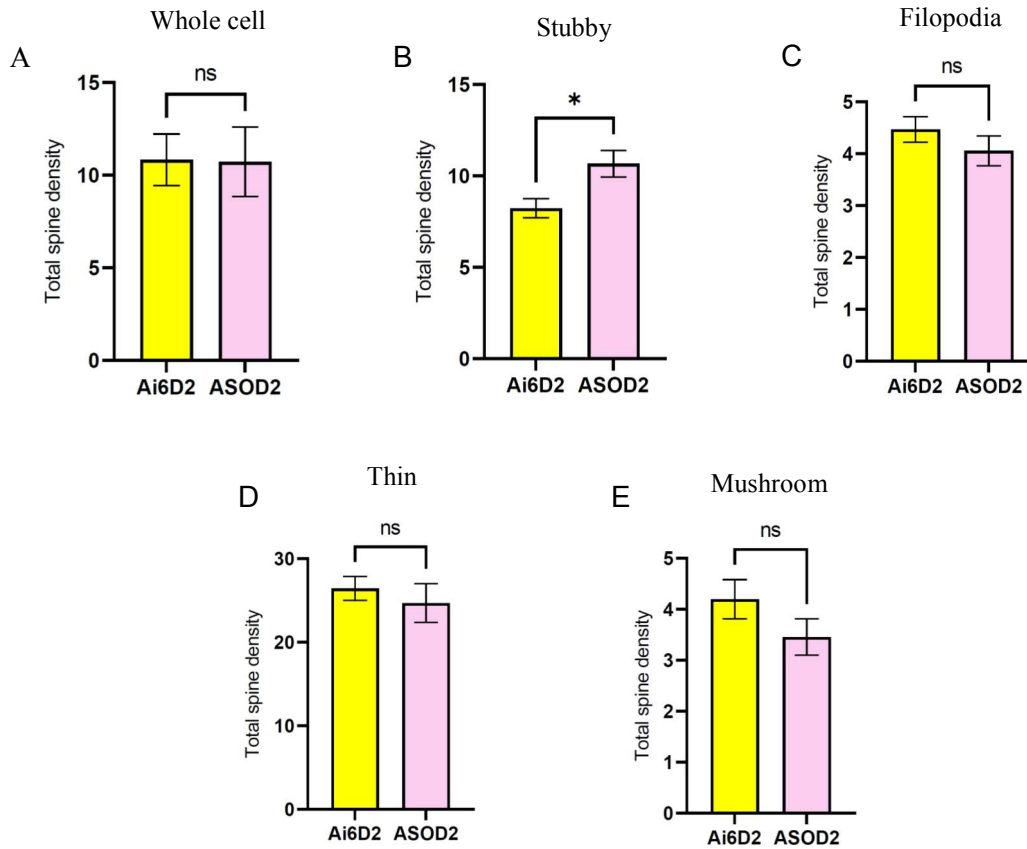


**Figure 16.** Whole cell dendritic spine density of female SIRT1- overexpress in D2-MSNs. (A) Whole cell spine density in female SIRT1-OVEXP-D2 mice ( $p=0.960$ ) (B) Stubby spine density ( $0.015$ ). (C) Filopodia density ( $p=0.324$ ). (D) Thin spine density ( $p=0.508$ ). (E) Mushroom spine density ( $p=0.236$ ).



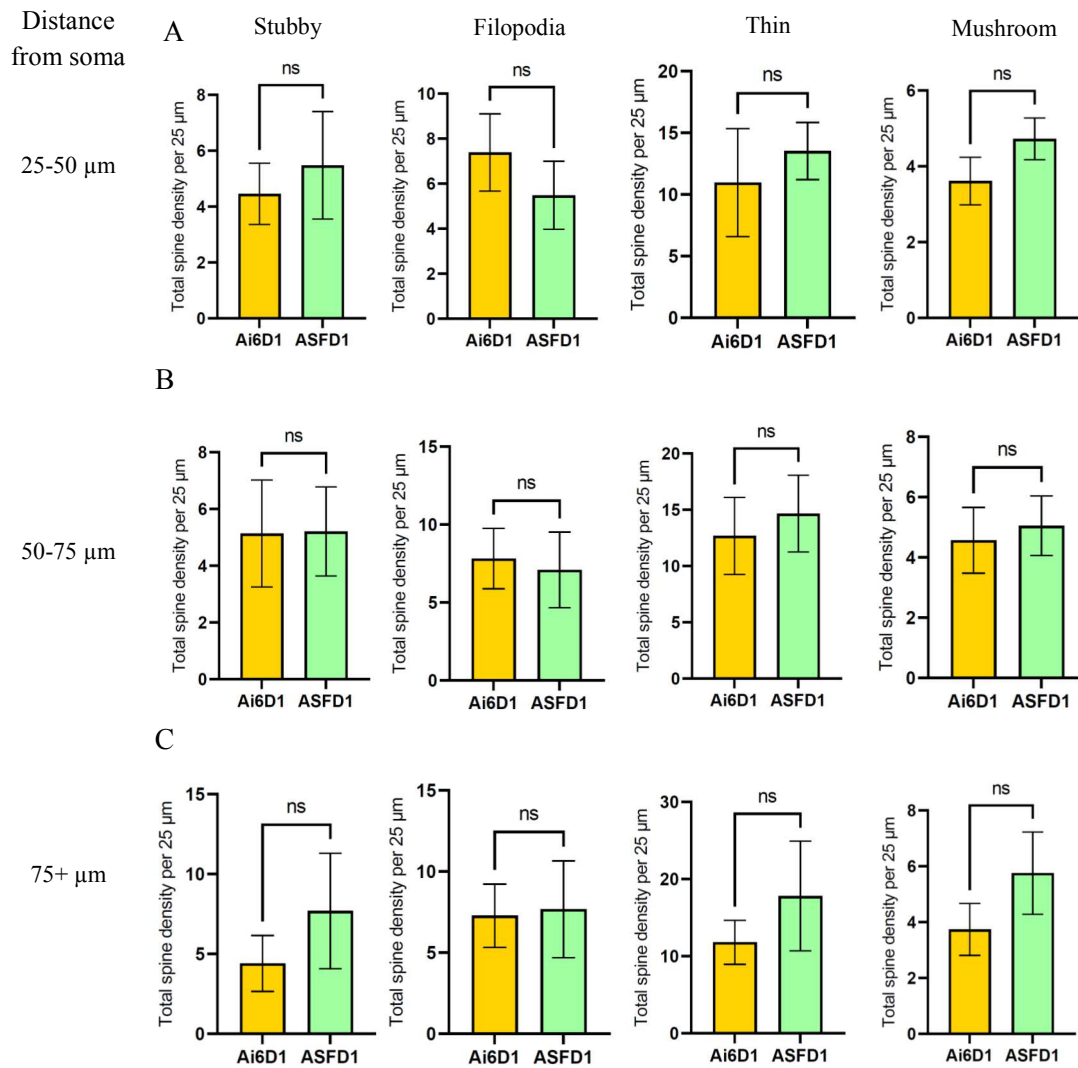


**Figure 17.** Male SIRT1-KO-D1 spine density by distance from soma. (A) Distance 25-50  $\mu\text{m}$  from soma: no significant difference between SIRT1-KO and control mice (stubby  $p=0.68$ ; filopodia,  $p=0.43$ ; thin,  $p=0.59$ ; mushroom,  $p=0.22$ ). (B) Distance 50- 75  $\mu\text{m}$  from soma: no significant difference between SIRT1-KO and control mice (stubby  $p=0.97$ ; filopodia,  $p=0.82$ ; thin,  $p=0.69$ ; mushroom,  $p=0.75$ ). (C) Distance 75+  $\mu\text{m}$  from soma: no significant difference between SIRT1-KO and control mice (stubby  $p=0.47$ ; filopodia,  $p=0.91$ ; thin,  $p=0.50$ ; mushroom,  $p=0.31$ ).

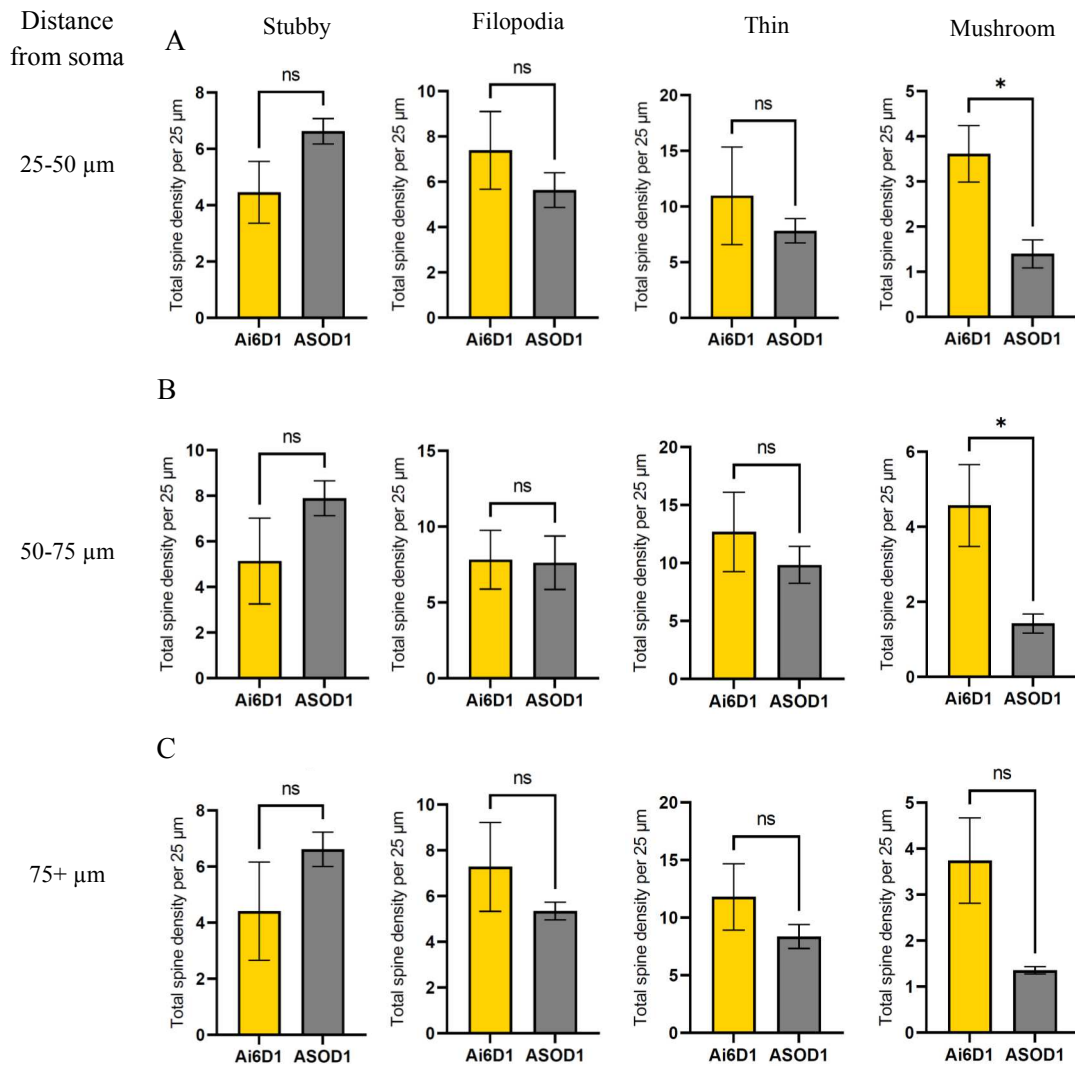


**Figure 18.** Male SIRT1- OVEXP-D1 spine density by distance from soma. (A) Distance 25-50 μm from soma: a significant difference between SIRT1-OVEXP and control mice was found in mushroom type spines ( $p=0.011$ ). No significant differences in other spine type (stubby  $p=0.08$ ; filopodia,  $p=0.34$ ; thin,  $p=0.46$ ). (B) Distance 50- 75 μm from soma: a significant difference between SIRT1-OVEXP and control mice in mushroom type spines ( $p=0.03$ ). No significant change was seen in other spine types (stubby  $p=0.22$ ; filopodia,  $p=0.94$ ; thin,  $p=0.47$ ). (C) Distance 75+ μm from soma: no significant difference between SIRT1-OVEXP and control mice (stubby  $p=0.34$ ; filopodia,  $p=0.44$ ; thin,  $p=0.97$ ; mushroom,  $p=0.08$ ).

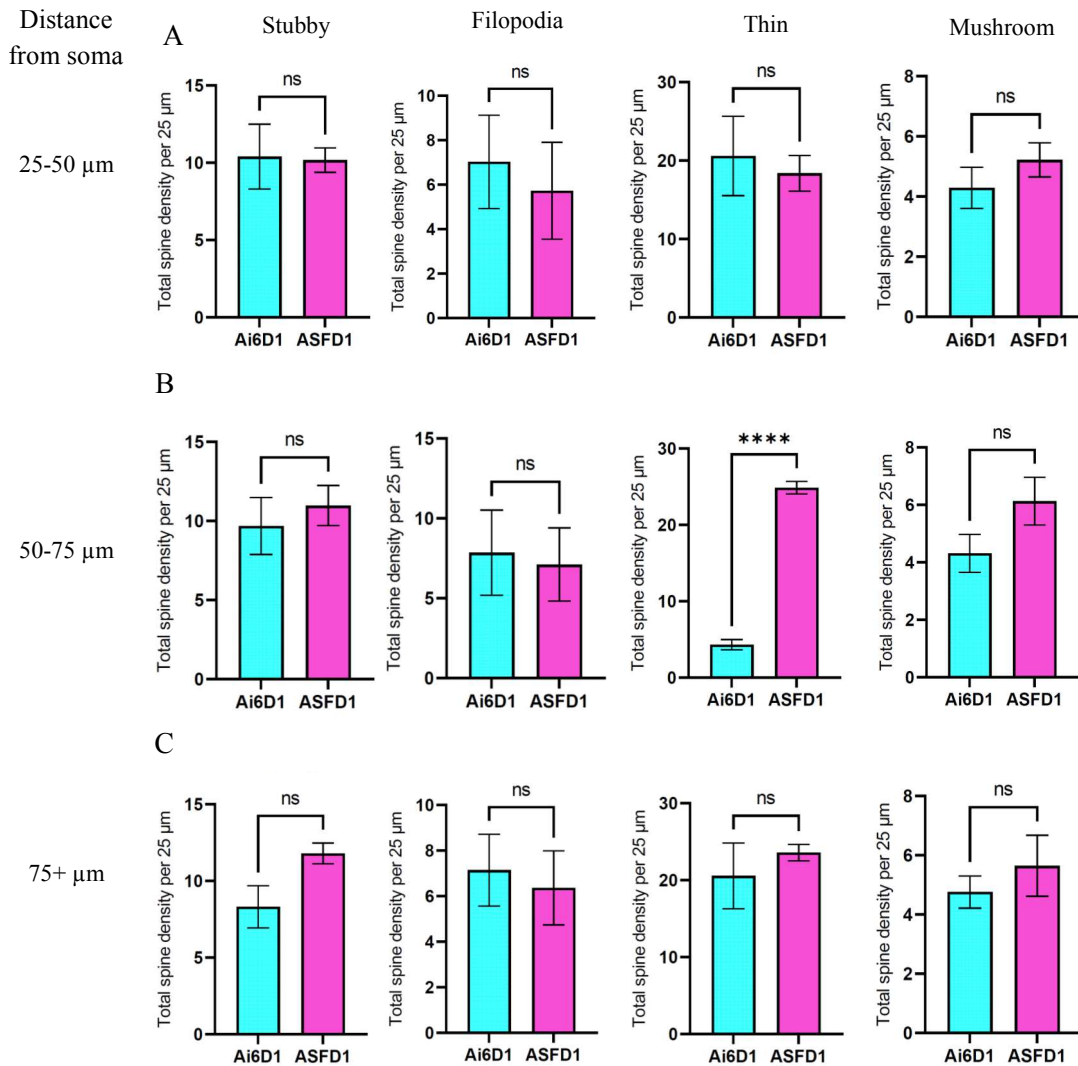


**Figure 19.** Female SIRT1-KO-D1 spine density by distance from soma. (A) Distance 25-50  $\mu\text{m}$  from soma: no significant difference between SIRT1-KO and control mice (stubby  $p=0.92$ ; filopodia,  $p=0.68$ ; thin,  $p=0.72$ ; mushroom,  $p=0.35$ ). (B) Distance 50-75  $\mu\text{m}$  from soma: there was a significant increase of thin spines ( $p<0.0001$ ) between SIRT1-KO and control mice (stubby  $p=0.59$ ; filopodia,  $p=0.84$ ; mushroom,  $p=0.12$ ). (C) Distance 75+  $\mu\text{m}$  from soma: no significant difference between SIRT1-KO and control mice (stubby  $p=0.07$ ; filopodia,  $p=0.74$ ; thin,  $p=0.56$ ; mushroom,  $p=0.44$ ).

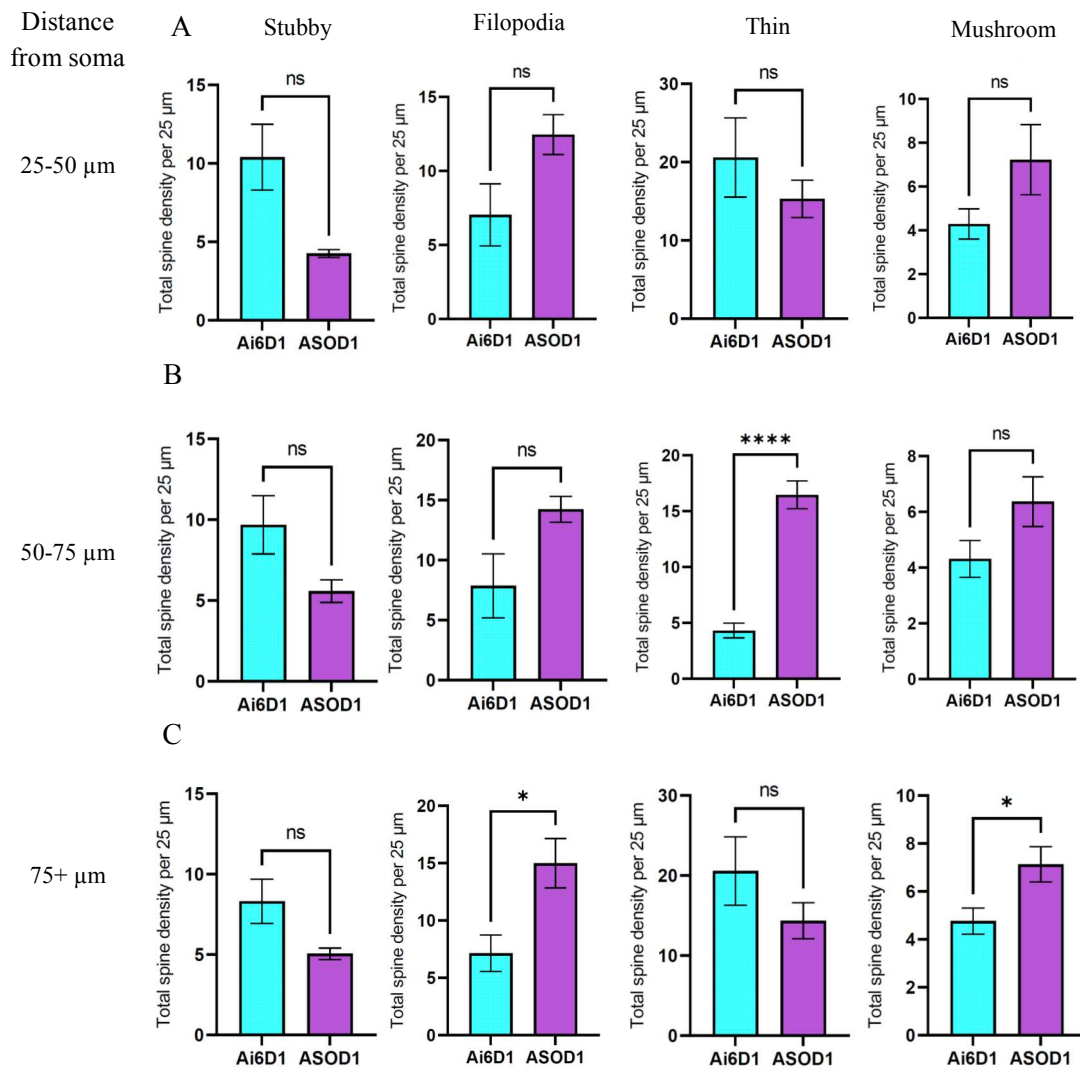


**Figure 20.** Female SIRT1-OVEXP-D1 spine density by distance from soma. (A) Distance 25-50 μm from soma: no significant difference between SIRT1-OVEXP and control mice was found (stubby  $p=0.07$ ; filopodia,  $p=0.11$ ; thin,  $p=0.47$ ; mushroom,  $p=0.09$ ). (B) Distance 50- 75 μm from soma: a significant difference between SIRT1-OVEXP and control mice in thin type spines ( $p<0.0001$ ). No significant change was seen in other spine types (stubby  $p=0.14$ ; filopodia,  $p=0.12$ ; mushroom,  $p=0.11$ ). (C) Distance 75+ μm from soma: a significant difference was observed in filopodia ( $p=0.02$ ) and mushroom spines ( $p=0.03$ ) between SIRT1-OVEXP and control mice (stubby  $p=0.12$ ; thin,  $p=0.33$ ).

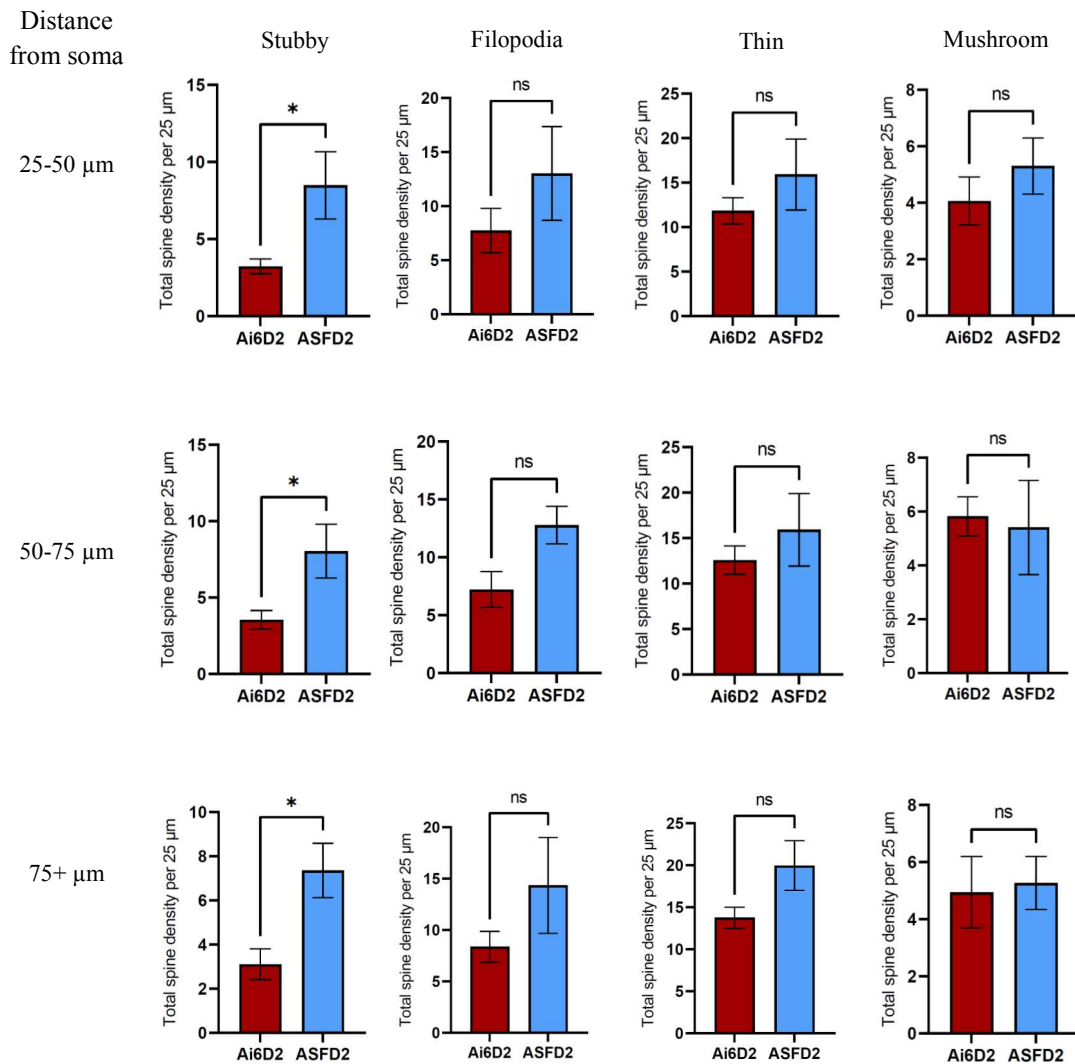


**Figure 21.** Male SIRT1-KO-D2 spine density by distance from soma. (A) Distance 25-50  $\mu\text{m}$  from soma: a significant increase of stubby spines ( $p=0.02$ ) was observed with no further differences between SIRT1-KO and control mice (filopodia,  $p=0.25$ ; thin,  $p=0.28$ ; mushroom,  $p=0.39$ ). (B) Distance 50-75  $\mu\text{m}$  from soma: there was a significant increase in the number of stubby spines ( $p=0.02$ ). No significant difference between SIRT1-KO and control mice were seen (filopodia,  $p=0.057$ ; thin,  $p=0.38$ ; mushroom,  $p=0.80$ ). (C) Distance 75+  $\mu\text{m}$  from soma: there was a significant increase in the number of stubby spines ( $p=0.017$ ). No further significant differences were observed (filopodia,  $p=0.18$ ; thin,  $p=0.06$ ; mushroom,  $p=0.86$ ).

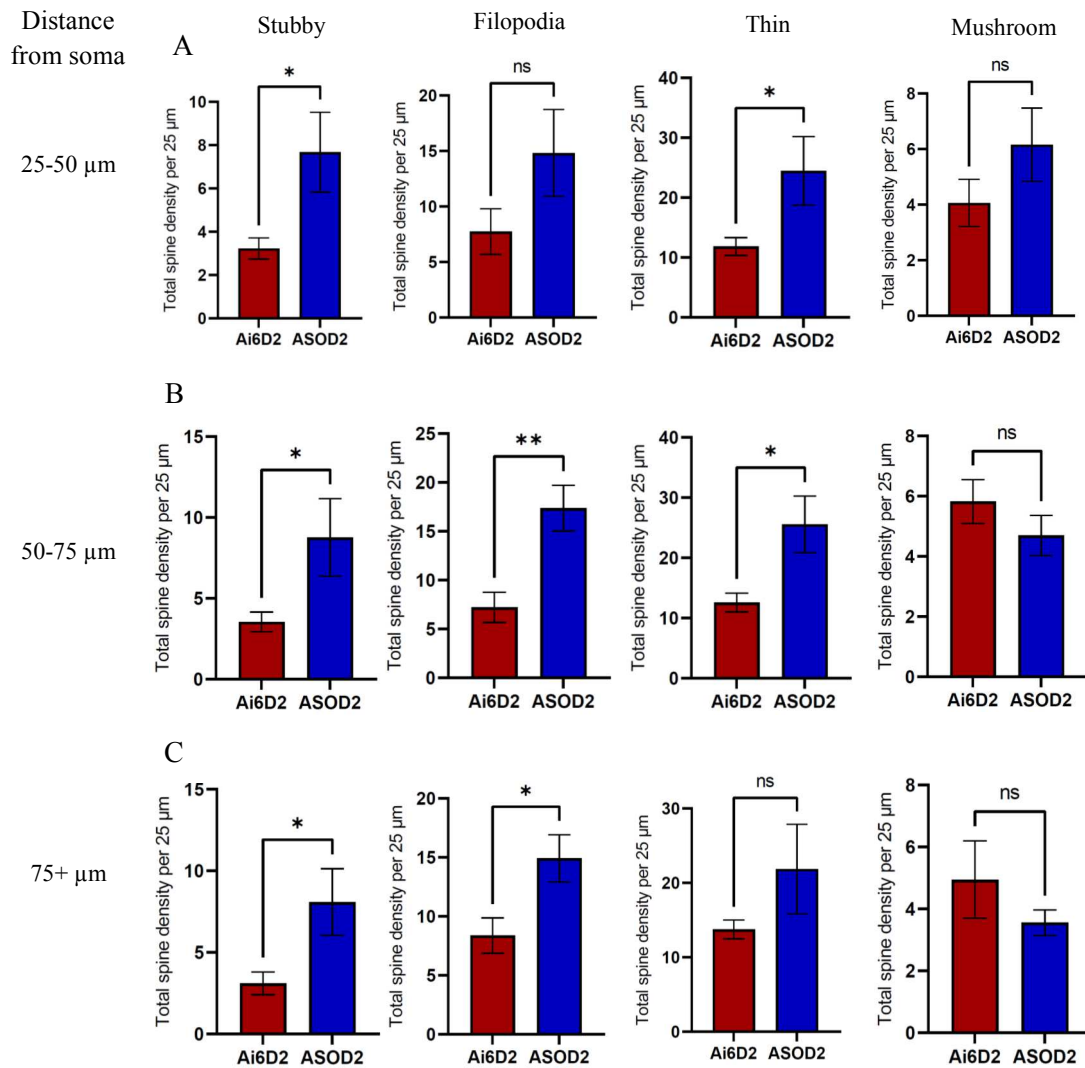


**Figure 22.** Male SIRT1-OVEXP-D2 spine density by distance from soma. (A) Distance 25-50  $\mu\text{m}$  from soma: a significant difference between SIRT1-OVEXP and control mice was found in stubby ( $p=0.02$ ), and thin spines ( $p=0.03$ ) with no change in filopodia ( $p=0.12$ ) or mushroom spines ( $p=0.20$ ). (B) Distance 50- 75  $\mu\text{m}$  from soma: a significant difference between SIRT1-OVEXP and control mice in stubby spines ( $p=0.03$ ), filopodia ( $p=0.008$ ), and thin spines ( $p=0.017$ ). No change was seen in mushroom spines ( $p=0.33$ ). (C) Distance 75+  $\mu\text{m}$  from soma: there was a significant increase in both stubby spines ( $p=0.03$ ) and filopodia ( $p=0.03$ ). No significant difference between SIRT1-OVEXP and control mice in thin (thin,  $p=0.97$ ) or mushroom ( $p=0.44$ ) spines.

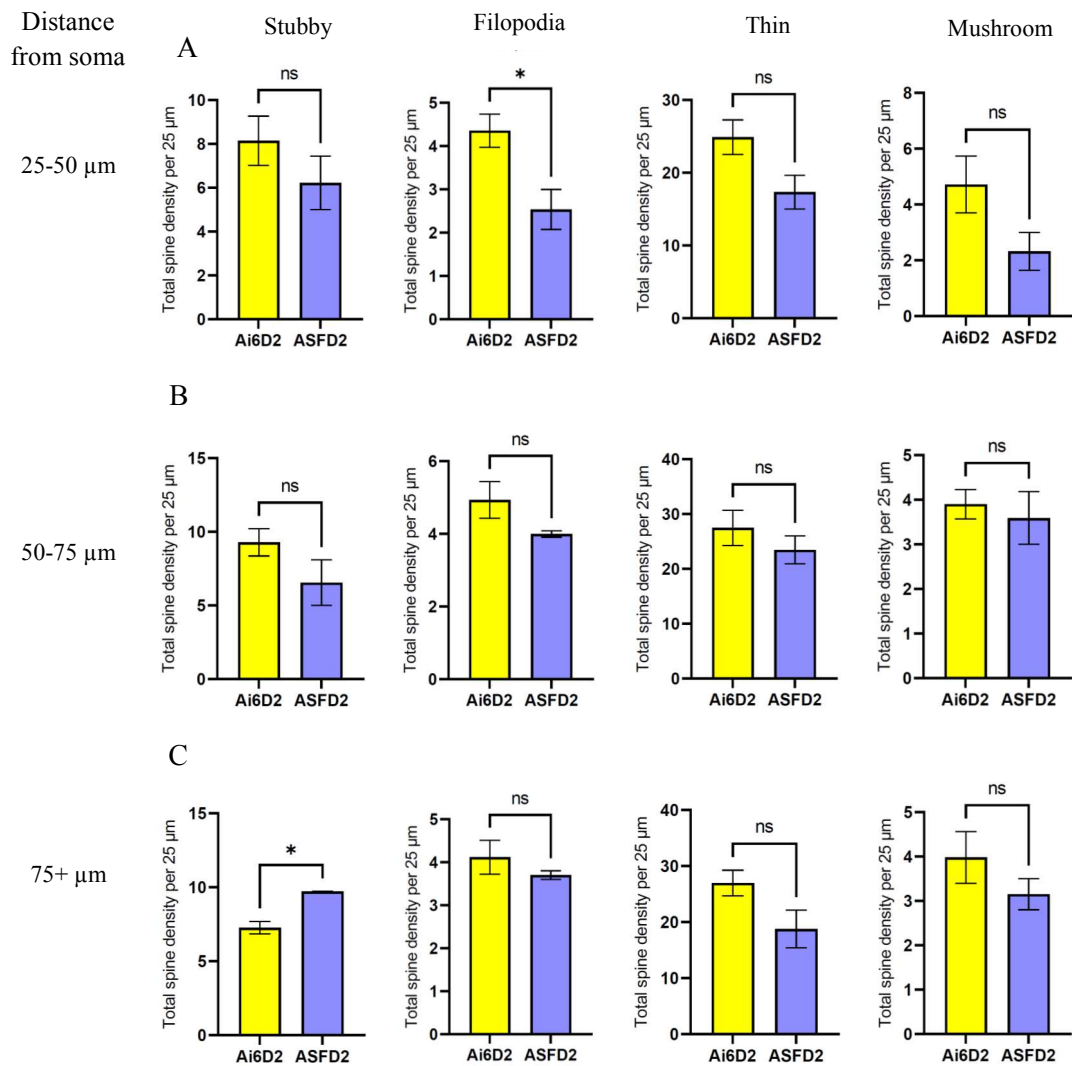


**Figure 23.** Female SIRT1-KO-D2 spine density by distance from soma. (A) Distance 25-50 μm from soma: there was a significant decrease in filopodia ( $p=0.04$ ). No other changes were seen between SIRT1-KO and control mice (stubby  $p=0.35$ ; thin,  $p=0.11$ ; mushroom,  $p=0.20$ ). (B) Distance 50-75 μm from soma: there were no significant changes between SIRT1-KO and control mice (stubby  $p=0.17$ ; filopodia,  $p=0.28$ ; thin,  $p=0.47$ ; mushroom,  $p=0.64$ ). (C) Distance 75+ μm from soma: there was a significant increase of stubby spines ( $p=0.01$ ) with no other significant differences between SIRT1-KO and control mice (filopodia,  $p=0.52$ ; thin,  $p=0.10$ ; mushroom,  $p=0.41$ ).

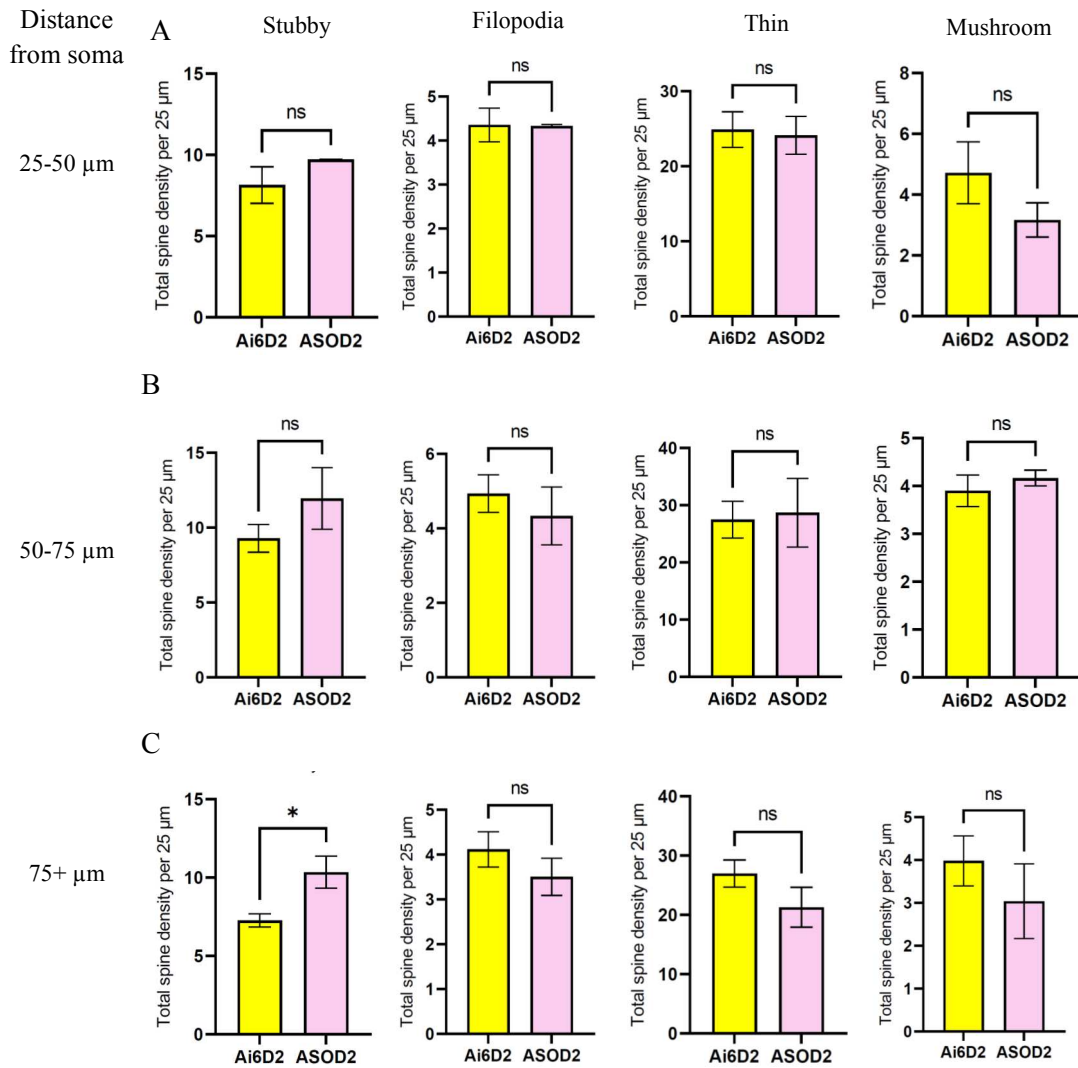


**Figure 24.** Female SIRT1-OVEXP-D2 spine density by distance from soma. (A) Distance 25-50 μm from soma: no significant difference between SIRT1-KO and control mice (stubby  $p=0.40$ ; filopodia,  $p=0.97$ ; thin,  $p=0.85$ ; mushroom,  $p=0.37$ ). (B) Distance 50- 75 μm from soma: no significant difference between SIRT1-KO and control mice (stubby  $p=0.22$ ; filopodia,  $p=0.53$ ; thin,  $p=0.85$ ; mushroom,  $p=0.62$ ). (C) Distance 75+ μm from soma: there was a significant increase in stubby spines ( $p=0.02$ ), and no significant difference between SIRT1-KO and control mice for other spine types (filopodia,  $p=0.39$ ; thin,  $p=0.22$ ; mushroom,  $p=0.41$ ).